



Article scientifique

Article

2019

Published version

Open Access

This is the published version of the publication, made available in accordance with the publisher's policy.

Measurement of distributions sensitive to the underlying event in inclusive Z boson production in pp collisions at $\sqrt{s} = 13$ TeV with the ATLAS detector

Collaborators: Adorni Braccesi Chiassi, Sofia; Akilli, Ece; Amrouche, Cherifa Sabrina; Benoit, Mathieu; Clark, Allan Geoffrey; Della Volpe, Domenico; Di Bello, Francesco Armando; Dubreuil, Arnaud; Ferrere, Didier; Gadatsch, Stefan; Golling, Tobias; Gonzalez Sevilla, Sergio Iacobucci, Giuseppe [**and 19 more**]

How to cite

ATLAS Collaboration. Measurement of distributions sensitive to the underlying event in inclusive Z boson production in pp collisions at $\sqrt{s} = 13$ TeV with the ATLAS detector. In: The European Physical Journal. C, Particles and Fields, 2019, vol. 79, p. 1–31. doi: 10.1140/epjc/s10052-019-7162-0

This publication URL: <https://archive-ouverte.unige.ch/unige:128788>

Publication DOI: [10.1140/epjc/s10052-019-7162-0](https://doi.org/10.1140/epjc/s10052-019-7162-0)



Measurement of distributions sensitive to the underlying event in inclusive Z boson production in pp collisions at $\sqrt{s} = 13$ TeV with the ATLAS detector

ATLAS Collaboration*

CERN, 1211 Geneva 23, Switzerland

Received: 24 May 2019 / Accepted: 19 July 2019 / Published online: 8 August 2019
© CERN for the benefit of the ATLAS collaboration 2019

Abstract This paper presents measurements of charged-particle distributions sensitive to the properties of the underlying event in events containing a Z boson decaying into a muon pair. The data were obtained using the ATLAS detector at the LHC in proton–proton collisions at a centre-of-mass energy of 13 TeV with an integrated luminosity of 3.2 fb^{-1} . Distributions of the charged-particle multiplicity and of the charged-particle transverse momentum are measured in regions of the azimuth defined relative to the Z boson direction. The measured distributions are compared with the predictions of various Monte Carlo generators which implement different underlying event models. The Monte Carlo model predictions qualitatively describe the data well, but with some significant discrepancies.

Contents

1	Introduction	1
2	Underlying event observables and measurement strategy	2
3	The ATLAS detector	3
4	Data and simulated event samples	3
5	Event and track selection	4
6	Corrections and systematic uncertainties	6
6.1	Unfolding	6
6.2	Background subtraction	6
6.3	Systematic uncertainties	6
7	Unfolded observables and comparison with model predictions	10
7.1	Overview of the results	10
7.2	Differential distributions	11
7.3	Underlying event activity as a function of p_T^Z	13
7.4	Comparison with other centre-of-mass energies	14
8	Discussion and conclusion	15
	References	17

* e-mail: atlas.publications@cern.ch

1 Introduction

A typical proton–proton (pp) collision studied at the LHC consists of a short-distance hard-scattering process and accompanying activity collectively termed the underlying event (UE). The hard-scattering processes have a momentum transfer sufficiently large that the strong coupling constant is small and the cross-section may be calculated perturbatively in quantum chromodynamics (QCD). The driving mechanisms for the production of the UE are at a much lower momentum scale. These mechanisms include partons not participating in the hard-scattering process (beam remnants), radiation processes and additional hard and semi-hard scatters in the same pp collision, termed multiple parton interactions (MPI). Phenomenological models are required to describe these processes using several free parameters determined from experiment. In addition to furthering the understanding of the proton’s internal structure and the related soft-QCD processes, accurate modelling of the UE is crucial for many data analyses at a hadron collider, either to precisely determine Standard Model quantities or to search for new particles and interactions.

The UE is not distinguishable from the hard scatter on an event-by-event basis. However, there are observables which are sensitive to the UE properties, as first introduced by the CDF Collaboration in proton–antiproton ($p\bar{p}$) collisions at a centre-of-mass energy of 1.8 TeV [1]. An example of such an observable can be defined by topological considerations, based on the activity measurement in the direction transverse¹ to a reference object.

¹ ATLAS uses a right-handed coordinate system with its origin at the nominal interaction point (IP) in the centre of the detector and the z-axis along the beam pipe. The x-axis points from the IP to the centre of the LHC ring, and the y-axis points upwards. Cylindrical coordinates (r, ϕ) are used in the transverse plane, ϕ being the azimuthal angle around the z-axis. The pseudorapidity is defined in terms of the polar angle θ as $\eta = -\ln \tan(\theta/2)$. Angular distance is measured in units of $\Delta R \equiv \sqrt{(\Delta\eta)^2 + (\Delta\phi)^2}$.

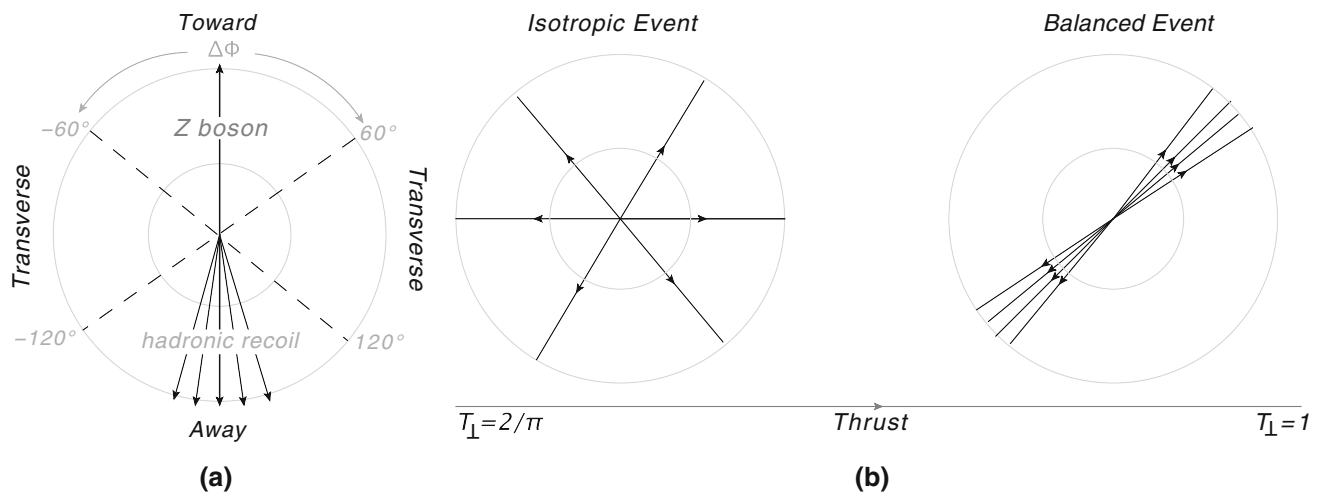


Fig. 1 **a** Illustration of away, transverse, and towards regions in the transverse plane defined relative to the direction of the Z boson. **b** Illustration of an isotropic and a balanced event topology in the transverse

plane with their corresponding values of thrust T_{\perp} . In these figures, the beams are travelling perpendicular to the plane of the page

The object in the event with the leading transverse momentum relates the UE activity to the scale of the momentum transfer in the hard interaction. In general, processes with leptonic final states like Drell–Yan events are experimentally clean and theoretically well understood, allowing reliable identification of the particles from the UE. The absence of QCD final-state radiation (FSR) permits a study of different kinematic regions with varying transverse momenta of the Z boson due to harder or softer initial-state radiation (ISR).

Previous measurements of distributions sensitive to the properties of the UE in Drell–Yan events were performed in pp collisions at a centre-of-mass energy of 7 TeV by the ATLAS [2] and CMS [3] Collaborations and at a centre-of-mass energy of 13 TeV by the CMS Collaboration [4]. Both measurements at $\sqrt{s} = 7$ TeV verified that the dependence of the UE activity on the dimuon invariant mass is qualitatively well described by the POWHEG+PYTHIA8 and Herwig++ sets of tuned parameters but with some significant discrepancies. Reference [2] provides distributions which are sensitive to the choice of parameters used in the various UE models.

This paper presents distributions of four observables sensitive to the UE in events containing a Z boson produced in pp collisions at a centre-of-mass energy of 13 TeV in the ATLAS detector at the LHC, where the singly produced Z boson decays into $\mu^+\mu^-$. Observables measured as a function of the transverse momentum of the Z boson, p_{T}^Z , in various regions of phase space are compared with predictions from several Monte Carlo (MC) event generators.

2 Underlying event observables and measurement strategy

Events containing two muons originating from the decay of a singly produced Z boson form a particularly interesting sample for studying the UE. The final-state Z boson is well-identified and colour neutral, so that interaction between the final-state leading particle and the UE is minimal. Gluon radiation from the quarks or gluons initiating the hard scatter are, however, an important consideration as these give the remainder of the event a non-zero transverse momentum and change the kinematics of the final-state. Observables are therefore measured in different regions of the transverse plane, which are defined relative to the direction of the Z boson as illustrated in Fig. 1.

A charged particle lies in the *away* region if its azimuthal angle relative to the Z boson direction $|\Delta\phi|$ is greater than 120° . This region is heavily dominated by the hadronic recoil against the Z boson from initial state quark/gluon radiation and is therefore not particularly sensitive to the UE. The *toward* ($|\Delta\phi| \leq 60^\circ$) and *transverse* ($60^\circ < |\Delta\phi| \leq 120^\circ$) regions contain less contamination from the hard process after subtraction of the two muons from the Z boson. The transverse region is sensitive to the UE because, by construction, it is perpendicular to the direction of the Z boson and hence is expected to have a lower level of activity from the hard-scattering process than the away region. The two *transverse* regions are differentiated on an event-by-event basis by their scalar sum of charged-particle p_T . The one with the larger sum is labelled *trans-max* and the other *trans-min* [5,6]. The trans-min region is highly sensitive to the UE activity because it is less likely that activity from recoiling jets leaks into this region.

Four distributions are studied to understand the UE activity. The first is the charged-particle transverse momentum $dN_{\text{ch}}/dp_{\text{T}}^{\text{ch}}$ distribution inclusive over all selected particles. The final spectrum for this variable is accumulated over all events and then normalized. The next three are evaluated on an event-by-event basis: the charged-particle multiplicity $dN_{\text{ev}}/d(N_{\text{ch}}/\delta\eta\delta\phi)$, the scalar sum of the transverse momentum of those particles $dN_{\text{ev}}/d(\Sigma p_{\text{T}}/\delta\eta\delta\phi)$, and the mean transverse momentum $dN_{\text{ev}}/d(\text{mean } p_{\text{T}})$, where mean p_{T} is the quotient of Σp_{T} and N_{ch} (provided $N_{\text{ch}} > 0$ in the corresponding region). The distributions of these variables are produced separately for charged particles lying in each of the regions described above. The charged-particle multiplicity and the scalar sum of transverse momenta are normalized relative to the area of the corresponding region in the η - ϕ space. This simplifies the comparison of the activity in different regions. The distributions are distinguished in different ranges of the Z boson transverse momentum p_{T}^Z and for two regions of transverse thrust T_{\perp} [7]. Transverse thrust characterizes the topology of the tracks in the event and is

$$T_{\perp} = \frac{\sum_i |\vec{p}_{\text{T},i} \cdot \hat{n}|}{\sum_i |\vec{p}_{\text{T},i}|}. \quad (1)$$

The thrust axis \hat{n} is the unit vector which maximizes T_{\perp} . Here the summation is done on an event-by-event basis over the transverse momenta p_{T} of all charged particles except the two muons. Transverse thrust has a maximum value of 1 for a pencil-like dijet topology and a minimum value of $2/\pi$ for a circularly symmetric distribution of particles in the transverse plane, as illustrated in Fig. 1. As proposed in Ref. [8], events with lower values of T_{\perp} are more sensitive to the MPI component of the UE. The two regions of thrust examined in this paper are $T_{\perp} < 0.75$ and $T_{\perp} \geq 0.75$, which are optimized to distinguish extra jet activity from the actual UE activity. A measurement of transverse thrust in combination with the UE activity was done at $\sqrt{s} = 7$ TeV [9], but it did not distinguish the transverse regions.

In this paper, all measurements are also performed inclusively in T_{\perp} . In total, the spectra of the four observables are measured in 96 regions of phase space, i.e. in eight bins of p_{T}^Z ; in the away, toward, trans-max, and trans-min regions; and for low, high, and inclusive T_{\perp} . The bin boundaries in p_{T}^Z are (0, 10, 20, 40, 60, 80, 120, 200, 500) GeV. In addition to distributions of the four observables, the arithmetic means $\langle N_{\text{ch}} \rangle$, $\langle \Sigma p_{\text{T}} \rangle$, and $\langle \text{mean } p_{\text{T}} \rangle$ are evaluated as functions of p_{T}^Z in each of the various regions of phase space.

3 The ATLAS detector

The ATLAS detector [10–12] at the LHC covers nearly the entire solid angle around the collision point. It consists of an

inner tracking detector (ID) surrounded by a thin superconducting solenoid, electromagnetic and hadronic calorimeters, and a muon spectrometer (MS) incorporating three large superconducting toroid magnets.

The ID is immersed in a 2 T axial magnetic field and provides charged-particle tracking in the range $|\eta| < 2.5$. A high-granularity silicon pixel detector typically provides four measurements per track and is surrounded by a silicon microstrip tracker (SCT), which usually provides four three-dimensional measurement points per track. These silicon detectors are complemented by a transition radiation tracker, which enables radially extended track reconstruction up to $|\eta| = 2.0$.

The MS comprises separate trigger and precision tracking chambers which measure the deflection of muons in a magnetic field generated by superconducting air-core toroids. The precision chamber system covers the region $|\eta| < 2.7$ with three layers of monitored drift tubes, complemented by cathode-strip chambers in the forward region, where the background is highest. The muon trigger system covers the range $|\eta| < 2.4$ with resistive-plate chambers in the barrel and thin-gap chambers in the endcap regions.

A two-level trigger system is used to select interesting events [13]. The level-1 trigger is implemented in hardware and uses a subset of the muon spectrometer and calorimeter information to reduce the event rate to around 100 kHz. This is followed by a software-based trigger which runs offline reconstruction algorithms and reduces the event rate to approximately 1 kHz.

4 Data and simulated event samples

Data recorded in 2015 with the ATLAS detector at the LHC in proton–proton collisions at a centre-of-mass energy of 13 TeV are used in this analysis. The data set corresponds to an integrated luminosity of 3.2 fb^{-1} . Only events recorded when the detector was fully operational are considered.

Simulated MC events are used both to estimate the contamination from background processes in data and to correct the measured data for detector inefficiency and resolution effects (Sect. 6.1).

The $Z \rightarrow \mu\mu$ signal process was simulated using the next-to-leading-order POWHEG [14, 15] event generator with the CT10 set of parton distribution functions (PDFs) [16] and interfaced to the PYTHIA 8.170 event generator [17, 18] to simulate the parton shower, hadronization and UE with the CTEQ6L1 PDF set and the AZNLO set of tuned parameters [19]. The latter option tunes the event generator to the p_{T}^Z measurement at $\sqrt{s} = 7$ TeV [19]. Hence, it retunes the overall UE activity by adjusting the PYTHIA MPI cut-off parameter to the UE activity of the previous measurement [2] in the lowest p_{T}^Z bin (0 to 5 GeV). PHOTOS [20] was used to simulate

Table 1 A summary of the fiducial volume definition of the measurement, the particle-level definition, and the main observables. The first row lists selection criteria for the signal muons (indicated with a μ

Fiducial volume (for muon selection)	$p_T^\mu > 25 \text{ GeV}, \eta < 2.4, 66 \text{ GeV} < m^{\mu\mu} < 116 \text{ GeV}$
Particle-level definition	$p_T > 0.5 \text{ GeV}, \eta < 2.5, \text{charge} \neq 0, \text{stable (i.e. a proper lifetime of } c\tau > 10 \text{ mm)}$

final-state electromagnetic radiation. The PYTHIA generator uses p_T -ordered parton showers and a hadronization model based on the fragmentation of colour strings. Its MPI model interleaves the ISR and FSR emissions with MPI scatters.

An alternative signal sample used for cross-checks and systematic uncertainty evaluations was simulated using SHERPA 2.2.0 [21], which has an independent implementation of the parton shower, hadronization, UE and FSR. The SHERPA samples utilize the NNPDF30NNLO PDF set [22] and were generated with the nominal tune set of version 2.2.0. The SHERPA generator uses leading-order matrix elements with a model for MPI similar to that of PYTHIA 8 but without interleaving the FSR. It implements a cluster hadronization model similar to that of Herwig++. SHERPA and PYTHIA impose the infrared cut-off for MPI as a smooth function. In contrast, Herwig++ implements it as a step function. A signal sample produced with the MC generator Herwig++ [23] using the UE-EE-5 tune [24] provided by the generator's authors and the corresponding CTEQ6L1 PDF set is compared with unfolded data in Sect. 7. This tuning uses energy extrapolation and was developed to describe the UE and double parton interaction effective cross-section. Herwig++ uses, similarly to PYTHIA, a leading-logarithm parton shower model matched to leading-order matrix element calculations, but it implements a cluster hadronization scheme with parton showering ordered by emission angle.

Three sources of background are estimated using MC samples: $Z \rightarrow \tau\tau$, $WW \rightarrow \mu\nu\mu\nu$, and the $t\bar{t}$ process, each of which was simulated using POWHEG [25,26] interfaced to PYTHIA8 or PYTHIA6 for $t\bar{t}$. The PYTHIA tune set for $Z \rightarrow \tau\tau$ and $WW \rightarrow \mu\nu\mu\nu$ is the same as was used for the signal process (AZNLO). The Perugia 2012 [27] tune set was used for simulation of the $t\bar{t}$ process.

Overlaid MC-generated minimum-bias events [28] simulate the effect of multiple interactions in the same bunch crossing (pile-up). These samples were produced with PYTHIA 8 using the A2 tune set [29] in combination with the MSTW2008LO PDF set. The A2 tune set was matched to the ATLAS minimum-bias measurement at $\sqrt{s} = 7 \text{ TeV}$ [30]. The mean number of interactions per bunch crossing (μ) during the 2015 data-taking with 25 ns bunch spacing was 13.5. The simulated samples are reweighted to reproduce the

as superscript) limited by the detector geometry, while the cut on the dimuon invariant mass $m^{\ell\ell}$ yields a low background contamination

distribution of the number of interactions per bunch crossing observed in the data.

The GEANT4 [31] program simulated the passage of particles through the ATLAS detector. Differences in muon reconstruction, trigger, and isolation efficiencies between MC simulation and data are evaluated using a tag-and-probe method [32], and the simulation is corrected accordingly. Additional factors applied to the MC events correct for the description of the muon energy and momentum scales and resolution, which are determined from fits to the observed Z boson line shapes in data and MC simulations [32]. Finally, correction factors adjust the distribution of the longitudinal position of the primary pp collision vertex [33] to the one observed in the data.

5 Event and track selection

Candidate $Z \rightarrow \mu\mu$ events are selected by requiring that at least one out of two single-muon triggers be satisfied. A high-threshold trigger requires a muon to have $p_T > 40 \text{ GeV}$, whilst a low-threshold trigger requires $p_T > 20 \text{ GeV}$ and the muon to be isolated from additional nearby tracks. All events are required to have a primary vertex (PV). The PV is defined as the reconstructed vertex in the event with the highest Σp_T of the associated tracks, consistent with the beam-spot position (spatial region inside the detector where collisions take place) and with at least two associated tracks with $p_T > 400 \text{ MeV}$.

The main selections to define the regions of phase space are summarized in Table 1. The reconstruction procedure for muon candidates combines tracks reconstructed in the inner detector with tracks reconstructed in the MS [32]. The reconstructed muons are required to have $p_T > 25 \text{ GeV}$ and $|\eta| < 2.4$. Track quality requirements are imposed to suppress backgrounds, and the muon candidate is required to be isolated using a p_T - and η -dependent 'gradient' isolation criterion [32] based on track and calorimeter information. Muon candidates consistent with having originated from the decay of a heavy quark are rejected by requiring the significance of the transverse impact parameter ($|d_0/\sigma(d_0)|$, with d_0 representing the transverse impact parameter and $\sigma(d_0)$ the related uncertainty) to be below 3. Furthermore, the muon candidates must be associated to the PV, i.e. the longitudi-

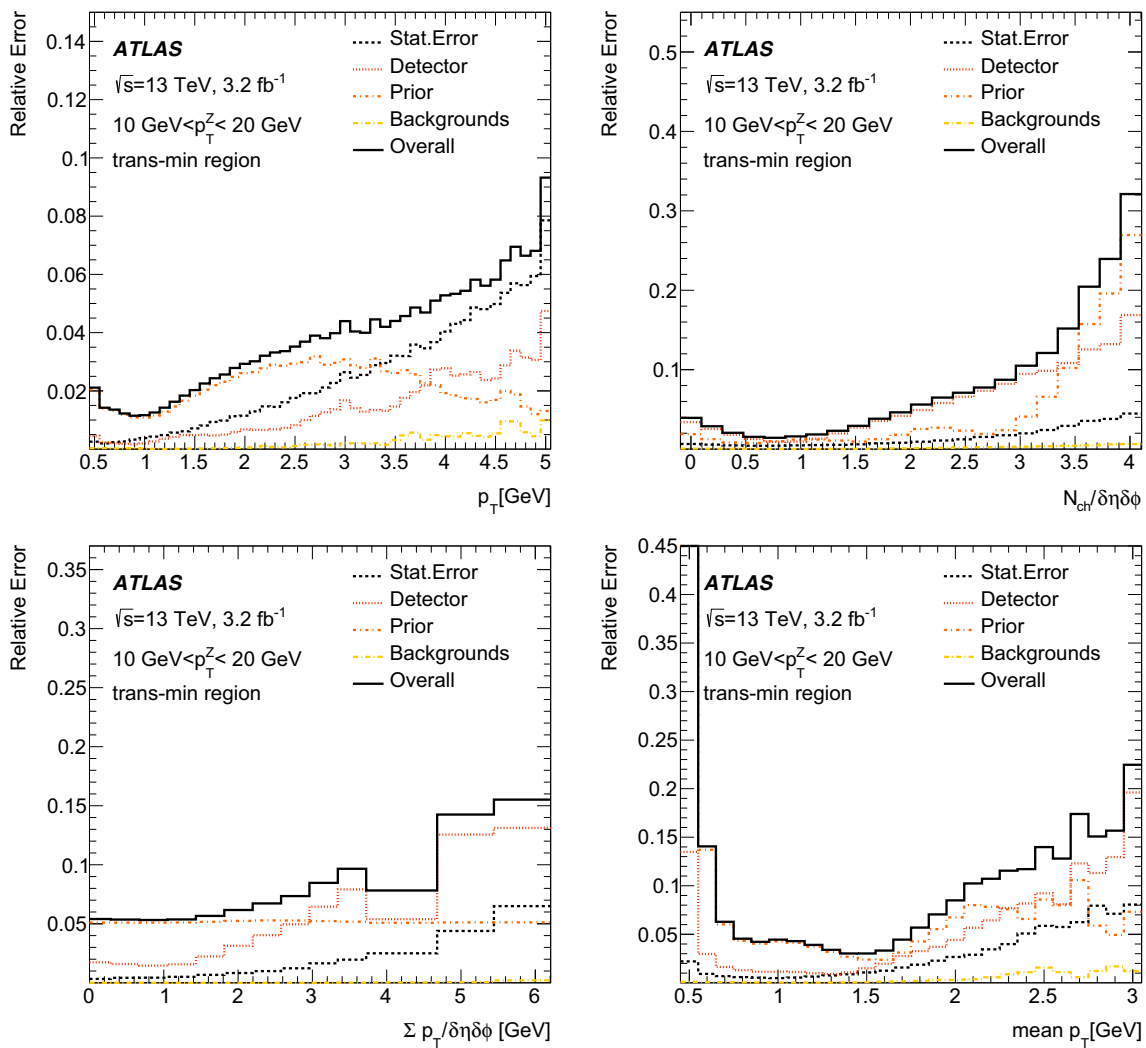


Fig. 2 Breakdown of systematic uncertainties in the p_T spectrum (upper left), the charged-particle multiplicity (N_{ch} , upper right), the scalar sum of the transverse momenta (Σp_T , lower left) and the mean transverse momentum (mean p_T , lower right) for events with $10 < p_T^Z$

< 20 GeV in the trans-min region inclusively in T_{\perp} . Here ‘Prior’ combines the two approaches to estimate the unfolding-related uncertainties. ‘Detector’ includes the modelling of the detector and the pile-up conditions

nal ($|z_0 \sin \theta|$) impact parameter is less than 0.5 mm. The variables d_0 and z_0 are measured relative to the PV.

Events are required to have exactly two opposite-charged muons satisfying the selection criteria above. The invariant mass of the dimuon system must be between 66 GeV and 116 GeV.

Tracks reconstructed in the ID from the passage of charged particles are used to form the UE observables. Each reconstructed track is required to have $p_T > 0.5$ GeV, $|\eta| < 2.5$, one hit in the innermost layer is required (if expected) and in total at least one hit in the pixel detector and at least six hits in the SCT. The tracks must have been assigned to the PV, i.e. the transverse and longitudinal impact parameters of the tracks relative to the PV must be smaller than 2 mm and 1.5 mm respectively. An additional requirement on the qual-

ity of the fit of the track to the hits in the detector applies to tracks with $p_T > 10$ GeV in order to suppress mismeasured tracks at high p_T . This criterion affects mainly the tracks associated with the muon candidates and has little impact on the predominantly low- p_T tracks of the UE activity.

The kinematics of the Z boson and of the charged particles in the event define the phase space of the fiducial region (particle level). This closely reflects the selection made on measured detector quantities outlined before. Simulated events are required to have two prompt muons that satisfy $p_T > 25$ GeV and $|\eta| < 2.4$ with each muon defined at the ‘bare’ level (after final-state QED radiation). The measurements are all reported in bins of p_T^Z , the results presented in this paper are not sensitive to the predicted shape of the p_T^Z spectrum, even though they are sensitive to jet activity in

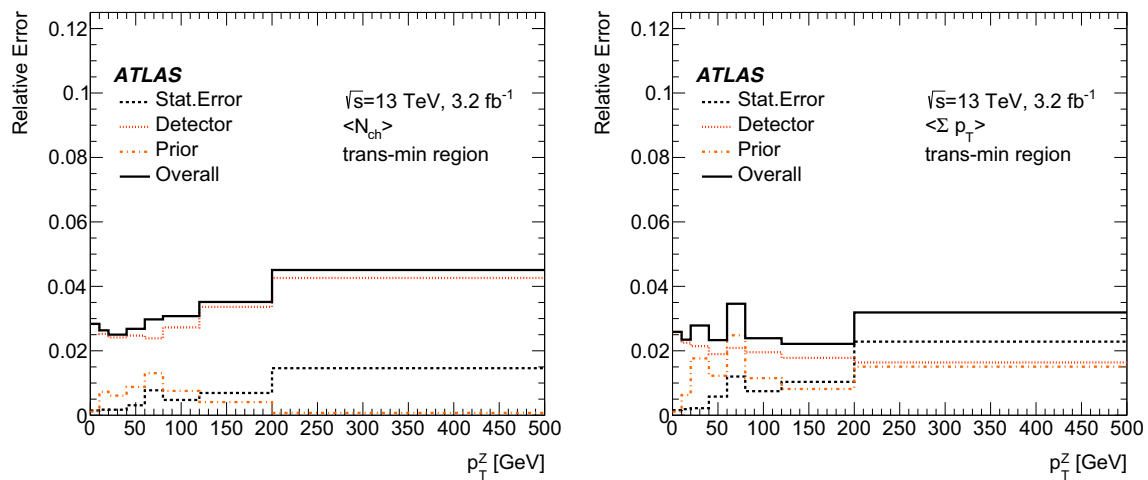


Fig. 3 A summary of the systematic uncertainties in the arithmetic mean of the N_{ch} and Σp_T spectra in the trans-min region as a function of p_T^Z . Here ‘Prior’ combines the two approaches to estimate the unfolding-related uncertainties. ‘Detector’ includes the modelling of the detector and the pile-up conditions

the event. As a cross-check the observables are constructed as defined before but the muons are unfolded to the ‘dressed’ level (i.e. collinear QED FSR is added to the ‘bare’ level muons) similar to the previous UE measurement in Z events [2]. The difference between the results after unfolding to different generator levels is below the percent level and is less than the uncertainty related to the unfolding procedure. Charged particles must be stable, i.e. have a proper lifetime with $c\tau > 10$ mm, with $p_T > 0.5$ GeV and $|\eta| < 2.5$.

The statistical uncertainties of the data and the MC simulations are propagated using the bootstrap method [34]. While the statistical error of the data is the limiting factor for all distributions at high p_T^Z , it does not limit the measurements in phase-space regions of lower p_T^Z , which are particularly important for tuning MC simulations.

6 Corrections and systematic uncertainties

6.1 Unfolding

An iterative Bayesian unfolding technique is used to correct the data for detector inefficiencies and resolution [35–37]. Response matrices connect each observable at the detector and particle levels; these are constructed using the POWHEG+PYTHIA8 signal MC sample which is overlaid with pile-up events at detector level. Each response matrix corresponds to a bin of p_T^Z or thrust, with the migration of events between p_T^Z or thrust bins corrected using a per-bin purity correction factor. In the context of MC simulations, the purity of one bin is defined as the fraction of events that are reconstructed in the same bin as the original particle level quantity. The bin intervals in p_T^Z and thrust are chosen to yield high purities (> 0.9 for the bins in p_T^Z and > 0.85 for

the two bins in T_{\perp}) enabling the per-bin corrections. For the observable $dN_{\text{ch}}/dp_T^{\text{ch}}$, two unfolding iterations are sufficient for convergence of the unfolding results, while for all other observables eight iterations are performed. The evaluation of the mean value of each observable in a bin of p_T^Z and thrust occurs after unfolding. The bin boundaries are the same at both the detector and particle levels.

6.2 Background subtraction

The background contributions to the selected data from the $Z \rightarrow \tau\tau$, $t\bar{t}$, and $WW \rightarrow \mu\nu\mu\nu$ processes are estimated using MC simulations. In total, these are about 0.7% of selected data events. This fraction varies from 0.9% for the lowest bin in p_T^Z to the per mille level for the highest p_T^Z bin. The background contribution from multijet processes is estimated using a data-driven technique based on the isolation and charge of the two reconstructed muons, similar to previous analyses [2]. The size of the multijet contribution in the data is less than 0.1%. The unfolding of the data is done after the subtraction of all MC and data-driven background estimates.

6.3 Systematic uncertainties

Systematic uncertainties can arise due to possible mismodelling of the muon momentum scale or resolution, as well as the reconstruction, identification, and isolation efficiencies. Furthermore, limited knowledge of the ID material distribution [38] dominates the uncertainties in the track reconstruction inefficiencies. Also the effect of falsely reconstructed tracks (when there is no corresponding charged particle) contributes to all observables.

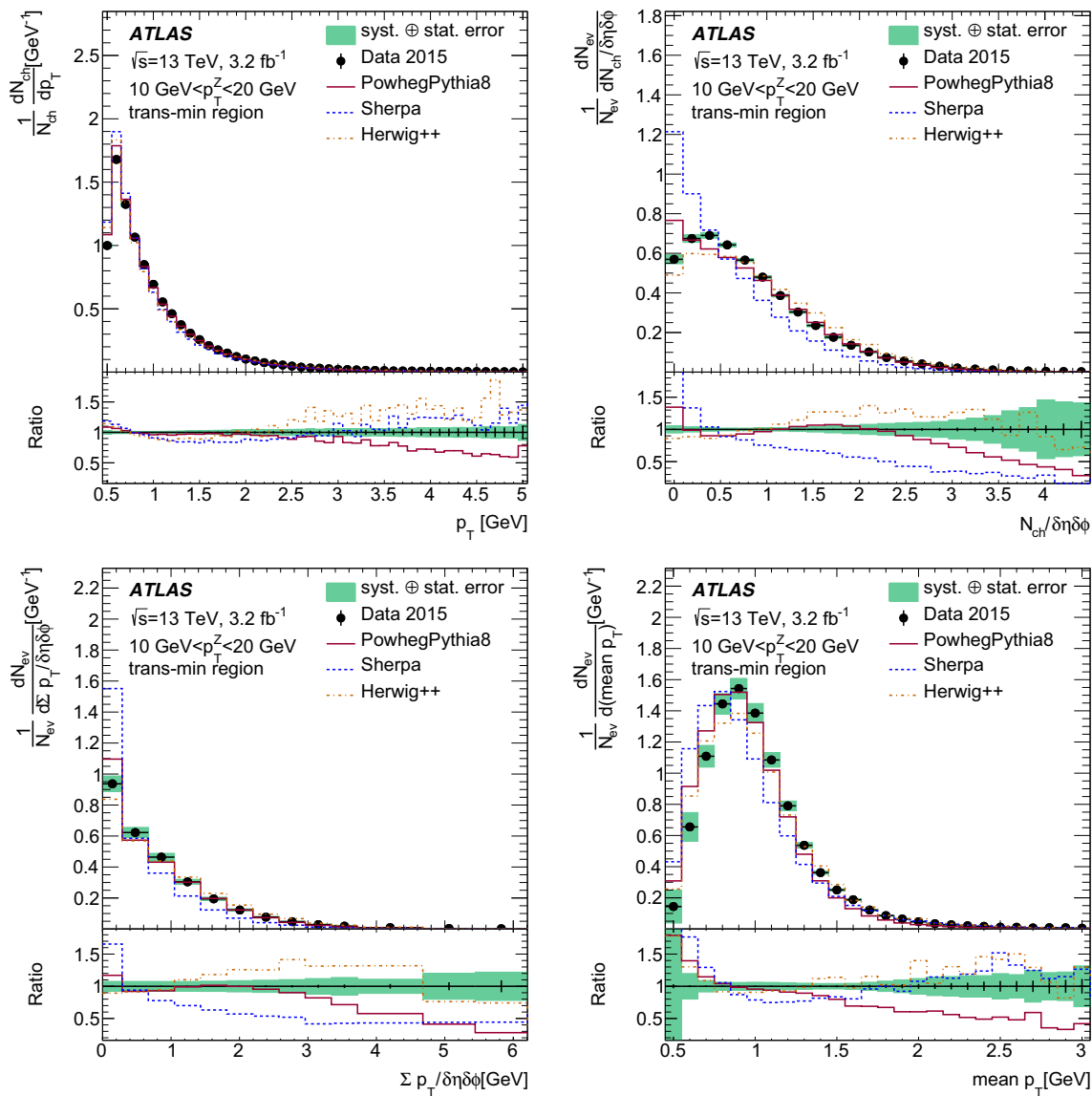


Fig. 4 Measured spectra of p_T (upper left), the charged-particle multiplicity, N_{ch} (upper right), the scalar sum of the transverse momentum of those particles, Σp_T , (lower left) and the mean transverse momentum, mean p_T (lower right) in the trans-min region inclusively in T_{\perp}

for events with $10 < p_T^Z < 20$ GeV. Predictions of POWHEG+PYTHIA, SHERPA and Herwig++ are compared with the data. The ratios shown are predictions over data

All uncertainties related to imperfect modelling of the detector are assessed using MC simulations. The data are first unfolded using the nominal MC simulation samples. Then the data are unfolded with MC samples where the parameter of the simulation which is affected by the mismodelling is varied by $\pm 1\sigma$ of its estimated uncertainty. The average of the up and down shifts is assigned as the corresponding systematic uncertainty.

Since the observables are primarily track-based, the track-related systematic uncertainties dominate the total detector-related uncertainty. These are of the order of 2% regardless of the observable and region. Systematic uncertainties related

to the muon reconstruction are a negligible fraction of the overall uncertainty.

Uncertainties due to mismodelling of the background processes are also considered. For the background processes modelled with MC simulations, the electroweak background normalization is varied by $\pm 5\%$ and the $t\bar{t}$ background normalization by $\pm 15\%$ (approximately within their theoretical uncertainties [39,40]) and the effect on the final measurements is estimated. The full effect of including the multijet background or not is taken as an uncertainty. The combined background-related uncertainties form a negligible fraction of the total systematic uncertainty. The dependence of the

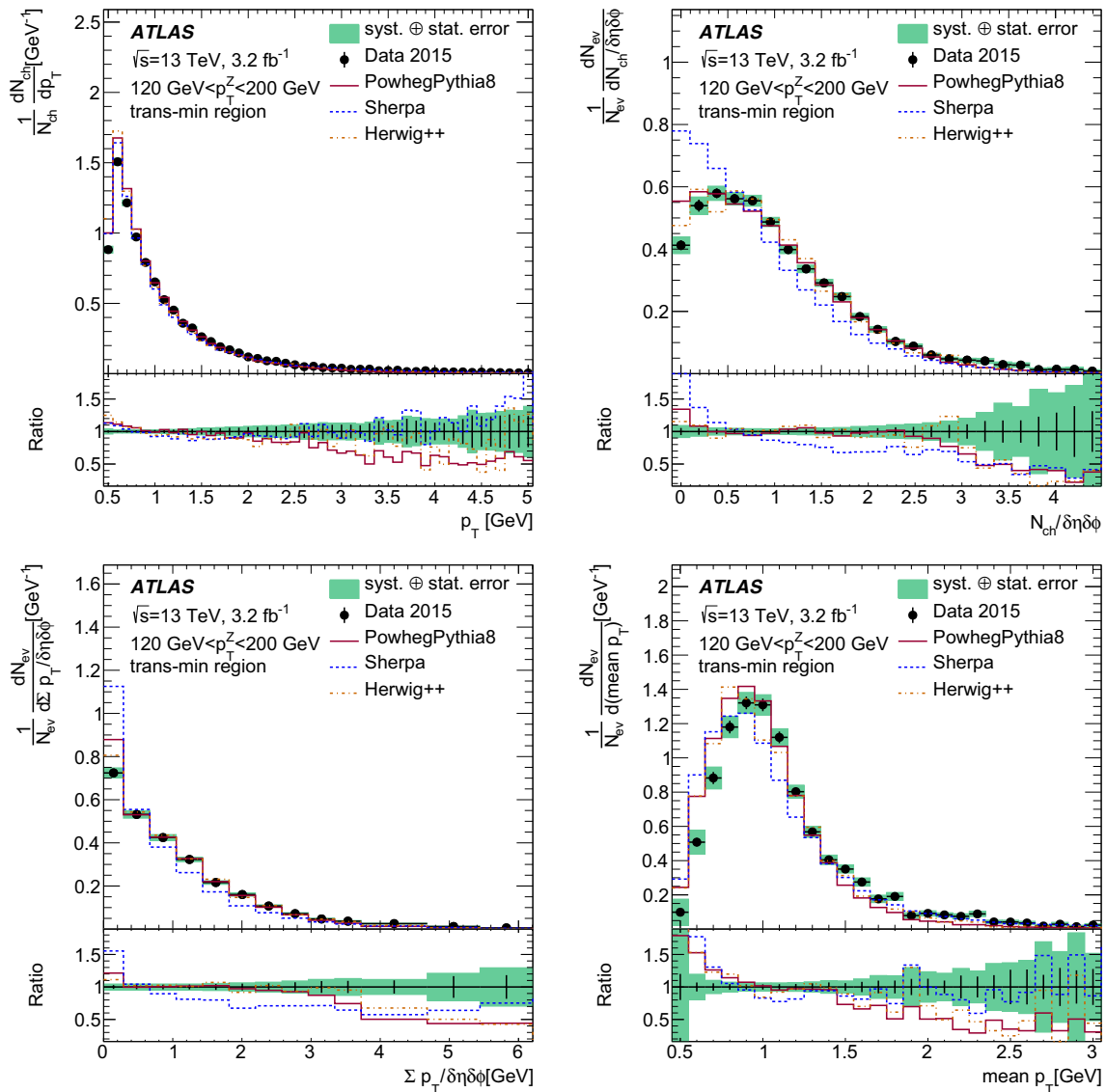


Fig. 5 Measured p_T spectra (upper left), the charged-particle multiplicity N_{ch} (upper right), the scalar sum of the transverse momentum of those particles Σp_T (lower left), and the mean transverse momentum, mean p_T (lower right) in the trans-min region inclusively in T_{\perp} for

events with $120 < p_T^Z < 200$ GeV. Predictions of POWHEG+PYTHIA, SHERPA, and Herwig++ are compared with the data. The ratios shown are predictions over data

background uncertainty on p_T^Z is negligible for this measurement.

An important consideration for these measurements is the modelling of the pile-up, since the MC simulations must correct for contamination from pile-up tracks through the unfolding procedure. When averaging over all simulated events about 13% of the selected tracks which are compatible with the primary vertex originate from pile-up.

A variation in the pile-up reweighting of the MC simulations is included to cover the uncertainty on the ratio between the predicted and measured inelastic cross-section in the fiducial volume defined by $M_X > 13$ GeV where M_X is the mass of the hadronic system [41]. The value of $\langle \mu \rangle$ assumed in the

MC simulations for the unfolding process is varied by $\pm 9\%$ from the nominal value. This uncertainty in the pile-up modelling is one of the largest sources of systematic uncertainty in the tails of the distributions of p_T , N_{ch} , Σp_T , and mean p_T , and for the mean distributions. The uncertainties related to the inaccuracies of the detector and pile-up modelling are combined and referred to as the ‘Detector’ uncertainty in the following figures.

Two additional cross-checks validate the pile-up modelling and the consistency of removing the pile-up effects via the unfolding technique. First, the unfolding procedure for all observables in all measurement bins is repeated for three intervals of $\langle \mu \rangle$, namely [8–10], [11–13] and [14–16].

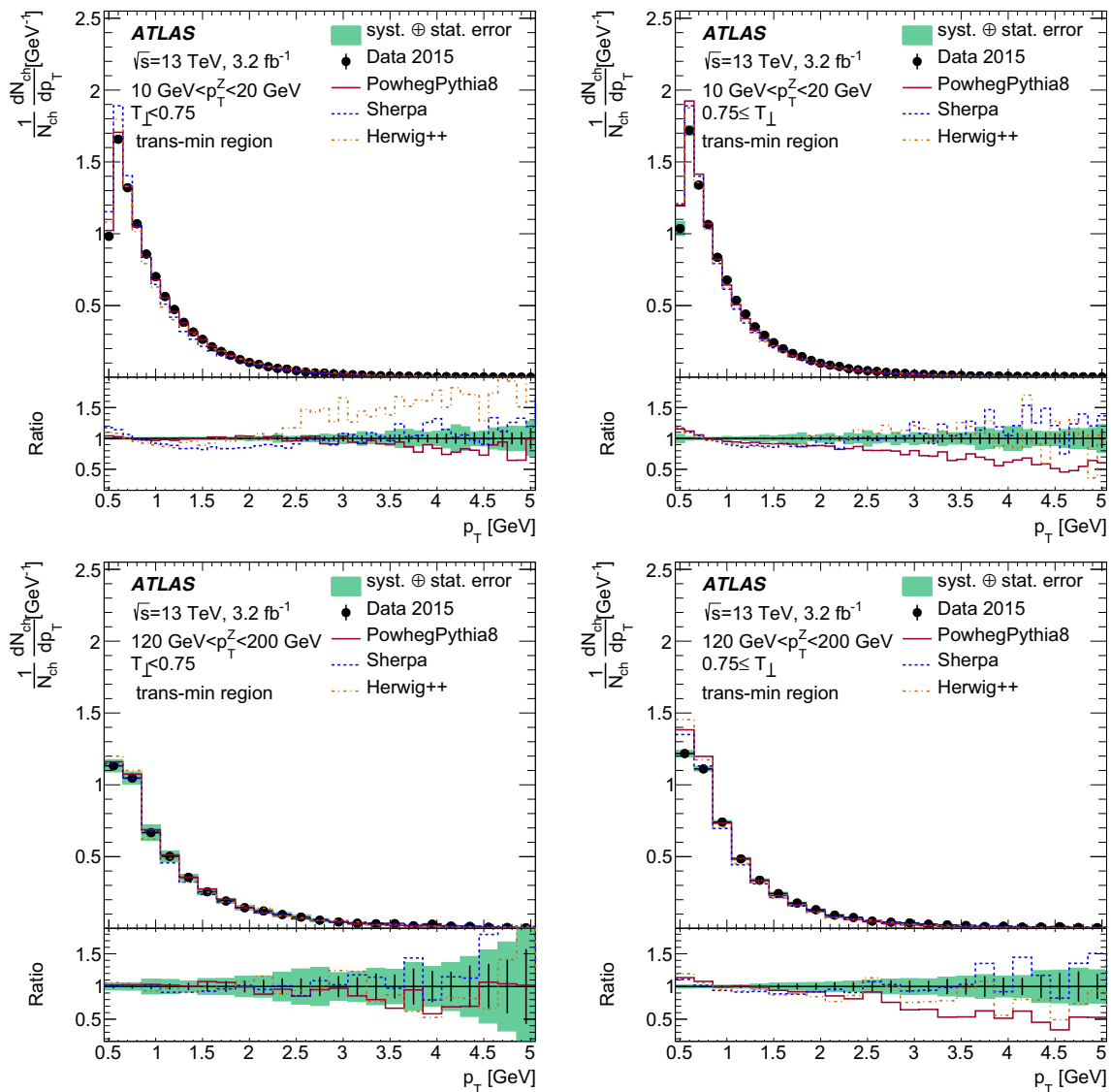


Fig. 6 Measured p_T spectra in the trans-min region for $T_{\perp} < 0.75$ (left) and $0.75 \leq T_{\perp}$ (right) for events with $10 < p_T^Z < 20$ GeV (upper row) and $120 < p_T^Z < 200$ GeV (lower row). Predictions of

POWHEG+PYTHIA, SHERPA, and Herwig++ are compared with the data. The ratios shown are predictions over data

A mismodelling of pile-up in MC simulations would manifest itself less in the interval of $8 \leq \langle \mu \rangle \leq 10$ and more in the interval of $14 \leq \langle \mu \rangle \leq 16$. The unfolded results for the three intervals are found to be fully compatible within their associated statistical uncertainties, confirming the consistency of the handling of pile-up in the unfolding process.

Secondly, a complementary data-driven technique based on the *Hit Backspace Once More* (HBOM) method [42] is used. The intention is to reproduce pile-up contaminations as realistically as possible. Hence, the track information associated with non-primary vertices in the data is bundled to form a pile-up library. A random sample is drawn from this library and used as an example of pile-up effects in data. If this random sample is added to an individual event, the pile-up effect

increases. A sampling of the library is subsequently used to pollute events with additional pile-up. Six iterations of pollution are applied, i.e. up to six random samples from the pile-up library are added to each event. Then the observables are constructed from these additionally contaminated events. Assuming the values of the observables evolve smoothly with each iteration of additional pile-up, an extrapolation in each bin to the value with zero pile-up vertices yields the HBOM estimate of pile-up subtracted data. The data are subsequently unfolded using a version of the POWHEG+PYTHIA signal MC samples without pile-up vertices. The results obtained using this method are consistent with the nominal procedure, and no additional uncertainty is assigned.

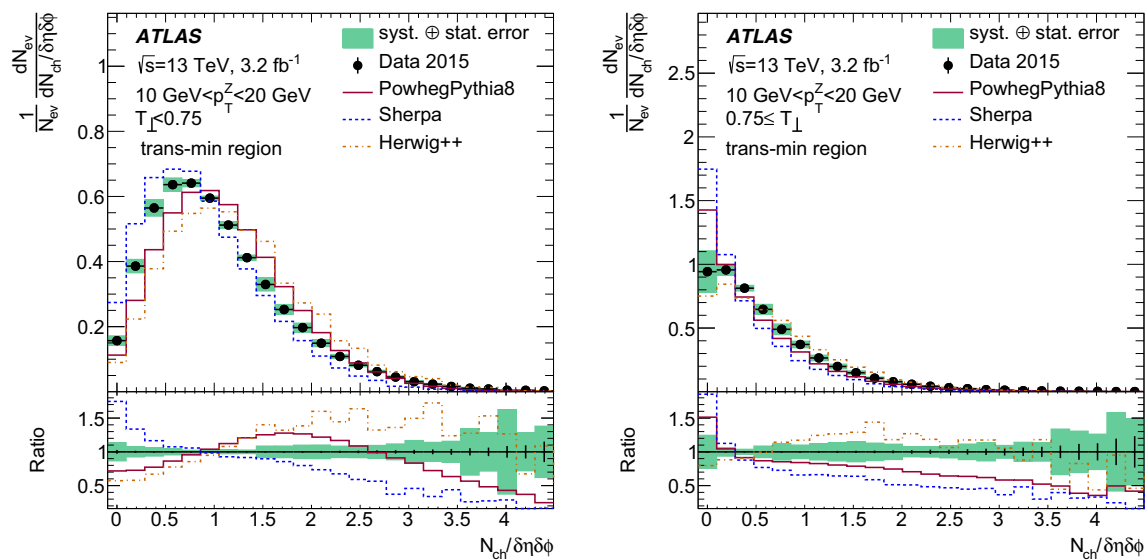


Fig. 7 Measured number of charged particles in the trans-min region for $T_{\perp} < 0.75$ (left) and $0.75 \leq T_{\perp}$ (right) for events with $10 < p_T^Z < 20$ GeV. Predictions of POWHEG+PYTHIA, SHERPA, and Herwig++ are compared with the data. The ratios shown are predictions over data

The uncertainty associated with the unfolding technique is evaluated using a data-driven method. It accounts for the dependence of the unfolding on the usage of prior knowledge from the MC simulation, i.e. the particle level quantities. The ratio of data to simulation at detector-level is evaluated and smoothed for each observable. The smoothed ratio is then used to reweight the simulations by applying the event-weight according to the particle level quantity. The reweighted detector-level distribution is then unfolded using the regular response matrix. The relative difference between the reweighted particle-level distribution and the reweighted and unfolded detector-level distribution is treated as a systematic uncertainty. This dependence on prior knowledge from the MC simulation is the dominant systematic uncertainty in most distributions at lower values of p_T^Z . An additional method of estimating the uncertainty related to the unfolding is to unfold the detector-level MC distributions generated with SHERPA using the unfolding matrices based on the POWHEG+PYTHIA MC sample. The results are compared with the particle level quantities predicted by SHERPA. After taking the uncertainty due to the MC prior into account, a slight discrepancy between the unfolded SHERPA sample and the particle-level distributions remains. Therefore, an additional contribution to the MC prior uncertainty is introduced to cover this remaining non-closure of the unfolded result and the SHERPA generator level. In general, it does not exceed the 2–4% level and is smoothed over the full range of the observable. In a few cases, this non-closure component dominates the MC prior uncertainty. These two separate unfolding uncertainties are added in quadrature in all figures.

All sources of systematic uncertainty are considered uncorrelated and are combined in quadrature. The MC prior uncertainty is one of the largest contributors to the total sys-

tematic uncertainty at all values of p_T and in each p_T^Z region. The statistical uncertainty of the data rises with increasing p_T^Z , contributing a significant fraction of the overall uncertainty. The breakdown of the individual sources of uncertainties for the four observables, p_T , N_{ch} , Σp_T , and mean p_T is illustrated in Fig. 2 for the example of events with $10 < p_T^Z < 20$ GeV in the trans-min region (the region most sensitive to the UE), inclusively in T_{\perp} .

Figure 3 shows the systematic uncertainties in the arithmetic mean of the N_{ch} and Σp_T spectra in the trans-min region as a function of p_T^Z inclusively in T_{\perp} . The largest contributions to the total systematic uncertainties of the mean distributions at all p_T^Z values come from either the MC prior uncertainty or the track-related uncertainties. The statistical uncertainties of the data become large for p_T^Z greater than around 200 GeV.

7 Unfolded observables and comparison with model predictions

7.1 Overview of the results

Distributions of p_T , N_{ch} , Σp_T , and mean p_T are obtained in slices of p_T^Z for the different regions defined in the transverse plane and different regions of T_{\perp} . The results for N_{ch} and Σp_T are normalized relative to the area of the region in η and ϕ . In addition to the measurements in slices of p_T^Z , the arithmetic means of N_{ch} , Σp_T , and mean p_T ($\langle N_{\text{ch}} \rangle$, $\langle \Sigma p_T \rangle$, and $\langle \text{mean } p_T \rangle$) are measured as a function of p_T^Z . Only a selection of the most relevant results is discussed in this section: the comparison of the unfolded data to the predictions of different MC generators focuses on the trans-min region.

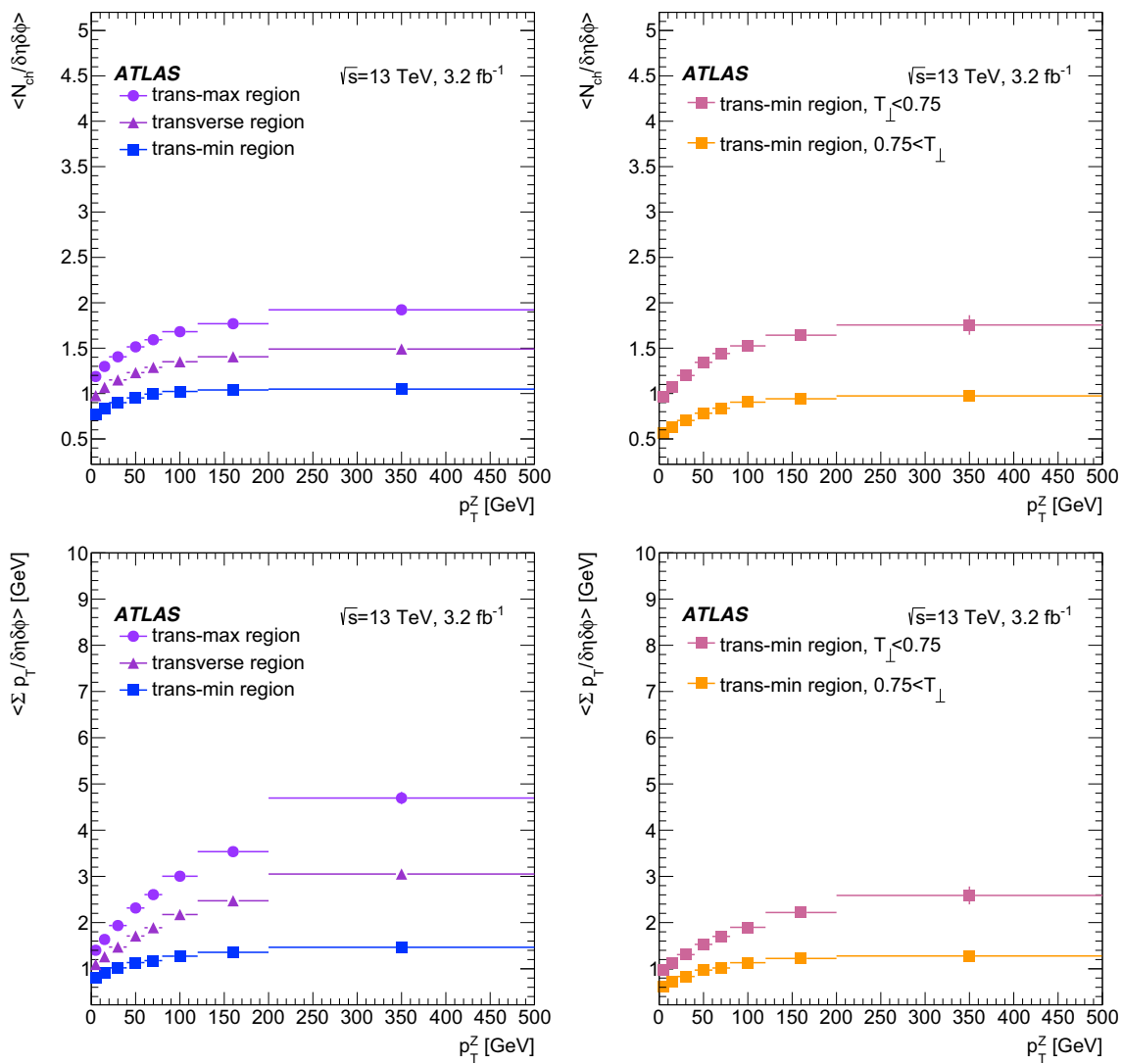


Fig. 8 The mean number of charged particles (upper row) and the mean of the scalar sum of the transverse momentum of those particles (lower row) per unit η - ϕ space as a function of p_T^Z in the full transverse region

While the toward region provides insights of similar importance for tuning MC generators after having removed the two muons, the discussion focuses on the trans-min region to better facilitate comparison with previous measurements. The UE activity in the toward region is higher compared with that in trans-min. This is expected since the trans-min region is defined as the subregion of the transverse region with the lower activity and for $Z \rightarrow \mu\mu$ events the UE activity is expected to be of similar magnitude in the toward and transverse regions. The trans-min region is statistically less affected by radiation and it is essentially the region where the contribution from ISR is subtracted. Apart from this difference in the amount of activity, the predictive performance of the different MC generators is comparable in the toward and trans-min regions. No significant difference in the predictive power between these regions is observed. Both $\langle N_{ch} \rangle$ and

and for the trans-min and trans-max regions inclusively in T_{\perp} (left) and in the trans-min region separated in T_{\perp} (right)

$\langle \Sigma p_T \rangle$ measured in the trans-min are compared with previous measurements of the UE in Z boson events at lower centre-of-mass energies.

7.2 Differential distributions

Figures 4 and 5 show the unfolded p_T spectrum, N_{ch} , Σp_T , and mean p_T for the trans-min region inclusively in T_{\perp} for events with p_T^Z between 10 and 20 GeV and between 120 and 200 GeV. The predictions from POWHEG+PYTHIA, SHERPA, and Herwig++ are compared with the data. The ratio of prediction to data is shown beneath each plot. None of the tested MC generators describes all aspects of the data well and in some regions the differences exceed the 70% level. Generally, the MC generators predict a higher number of particles with small p_T than is observed in data (see top left of Figs. 4,

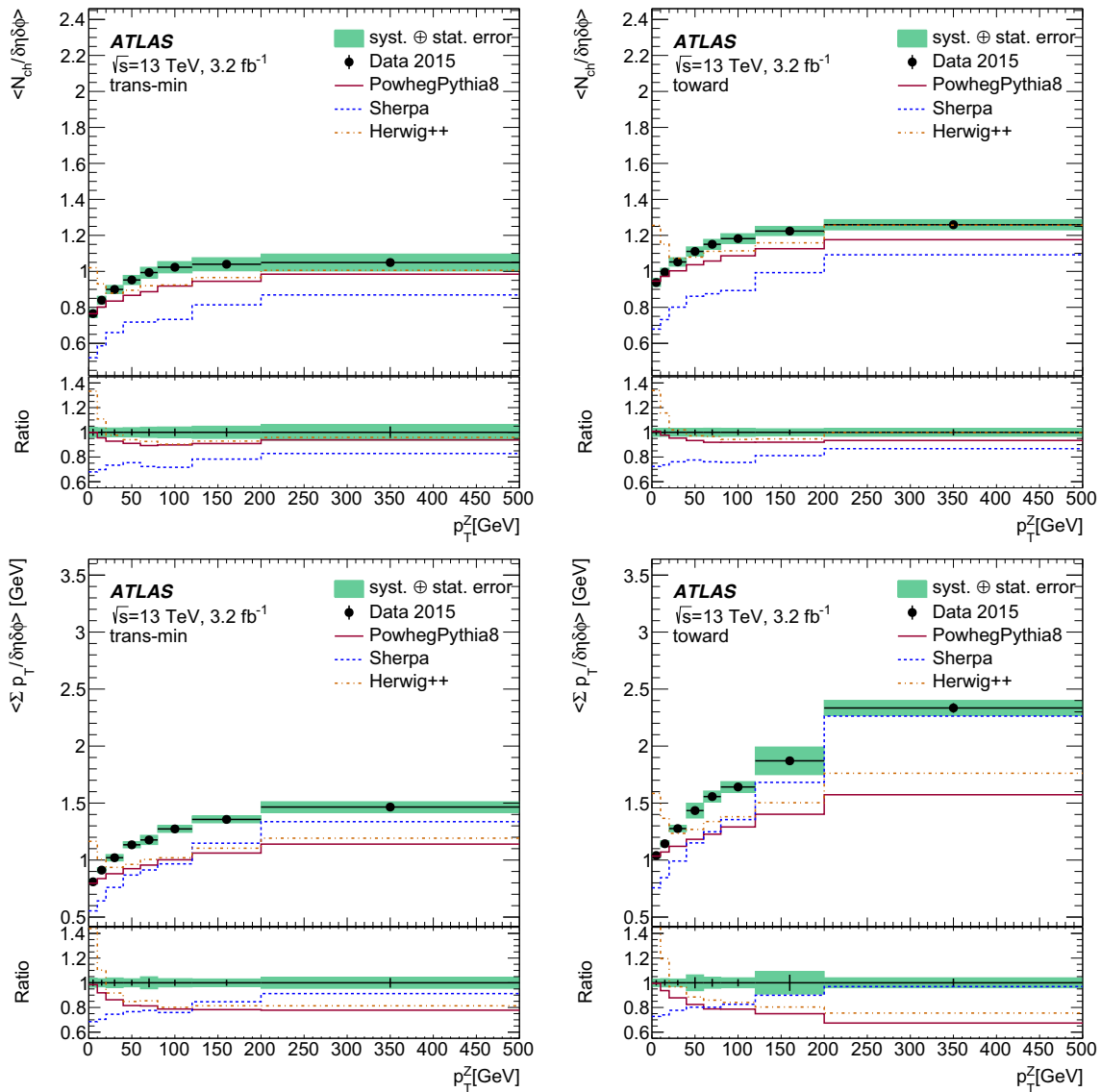


Fig. 9 Comparison of measured arithmetic means of the N_{ch} (upper row) and Σp_T (lower row) as functions of p_T^Z for the trans-min (left) and towards (right) region inclusively in T_\perp . Predictions of

POWHEG+PYTHIA, SHERPA and Herwig++ are compared with the data. The ratios shown are predictions over data

5). This is consistent with the MC predictions tending to lower values of mean p_T , as is shown on the lower right plots of Figs. 4 and 5. The largest differences between data and simulation are at low N_{ch} and low Σp_T , and arise due to the steeper transverse momentum spectrum of charged particles in MC simulations. POWHEG+PYTHIA and SHERPA predict a higher fraction of events with fewer charged particles and a consistently smaller sum of p_T . However, Herwig++ slightly overestimates the fraction of particles with $p_T > 2.5$ GeV and is qualitatively closer to the shape of the distributions of N_{ch} and Σp_T . With rising p_T^Z , the data p_T spectrum becomes harder, and N_{ch} , Σp_T , and mean p_T increase. The relative discrepancy remains the same in comparisons with the generator predictions.

The dependence on T_\perp is illustrated in Fig. 6 for the unfolded p_T spectrum in the trans-min region for events with $10 < p_T^Z < 20$ GeV and $120 < p_T^Z < 200$ GeV. Similar to the results for the measurement inclusive in T_\perp , the MC generators predict a higher fraction of particles with low p_T than present in data. The predictions of POWHEG+PYTHIA are closer to the measured distributions in the lower p_T^Z region, but SHERPA describes better the full p_T range in the higher p_T^Z bin. The Herwig++ simulations have significant statistical fluctuations at higher p_T . The most striking difference between the different regions in T_\perp is observed for the POWHEG+PYTHIA generator when focusing on the low p_T^Z bins for N_{ch} as presented in Fig. 7. In MPI-sensitive regions (left plot in Fig. 7) the distribution of

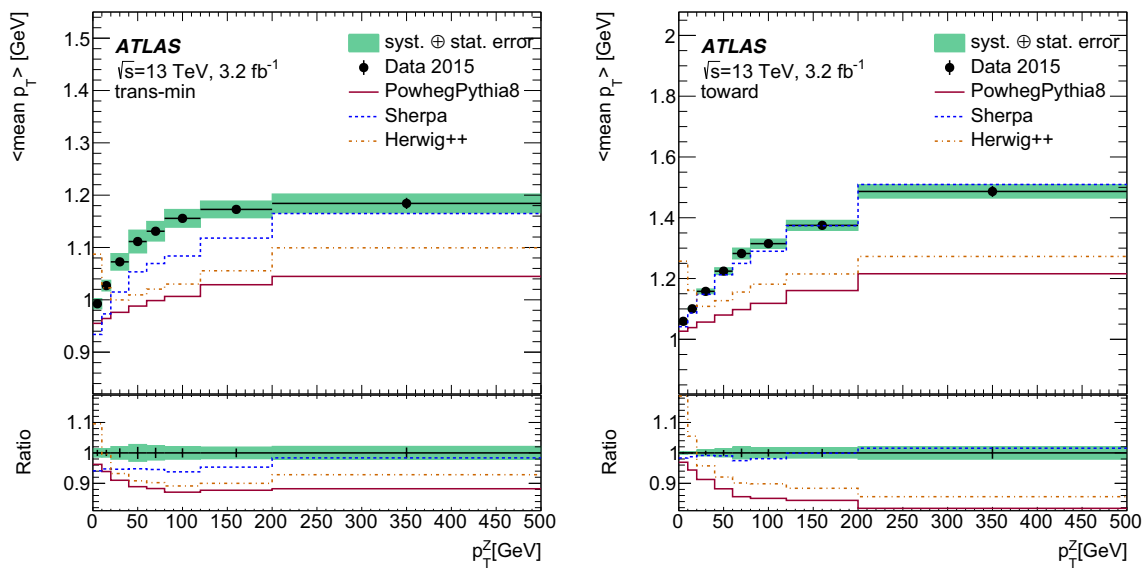


Fig. 10 Comparison of measured arithmetic means of mean p_T as functions of p_T^Z for the trans-min (left) and towards (right) regions inclusively, and in regions of T_\perp . Predictions of POWHEG+PYTHIA, SHERPA,

and Herwig++ are compared with the data. The ratios shown are predictions over data

N_{ch} by POWHEG+PYTHIA is shifted towards higher numbers of charged-particles relative to the data, i.e. overshooting the data in the range $1 \leq N_{ch}/\delta\eta\delta\phi \leq 2.5$. But in the high thrust region (right plot) the MC generator underestimates the data almost over the full range except for the first two bins. In contrast, the performances of SHERPA and Herwig++ are consistent when comparing the low and high thrust regions for N_{ch} ; Herwig++ overestimates N_{ch} , and SHERPA underestimates it. The same effect is observed for the distributions of Σp_T but is less significant and therefore not presented. As pointed out in Ref. [8], the regions of high values of T_\perp are dominated by extra jet activity which is not adequately modelled in POWHEG+PYTHIA, as shown in the right plots in Figs. 6 and 7.

7.3 Underlying event activity as a function of p_T^Z

Figure 8 shows the mean number of charged particles and the mean of the scalar sum of the transverse momenta of those particles per unit $\eta-\phi$ space as a function of p_T^Z in the transverse, trans-min, and trans-max regions inclusively in T_\perp . The trans-min region is further separated by T_\perp in the right plots of Fig. 8. In the trans-min region, the UE-sensitive variables N_{ch} and Σp_T rise slowly with increasing Z boson transverse momentum. In contrast, the observables in the trans-max region have a strong dependence on p_T^Z . This is because it is heavily contaminated with the Z boson hadronic recoil leaking into the transverse region. The slope of the UE activity in the trans-min region as a function of p_T^Z for events of high T_\perp is similar to the inclusive measurement. The total amount of activity measured in the trans-min region for events with high T_\perp is lower than the inclusive measure-

ment due to the correlation of activity in the transverse region and T_\perp . Furthermore, the right-hand plots of Fig. 8 demonstrate that the UE activity is higher for events with lower T_\perp , as expected [8]. Lower values of T_\perp also increase the dependence on p_T^Z in the trans-min region.

The MC modelling of individual measurements in all 96 phase-space regions is further investigated by comparing the measured arithmetic means of the N_{ch} , Σp_T , and mean p_T as functions of p_T^Z . Figures 9 and 10 show comparisons with the predictions of POWHEG+PYTHIA, SHERPA, and Herwig++ for the trans-min and towards regions inclusively in T_\perp . The predictions fail to describe the data in either of the regimes. For $p_T^Z > 20$ GeV, Herwig++ predicts a slower rise in UE activity with rising p_T^Z than in the measured distributions. On the other hand, POWHEG+PYTHIA and SHERPA qualitatively describe the ‘turn-on’ effect of the UE activity, i.e. a steeper slope at low p_T^Z which vanishes at higher values of p_T^Z . For POWHEG+PYTHIA, the rise of the UE activity is underestimated, and hence the discrepancy with data grows with p_T^Z and stabilizes around $p_T^Z = 100$ GeV. Only in the toward region of the mean of the mean p_T is SHERPA in good agreement with the data.

The p_T^Z dependence for the two regions of T_\perp in the trans-min region is summarized in Figs. 11 and 12. In the low T_\perp region, the prediction by SHERPA improves, e.g. for N_{ch} the discrepancy shrinks from about 30% to roughly 10%. Referring to the same observable, POWHEG+PYTHIA is in agreement with data for $p_T^Z > 80$ GeV in the low T_\perp regime within the uncertainties. For the selection on high T_\perp all generators underestimate the UE activity. SHERPA provides the best description of the data in $\langle \text{mean } p_T \rangle$. Apart from the toward

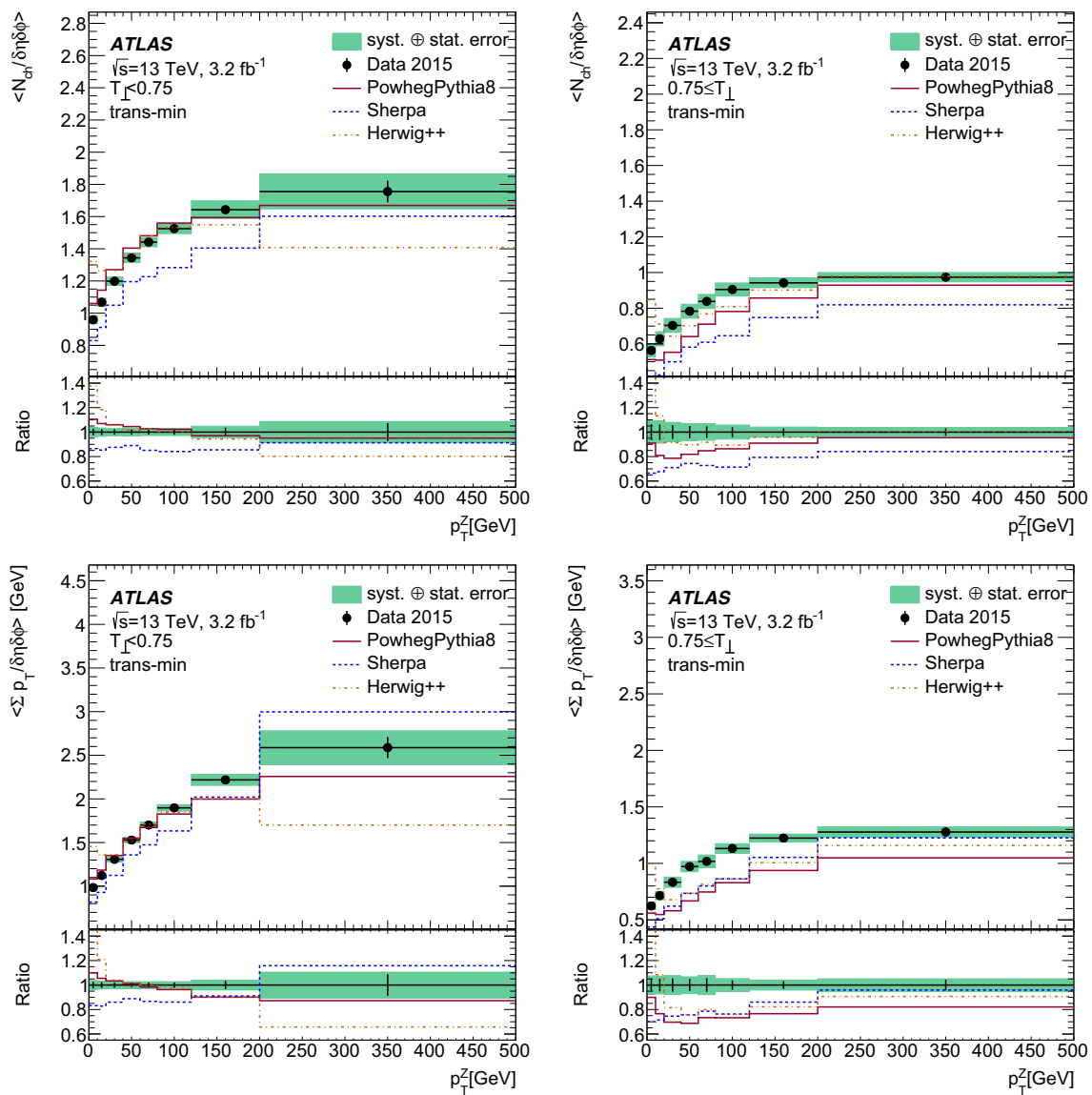


Fig. 11 Comparison of measured arithmetic means of the N_{ch} (upper row) and Σp_T (lower row) as functions of p_T^Z for $T_\perp < 0.75$ (left) and $0.75 \leq T_\perp$ (right) for the trans-min region. Predictions of

POWHEG+PYTHIA, SHERPA, and Herwig++ are compared with the data. The ratios shown are predictions over data

region, it tends to a constant underestimation but agrees with the overall shape. The agreement of POWHEG+PYTHIA with data is better for $T_\perp < 0.75$ than for the inclusive measurement. The predictions of Herwig++ in the trans-min region improve with higher values of p_T^Z and also in events of lower T_\perp . However, the discrepancy between Herwig++ and the data in the lowest bins remains regardless of the selected region.

7.4 Comparison with other centre-of-mass energies

Figure 13 presents a comparison of the measured $\langle N_{ch} \rangle$ and $\langle \Sigma p_T \rangle$ for different centre-of-mass energies. The results for $\sqrt{s} = 7$ TeV are taken from the previous ATLAS measure-

ment of the UE activity in Z boson events [2]. The event selection criteria are similar to the analysis presented in this paper, but the previous measurement also includes the $Z \rightarrow e^+e^-$ channel. The CDF measurements at $\sqrt{s} = 1.96$ TeV [43] are also included in the comparison. The CDF analyses used Drell–Yan lepton pairs in a smaller invariant mass window ($70 < m_{\mu\mu} < 110$ GeV) in $p\bar{p}$ collisions. The relative uncertainties of the two ATLAS measurements are of similar sizes, while the CDF measurements have large statistical fluctuations for $p_T^{Z/\mu\mu} > 30$ GeV. All three measurements show qualitatively the same behaviour, i.e. a growing UE activity with higher values of p_T^Z . With higher centre-of-mass energies, more energy is available for the processes forming the

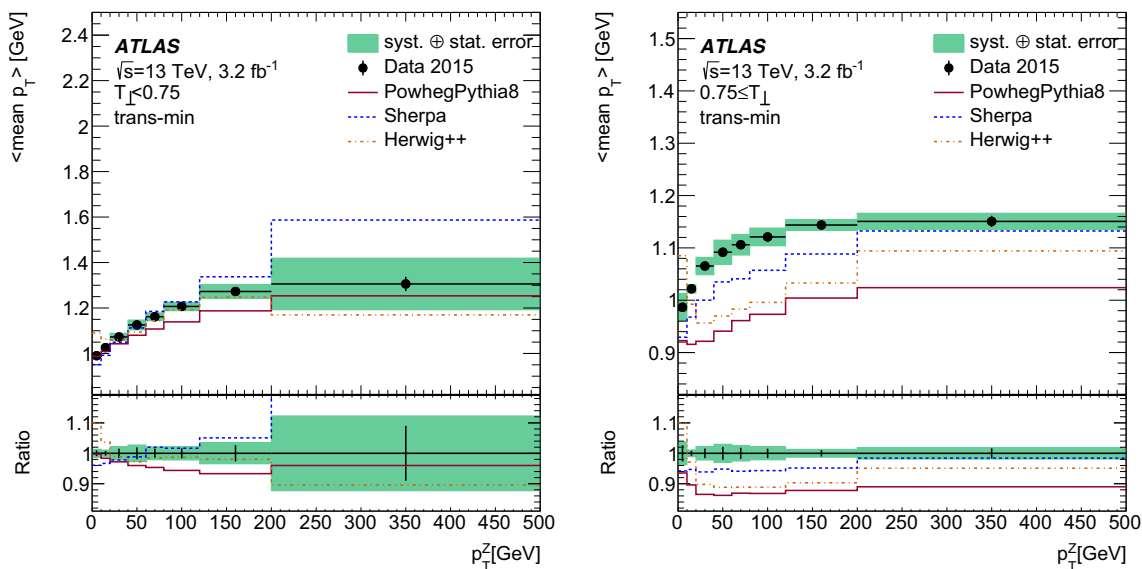


Fig. 12 Comparison of the measured arithmetic mean of mean p_T as a function of p_T^Z for ranges of T_\perp in the trans-min region. Predictions of POWHEG+PYTHIA, SHERPA, and Herwig++ are compared with the data. The ratios shown are predictions over data

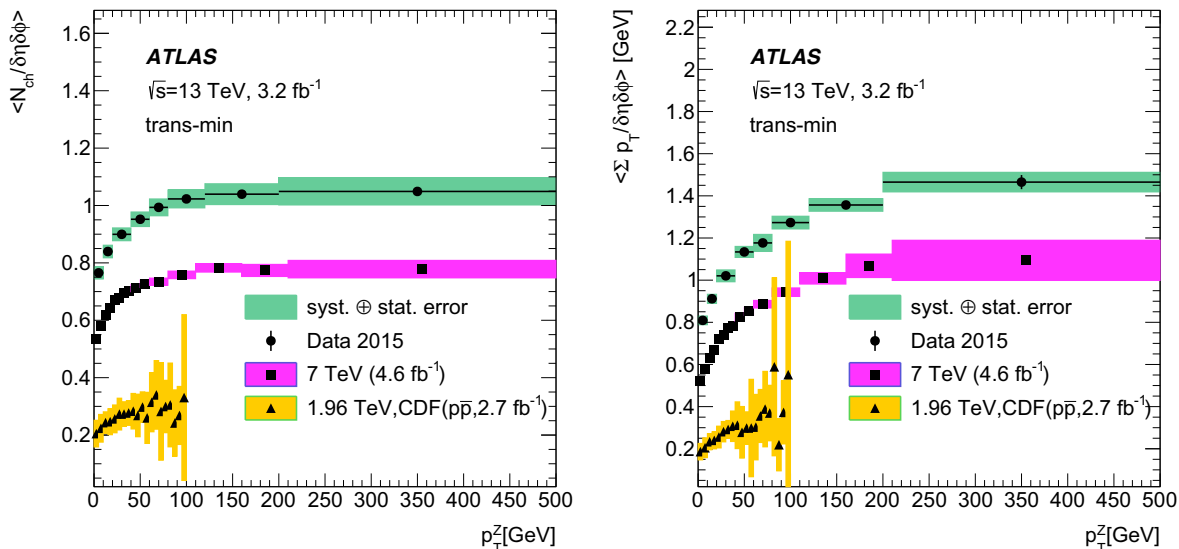


Fig. 13 The distributions of $\langle N_{ch} \rangle$ and $\langle \sum p_T \rangle$ measured at $\sqrt{s} = 13$ TeV compared with the results of the previous ATLAS measurements at $\sqrt{s} = 7$ TeV [2] and the CDF measurements at $\sqrt{s} = 1.96$ TeV [43].

The error bars correspond to the full uncertainties of the corresponding measurement

UE e.g. MPI. Hence, the rise of the UE activity as a function of \sqrt{s} is expected.

8 Discussion and conclusion

Measurements of four observables sensitive to the activity of the UE in $Z \rightarrow \mu\mu$ events are presented using 3.2 fb^{-1} of $\sqrt{s} = 13$ TeV pp collision data collected with the ATLAS detector at the LHC in 2015. Those observables are the p_T of charged particles, the number of charged particles per event (N_{ch}), the

sum of charged-particle p_T per event ($\sum p_T$), and the mean of charged-particle p_T per event (mean p_T). They are measured in intervals of the Z boson p_T and in different azimuthal regions of the detector relative to the Z boson direction. The arithmetic means of the distributions are plotted as functions of the Z boson p_T , inclusively of and in regions of transverse thrust.

The predictions from three Monte Carlo generators (POWHEG+PYTHIA8, SHERPA and Herwig++) are compared with the data. In general, all tested generators and tunes show significant deviations from the data distributions regardless

of the observable. The arithmetic means of the observables deduced from the predictions of POWHEG+PYTHIA8 and SHERPA match the main features of the UE activity in the fiducial region. The turn-on effect, i.e. the rising activity as a function of the hard-scatter scale (here p_T^Z), is visible as a saturation of this effect for higher values of p_T^Z . In contrast to the other generators, Herwig++ fails to reproduce the turn-on effect at low p_T^Z as it predicts that the UE activity decreases as a function of p_T^Z when considered only in the $p_T^Z < 20$ GeV region. Otherwise, all generators underestimate the activity of the UE when quantified as the arithmetic mean of the observables for inclusive T_\perp . The generators predict the mean values better in comparison with the data when focusing on the MPI-sensitive regions. POWHEG+PYTHIA8 is in agreement with data within the uncertainties for $\langle N_{\text{ch}} \rangle$ and $\langle \Sigma p_T \rangle$, indicating an adequate handling of the MPI activity. However, since the predictive power shrinks for the region with $T_\perp \geq 0.75$ in comparison with the inclusive measurement, the simulation of contributions other than MPI to the UE activity needs to be improved. Reference [8] points out that the region with $T_\perp > 0.75$ is dominated by extra jet activity, giving a first indication for a possible improvement of the MC generator prediction. This conclusion is valid when focusing on POWHEG+PYTHIA8 for different regions of T_\perp for individual bins of p_T^Z .

In comparison with the measurements at $\sqrt{s} = 7$ TeV [2], the performance of Herwig++ is consistent for $p_T^Z > 20$ GeV. Both measurements use the energy-extrapolation tunes [24] provided by the Herwig++ authors, i.e. UE-EE-3 for $\sqrt{s} = 7$ TeV and in the analysis presented here UE-EE-5. The latter tune was additionally validated against Tevatron and LHC measurements at $\sqrt{s} = 900$ GeV and $\sqrt{s} = 7$ TeV [44]. The prediction of Herwig++ is slightly better for the distributions of $\langle N_{\text{ch}} \rangle$ and $\langle \Sigma p_T \rangle$ at higher values of p_T^Z . In the previous measurements, the divergence increased with p_T^Z , which might be related to improper modelling of the impact parameter. Apart from overestimating the mean activity, Herwig++ improved relative to the $\sqrt{s} = 7$ TeV measurements in the description of the shape of $dN_{\text{ev}}/d(\Sigma p_T/\delta\eta\delta\phi)$, $dN_{\text{ev}}/d(\text{mean } p_T)$, and $dN_{\text{ev}}/d(N_{\text{ch}}/\delta\eta\delta\phi)$ in the presented p_T^Z -bins. Qualitatively it performs better than the other generators.

POWHEG+PYTHIA8 performs as well at $\sqrt{s} = 13$ TeV as it does at $\sqrt{s} = 7$ TeV, but is tuned with AU2 (only the MPI part was tuned by ATLAS using $\sqrt{s} = 7$ TeV UE data) in the previous measurements. Nevertheless, this indicates that the MPI energy extrapolation of PYTHIA8 works well, which is in agreement with the better description for distributions at low T_\perp .

In contrast, while at $\sqrt{s} = 7$ TeV SHERPA version 1.4.0 with the CT10 PDF set consistently overestimates the UE activity metrics $\langle N_{\text{ch}} \rangle$ and $\langle \Sigma p_T \rangle$ by 5% to 15%, the present analysis and SHERPA version reveal a continuous underesti-

mation. At $\sqrt{s} = 13$ TeV, the discrepancy relative to the data decreases with higher values of p_T^Z .

Acknowledgements We thank CERN for the very successful operation of the LHC, as well as the support staff from our institutions without whom ATLAS could not be operated efficiently. We acknowledge the support of ANPCyT, Argentina; YerPhI, Armenia; ARC, Australia; BMWFW and FWF, Austria; ANAS, Azerbaijan; SSTC, Belarus; CNPq and FAPESP, Brazil; NSERC, NRC and CFI, Canada; CERN; CONICYT, Chile; CAS, MOST and NSFC, China; COLCIENCIAS, Colombia; MSMT CR, MPO CR and VSC CR, Czech Republic; DNRF and DNSRC, Denmark; IN2P3-CNRS, CEA-DRF/IRFU, France; SRNSFG, Georgia; BMBF, HGF, and MPG, Germany; GSRT, Greece; RGC, Hong Kong SAR, China; ISF and Benozziyo Center, Israel; INFN, Italy; MEXT and JSPS, Japan; CNRST, Morocco; NWO, The Netherlands; RCN, Norway; MNiSW and NCN, Poland; FCT, Portugal; MNE/IFA, Romania; MES of Russia and NRC KI, Russian Federation; JINR; MESTD, Serbia; MSSR, Slovakia; ARRS and MIZŠ, Slovenia; DST/NRF, South Africa; MINECO, Spain; SRC and Wallenberg Foundation, Sweden; SERI, SNSF and Cantons of Bern and Geneva, Switzerland; MOST, Taiwan; TAEK, Turkey; STFC, UK; DOE and NSF, USA. In addition, individual groups and members have received support from BCKDF, CANARIE, CRC and Compute Canada, Canada; COST, ERC, ERDF, Horizon 2020, and Marie Skłodowska-Curie Actions, European Union; Investissements d’Avenir Labex and Idex, ANR, France; DFG and AvH Foundation, Germany; Herakleitos, Thales and Aristeia programmes co-financed by EU-ESF and the Greek NSRF, Greece; BSF-NSF and GIF, Israel; CERCA Programme Generalitat de Catalunya, Spain; The Royal Society and Leverhulme Trust, UK. The crucial computing support from all WLCG partners is acknowledged gratefully, in particular from CERN, the ATLAS Tier-1 facilities at TRIUMF (Canada), NDGF (Denmark, Norway, Sweden), CC-IN2P3 (France), KIT/GridKA (Germany), INFN-CNAF (Italy), NL-T1 (The Netherlands), PIC (Spain), ASGC (Taiwan), RAL (UK) and BNL (USA), the Tier-2 facilities worldwide and large non-WLCG resource providers. Major contributors of computing resources are listed in Ref. [45].

Data Availability Statement This manuscript has no associated data or the data will not be deposited. [Authors’ comment: All ATLAS scientific output is published in journals, and preliminary results are made available in Conference Notes. All are openly available, without restriction on use by external parties beyond copyright law and the standard conditions agreed by CERN. Data associated with journal publications are also made available: tables and data from plots (e.g. cross section values, likelihood profiles, selection efficiencies, cross section limits, ...) are stored in appropriate repositories such as HEPDATA (<http://hepdata.cedar.ac.uk/>). ATLAS also strives to make additional material related to the paper available that allows a reinterpretation of the data in the context of new theoretical models. For example, an extended encapsulation of the analysis is often provided for measurements in the framework of RIVET (<http://rivet.hepforge.org/>).” This information is taken from the ATLAS Data Access Policy, which is a public document that can be downloaded from <http://opendata.cern.ch/record/413> [opendata.cern.ch].]

Open Access This article is distributed under the terms of the Creative Commons Attribution 4.0 International License (<http://creativecommons.org/licenses/by/4.0/>), which permits unrestricted use, distribution, and reproduction in any medium, provided you give appropriate credit to the original author(s) and the source, provide a link to the Creative Commons license, and indicate if changes were made. Funded by SCOAP³.

References

1. CDF Collaboration, Charged jet evolution and the underlying event in $p\bar{p}$ collisions at 1.8 TeV, Phys. Rev. D **65**, 092002 (2002)
2. ATLAS Collaboration, Measurement of distributions sensitive to the underlying event in inclusive Z-boson production in pp collisions at $\sqrt{s} = 7$ TeV with the ATLAS detector. Eur. Phys. J. C **74**, 3195 (2014). [arXiv:1409.3433](#) [hep-ex]
3. CMS Collaboration, Measurement of the underlying event in the Drell–Yan process in proton–proton collisions at $\sqrt{s} = 7$ TeV. Eur. Phys. J. C **72**, 2080 (2012). [arXiv:1204.1411](#) [hep-ex]
4. CMS Collaboration, Measurement of the underlying event activity in inclusive Z boson production in proton–proton collisions at $\sqrt{s} = 13$ TeV. JHEP **07**, 032 (2018). [arXiv:1711.04299](#) [hep-ex]
5. G. Marchesini, B.R. Webber, Associated transverse energy in hadronic jet production. Phys. Rev. D **38**, 3419 (1988)
6. J. Pumplin, Hard underlying event correction to inclusive jet cross-sections. Phys. Rev. D **57**, 5787 (1998). [arXiv:hep-ph/9708464](#) [hep-ph]
7. A. Banfi, G.P. Salam, G. Zanderighi, Phenomenology of event shapes at hadron colliders. JHEP **06**, 038 (2010). [arXiv:1001.4082](#) [hep-ph]
8. D. Kar, D.S. Rafanoharana, Probing underlying event in Z-boson events using event shape observables. Int. J. Mod. Phys. A **34**, 1950022 (2018). [arXiv:1801.05218](#) [hep-ph]
9. ATLAS Collaboration, Measurement of event-shape observables in $Z \rightarrow \ell^+ \ell^-$ events in pp collisions at $\sqrt{s} = 7$ TeV with the ATLAS detector at the LHC. Eur. Phys. J. C **76**, 375 (2016). [arXiv:1602.08980](#) [hep-ex]
10. ATLAS Collaboration, The ATLAS Experiment at the CERN Large Hadron Collider. JINST **3**, S08003 (2008)
11. ATLAS Collaboration, ATLAS Insertable B-Layer Technical Design Report. ATLAS-TDR-19 (2010). <https://cds.cern.ch/record/1291633>, Addendum: ATLAS-TDR-19-ADD-1, 2012. <https://cds.cern.ch/record/1451888>. Accessed 1 Oct 2018
12. B. Abbott et al., Production and integration of the ATLAS Insertable B-Layer. JINST **13**, T05008 (2018). [arXiv:1803.00844](#) [physics.ins-det]
13. ATLAS Collaboration, Performance of the ATLAS trigger system in 2015. Eur. Phys. J. C **77**, 317 (2017). [arXiv:1611.09661](#) [hep-ex]
14. S. Alioli, P. Nason, C. Oleari, E. Re, NLO vector-boson production matched with shower in POWHEG. JHEP **07**, 060 (2008). [arXiv:0805.4802](#) [hep-ph]
15. S. Alioli, P. Nason, C. Oleari, E. Re, A general framework for implementing NLO calculations in shower Monte Carlo programs: the POWHEG BOX. JHEP **06**, 043 (2010). [arXiv:1002.2581](#) [hep-ph]
16. J. Pumplin et al., New generation of parton distributions with uncertainties from global QCD analysis. JHEP **07**, 012 (2002). [arXiv:hep-ph/0201195](#)
17. T. Sjöstrand, S. Mrenna, P.Z. Skands, PYTHIA 6.4 physics and manual. JHEP **05**, 026 (2006). [arXiv:hep-ph/0603175](#)
18. T. Sjöstrand, S. Mrenna, P.Z. Skands, A brief introduction to PYTHIA 8.1. Comput. Phys. Commun. **178**, 852 (2008). [arXiv:0710.3820](#) [hep-ph]
19. ATLAS Collaboration, Measurement of the Z/γ^* boson transverse momentum distribution in pp collisions at $\sqrt{s} = 7$ TeV with the ATLAS detector. JHEP **09**, 145 (2014). [arXiv:1406.3660](#) [hep-ex]
20. P. Golonka, Z. Was, PHOTOS Monte Carlo: a precision tool for QED corrections in Z and W decays. Eur. Phys. J. C **45**, 97 (2006). [arXiv:hep-ph/0506026](#)
21. T. Gleisberg et al., Event generation with SHERPA 1.1. JHEP **02**, 007 (2009). [arXiv:0811.4622](#) [hep-ph]
22. R.D. Ball et al., Parton distributions for the LHC Run II. JHEP **04**, 040 (2015). [arXiv:1410.8849](#) [hep-ph]
23. M. Bähr et al., Herwig++ physics and manual. Eur. Phys. J. C **58**, 639 (2008). [arXiv:0803.0883](#) [hep-ph]
24. S. Gieseke, C. Rohr, A. Siodmok, Colour reconnections in Herwig++. Eur. Phys. J. C **72**, 2225 (2012). [arXiv:1206.0041](#) [hep-ph]
25. T. Melia, P. Nason, R. Rötsch, G. Zanderighi, W+W-, WZ and ZZ production in the POWHEG BOX. JHEP **2011**, 78 (2011). [arXiv:1107.5051](#) [hep-ph]
26. S. Frixione, P. Nason, G. Ridolfi, A positive-weight next-to-leading-order Monte Carlo for heavy flavour hadroproduction. JHEP **09**, 126 (2007). [arXiv:0707.3088](#) [hep-ph]
27. P.Z. Skands, Tuning Monte Carlo generators: the Perugia tunes. Phys. Rev. D **82**, 074018 (2010). [arXiv:1005.3457](#) [hep-ph]
28. ATLAS Collaboration, The ATLAS simulation infrastructure. Eur. Phys. J. C **70**, 823 (2010). [arXiv:1005.4568](#) [physics.ins-det]
29. ATLAS Collaboration, Further ATLAS tunes of PYTHIA 6 and Pythia 8, ATL-PHYS-PUB-2011-014 (2011). <https://cds.cern.ch/record/1400677>. Accessed 15 Nov 2018
30. ATLAS Collaboration, Measurement of the jet fragmentation function and transverse profile in proton–proton collisions at a center-of-mass energy of 7 TeV with the ATLAS detector. Eur. Phys. J. C **71**, 1795 (2011). [arXiv:1109.5816](#) [hep-ex]
31. S. Agostinelli et al., GEANT4-A simulation toolkit. Nucl. Instrum. Methods A **506**, 250 (2003)
32. ATLAS Collaboration, Muon reconstruction performance of the ATLAS detector in proton–proton collision data at $\sqrt{s} = 13$ TeV. Eur. Phys. J. C **76**, 292 (2016). [arXiv:1603.05598](#) [hep-ex]
33. ATLAS Collaboration, Performance of primary vertex reconstruction in proton–proton collisions at $\sqrt{s} = 7$ TeV in the ATLAS experiment. ATLAS-CONF-2010-069 (2010). <https://cds.cern.ch/record/1281344>. Accessed 15 Nov 2018
34. B. Efron, Bootstrap methods: another look at the Jackknife. Ann. Stat. **7**, 1 (1979)
35. G. D’Agostini, A Multidimensional unfolding method based on Bayes’ theorem. Nucl. Instrum. Methods A **362**, 487 (1995)
36. G. D’Agostini, Improved iterative Bayesian unfolding (2010). [arXiv:1010.0632](#) [physics.data-an]
37. T. Auye, Unfolding algorithms and tests using RooUnfold (2011). [arXiv:1105.1160](#) [physics.data-an]
38. ATLAS Collaboration, Study of the material of the ATLAS inner detector for Run 2 of the LHC, JINST **12**, P12009 (2017). [arXiv:1707.02826](#) [hep-ex]
39. ATLAS Collaboration, Measurement of the WW cross section in $\sqrt{s} = 7$ TeV pp collisions with the ATLAS detector and limits on anomalous gauge couplings. Phys. Lett. B **712**, 289 (2012). [arXiv:1203.6232](#) [hep-ex]
40. ATLAS Collaboration, Measurement of the top quark pair production cross section in pp collisions at $\sqrt{s} = 7$ TeV in dilepton final states with ATLAS. Phys. Lett. B **707**, 459 (2012). [arXiv:1108.3699](#) [hep-ex]
41. ATLAS Collaboration, Measurement of the inelastic proton–proton cross section at $\sqrt{s} = 13$ TeV with the ATLAS Detector at the LHC. Phys. Rev. Lett. **117**, 182002 (2016). [arXiv:1606.02625](#) [hep-ex]
42. J.W. Monk, C. Oropeza-Barrera, The HBOM method for unfolding detector effects. Nucl. Instrum. Methods A **701**, 17 (2013). [arXiv:1111.4896](#) [hep-ex]
43. C.D.F. Collaboration, Studying the underlying event in Drell–Yan and high transverse momentum jet production at the Tevatron. Phys. Rev. D **82**, 034001 (2010). [arXiv:1003.3146](#) [hep-ex]
44. M.H. Seymour, A. Siodmok, Constraining MPI models using σ_{eff} and recent tevatron and LHC underlying event data. JHEP **10**, 113 (2013). [arXiv:1307.5015](#) [hep-ph]
45. ATLAS Collaboration, ATLAS Computing Acknowledgements, ATL-GEN-PUB-2016-002. <https://cds.cern.ch/record/2202407>. Accessed 1 Mar 2019

ATLAS Collaboration

G. Aad¹⁰¹, B. Abbott¹²⁸, D. C. Abbott¹⁰², O. Abidinov^{13,*}, A. Abed Abud^{70a,70b}, K. Abeling⁵³, D. K. Abhayasinghe⁹³, S. H. Abidi¹⁶⁷, O. S. AbouZeid⁴⁰, N. L. Abraham¹⁵⁶, H. Abramowicz¹⁶¹, H. Abreu¹⁶⁰, Y. Abulaiti⁶, B. S. Acharya^{66a,66b,n}, B. Achkar⁵³, S. Adachi¹⁶³, L. Adam⁹⁹, C. Adam Bourdarios¹³², L. Adamczyk^{83a}, L. Adamek¹⁶⁷, J. Adelman¹²¹, M. Adersberger¹¹⁴, A. Adiguzel^{12c,ai}, S. Adorni⁵⁴, T. Adye¹⁴⁴, A. A. Affolder¹⁴⁶, Y. Afik¹⁶⁰, C. Agapopoulou¹³², M. N. Agaras³⁸, A. Aggarwal¹¹⁹, C. Agheorghiesei^{27c}, J. A. Aguilar-Saavedra^{140a,140f,ah}, F. Ahmadov⁷⁹, W. S. Ahmed¹⁰³, X. Ai^{15a}, G. Aielli^{73a,73b}, S. Akatsuka⁸⁵, T. P. A. Åkesson⁹⁶, E. Akilli⁵⁴, A. V. Akimov¹¹⁰, K. Al Khoury¹³², G. L. Alberghi^{23a,23b}, J. Albert¹⁷⁶, M. J. Alconada Verzini⁸⁸, S. Alderweireldt³⁶, M. Aleksa³⁶, I. N. Aleksandrov⁷⁹, C. Alexa^{27b}, D. Alexandre¹⁹, T. Alexopoulos¹⁰, A. Alfonsi¹²⁰, M. Alhroob¹²⁸, B. Ali¹⁴², G. Alimonti^{68a}, J. Alison³⁷, S. P. Alkire¹⁴⁸, C. Allaire¹³², B. M. M. Allbrooke¹⁵⁶, B. W. Allen¹³¹, P. P. Allport²¹, A. Aloisio^{69a,69b}, A. Alonso⁴⁰, F. Alonso⁸⁸, C. Alpigiani¹⁴⁸, A. A. Alshehri⁵⁷, M. Alvarez Estevez⁹⁸, D. Álvarez Piqueras¹⁷⁴, M. G. Alvigi^{69a,69b}, Y. Amaral Coutinho^{80b}, A. Ambler¹⁰³, L. Ambroz¹³⁵, C. Amelung²⁶, D. Amidei¹⁰⁵, S. P. Amor Dos Santos^{140a}, S. Amoroso⁴⁶, C. S. Amrouche⁵⁴, F. An⁷⁸, C. Anastopoulos¹⁴⁹, N. Andari¹⁴⁵, T. Andeen¹¹, C. F. Anders^{61b}, J. K. Anders²⁰, A. Andreazza^{68a,68b}, V. Andrei^{61a}, C. R. Anelli¹⁷⁶, S. Angelidakis³⁸, A. Angerami³⁹, A. V. Anisenkov^{122a,122b}, A. Annovi^{71a}, C. Antel^{61a}, M. T. Anthony¹⁴⁹, M. Antonelli⁵¹, D. J. A. Antrim¹⁷¹, F. Anulli^{72a}, M. Aoki⁸¹, J. A. Aparisi Pozo¹⁷⁴, L. Aperio Bella³⁶, G. Arabidze¹⁰⁶, J. P. Araque^{140a}, V. Araujo Ferraz^{80b}, R. Araujo Pereira^{80b}, C. Arcangeletti⁵¹, A. T. H. Arce⁴⁹, F. A. Arduh⁸⁸, J.-F. Arguin¹⁰⁹, S. Argyropoulos⁷⁷, J.-H. Arling⁴⁶, A. J. Armbruster³⁶, L. J. Armitage⁹², A. Armstrong¹⁷¹, O. Arnaez¹⁶⁷, H. Arnold¹²⁰, A. Artamonov^{111,*}, G. Artoni¹³⁵, S. Artz⁹⁹, S. Asai¹⁶³, N. Asbah⁵⁹, E. M. Asimakopoulou¹⁷², L. Asquith¹⁵⁶, K. Assamagan²⁹, R. Astalos^{28a}, R. J. Atkin^{33a}, M. Atkinson¹⁷³, N. B. Atlay¹⁵¹, H. Atmani¹³², K. Augsten¹⁴², G. Avolio³⁶, R. Avramidou^{60a}, M. K. Ayoub^{15a}, A. M. Azoulay^{168b}, G. Azuelos^{109,ax}, M. J. Baca²¹, H. Bachacou¹⁴⁵, K. Bachas^{67a,67b}, M. Backes¹³⁵, F. Backman^{45a,45b}, P. Bagnaia^{72a,72b}, M. Bahmani⁸⁴, H. Bahrasemani¹⁵², A. J. Bailey¹⁷⁴, V. R. Bailey¹⁷³, J. T. Baines¹⁴⁴, M. Bajic⁴⁰, C. Bakalis¹⁰, O. K. Baker¹⁸³, P. J. Bakker¹²⁰, D. Bakshi Gupta⁸, S. Balaji¹⁵⁷, E. M. Baldin^{122a,122b}, P. Balek¹⁸⁰, F. Balli¹⁴⁵, W. K. Balunas¹³⁵, J. Balz⁹⁹, E. Banas⁸⁴, A. Bandyopadhyay²⁴, Sw. Banerjee^{181,i}, A. A. E. Bannoura¹⁸², L. Barak¹⁶¹, W. M. Barbe³⁸, E. L. Barberio¹⁰⁴, D. Barberis^{55a,55b}, M. Barbero¹⁰¹, T. Barillari¹¹⁵, M.-S. Barisits³⁶, J. Barkeloo¹³¹, T. Barklow¹⁵³, R. Barnea¹⁶⁰, S. L. Barnes^{60c}, B. M. Barnett¹⁴⁴, R. M. Barnett¹⁸, Z. Barnovska-Blenessy^{60a}, A. Baroncelli^{60a}, G. Barone²⁹, A. J. Barr¹³⁵, L. Barranco Navarro¹⁷⁴, F. Barreiro⁹⁸, J. Barreiro Guimarães da Costa^{15a}, S. Barsov¹³⁸, R. Bartoldus¹⁵³, G. Bartolini¹⁰¹, A. E. Barton⁸⁹, P. Bartos^{28a}, A. Basalae⁴⁶, A. Bassalat^{132,aq}, R. L. Bates⁵⁷, S. J. Batista¹⁶⁷, S. Batlamous^{35c}, J. R. Batley³², B. Batool¹⁵¹, M. Battaglia¹⁴⁶, M. Bauce^{72a,72b}, F. Bauer¹⁴⁵, K. T. Bauer¹⁷¹, H. S. Bawa^{31,j}, J. B. Beacham⁴⁹, T. Beau¹³⁶, P. H. Beauchemin¹⁷⁰, F. Becherer⁵², P. Bechtel²⁴, H. C. Beck⁵³, H. P. Beck^{20,r}, K. Becker⁵², M. Becker⁹⁹, C. Becot⁴⁶, A. Beddall^{12d}, A. J. Beddall^{12a}, V. A. Bednyakov⁷⁹, M. Bedognetti¹²⁰, C. P. Bee¹⁵⁵, T. A. Beermann⁷⁶, M. Begalli^{80b}, M. Begel²⁹, A. Behera¹⁵⁵, J. K. Behr⁴⁶, F. Beisiegel²⁴, A. S. Bell⁹⁴, G. Bella¹⁶¹, L. Bellagamba^{23b}, A. Bellerive³⁴, P. Bellos⁹, K. Beloborodov^{122a,122b}, K. Belotskiy¹¹², N. L. Belyaev¹¹², D. Benchechroun^{35a}, N. Benekos¹⁰, Y. Benhammou¹⁶¹, D. P. Benjamin⁶, M. Benoit⁵⁴, J. R. Bensinger²⁶, S. Bentvelsen¹²⁰, L. Beresford¹³⁵, M. Beretta⁵¹, D. Berge⁴⁶, E. Bergeaas Kuutmann¹⁷², N. Berger⁵, B. Bergmann¹⁴², L. J. Bergsten²⁶, J. Beringer¹⁸, S. Berlendis⁷, N. R. Bernard¹⁰², G. Bernardi¹³⁶, C. Bernius¹⁵³, T. Berry⁹³, P. Berta⁹⁹, C. Bertella^{15a}, I. A. Bertram⁸⁹, G. J. Besjes⁴⁰, O. Bessidskaia Bylund¹⁸², N. Besson¹⁴⁵, A. Bethani¹⁰⁰, S. Bethke¹¹⁵, A. Betti²⁴, A. J. Bevan⁹², J. Beyer¹¹⁵, R. Bi¹³⁹, R. M. Bianchi¹³⁹, O. Biebel¹¹⁴, D. Biedermann¹⁹, R. Bielski³⁶, K. Bierwagen⁹⁹, N. V. Biesuz^{71a,71b}, M. Biglietti^{74a}, T. R. V. Billoud¹⁰⁹, M. Bindi⁵³, A. Bingul^{12d}, C. Bini^{72a,72b}, S. Biondi^{23a,23b}, M. Birman¹⁸⁰, T. Bisanz⁵³, J. P. Biswal¹⁶¹, A. Bitadze¹⁰⁰, C. Bittrich⁴⁸, K. Björke¹³⁴, K. M. Black²⁵, T. Blazek^{28a}, I. Bloch⁴⁶, C. Blocker²⁶, A. Blue⁵⁷, U. Blumenschein⁹², G. J. Bobbink¹²⁰, V. S. Bobrovnikov^{122a,122b}, S. S. Bocchetta⁹⁶, A. Bocci⁴⁹, D. Boerner⁴⁶, D. Bogavac¹⁴, A. G. Bogdanichikov^{122a,122b}, C. Bohm^{45a}, V. Boisvert⁹³, P. Bokan^{53,172}, T. Bold^{83a}, A. S. Boldyrev¹¹³, A. E. Bolz^{61b}, M. Bomben¹³⁶, M. Bona⁹², J. S. Bonilla¹³¹, M. Boonekamp¹⁴⁵, H. M. Borecka-Bielska⁹⁰, A. Borisov¹²³, G. Borissov⁸⁹, J. Bortfeldt³⁶, D. Bortoletto¹³⁵, V. Bortolotto^{73a,73b}, D. Boscherini^{23b}, M. Bosman¹⁴, J. D. Bossio Sola¹⁰³, K. Bouaouda^{35a}, J. Boudreau¹³⁹, E. V. Bouhova-Thacker⁸⁹, D. Boumediene³⁸, S. K. Boutle⁵⁷, A. Boveia¹²⁶, J. Boyd³⁶, D. Boye^{33b,ar}, I. R. Boyko⁷⁹, A. J. Bozson⁹³, J. Bracinik²¹, N. Brahimi¹⁰¹, G. Brandt¹⁸², O. Brandt^{61a}, F. Braren⁴⁶, U. Bratzler¹⁶⁴, B. Brau¹⁰², J. E. Brau¹³¹, W. D. Breaden Madden⁵⁷, K. Brendlinger⁴⁶, L. Brenner⁴⁶, R. Brenner¹⁷², S. Bressler¹⁸⁰, B. Brickwedde⁹⁹, D. L. Briglin²¹, D. Britton⁵⁷, D. Britzger¹¹⁵, I. Brock²⁴, R. Brock¹⁰⁶, G. Brooijmans³⁹, W. K. Brooks^{147b}, E. Brost¹²¹, J. H. Broughton²¹, P. A. Bruckman de Renstrom⁸⁴, D. Bruncko^{28b}, A. Bruni^{23b}, G. Bruni^{23b}, L. S. Bruni¹²⁰, S. Bruno^{73a,73b}, B. H. Brunt³², M. Bruschi^{23b}, N. Bruscino¹³⁹, P. Bryant³⁷, L. Bryngemark⁹⁶, T. Buanes¹⁷, Q. Buat³⁶, P. Buchholz¹⁵¹, A. G. Buckley⁵⁷, I. A. Budagov⁷⁹, M. K. Bugge¹³⁴, F. Bühner⁵², O. Bulekov¹¹², T. J. Burch¹²¹, S. Burdin⁹⁰, C. D. Burgard¹²⁰,

A. M. Burger¹²⁹, B. Burghgrave⁸, K. Burka⁸⁴, J. T. P. Burr⁴⁶, J. C. Burzynski¹⁰², V. Büscher⁹⁹, E. Buschmann⁵³, P. J. Bussey⁵⁷, J. M. Butler²⁵, C. M. Buttar⁵⁷, J. M. Butterworth⁹⁴, P. Butti³⁶, W. Buttinger³⁶, A. Buzatu¹⁵⁸, A. R. Buzykaev^{122a,122b}, G. Cabras^{23a,23b}, S. Cabrera Urbán¹⁷⁴, D. Caforio⁵⁶, H. Cai¹⁷³, V. M. M. Cairo¹⁵³, O. Cakir^{4a}, N. Calace³⁶, P. Calafiura¹⁸, A. Calandri¹⁰¹, G. Calderini¹³⁶, P. Calfayan⁶⁵, G. Callea⁵⁷, L. P. Caloba^{80b}, S. Calvente Lopez⁹⁸, D. Calvet³⁸, S. Calvet³⁸, T. P. Calvet¹⁵⁵, M. Calvetti^{71a,71b}, R. Camacho Toro¹³⁶, S. Camarda³⁶, D. Camarero Munoz⁹⁸, P. Camarri^{73a,73b}, D. Cameron¹³⁴, R. Caminal Armadans¹⁰², C. Camincher³⁶, S. Campana³⁶, M. Campanelli⁹⁴, A. Camplani⁴⁰, A. Campoverde¹⁵¹, V. Canale^{69a,69b}, A. Canesse¹⁰³, M. Cano Bret^{60c}, J. Cantero¹²⁹, T. Cao¹⁶¹, Y. Cao¹⁷³, M. D. M. Capeans Garrido³⁶, M. Capua^{41a,41b}, R. Cardarelli^{73a}, F. C. Cardillo¹⁴⁹, I. Carli¹⁴³, T. Carli³⁶, G. Carlino^{69a}, B. T. Carlson¹³⁹, L. Carminati^{68a,68b}, R. M. D. Carney^{45a,45b}, S. Caron¹¹⁹, E. Carquin^{147b}, S. Carrá⁴⁶, J. W. S. Carter¹⁶⁷, M. P. Casado^{14.e}, A. F. Casha¹⁶⁷, D. W. Casper¹⁷¹, R. Castelijn¹²⁰, F. L. Castillo¹⁷⁴, V. Castillo Gimenez¹⁷⁴, N. F. Castro^{140a,140e}, A. Catinaccio³⁶, J. R. Catmore¹³⁴, A. Cattai³⁶, J. Caudron²⁴, V. Cavaliere²⁹, E. Cavallaro¹⁴, D. Cavalli^{68a}, M. Cavalli-Sforza¹⁴, V. Cavasinni^{71a,71b}, E. Celebi^{12b}, F. Ceradini^{74a,74b}, L. Cerda Alberich¹⁷⁴, K. Cerny¹³⁰, A. S. Cerqueira^{80a}, A. Cerri¹⁵⁶, L. Cerrito^{73a,73b}, F. Cerutti¹⁸, A. Cervelli^{23a,23b}, S. A. Cetin^{12b}, D. Chakraborty¹²¹, S. K. Chan⁵⁹, W. S. Chan¹²⁰, W. Y. Chan⁹⁰, J. D. Chapman³², B. Chargeishvili^{159b}, D. G. Charlton²¹, T. P. Charman⁹², C. C. Chau³⁴, S. Che¹²⁶, A. Chegwidan¹⁰⁶, S. Chekanov⁶, S. V. Chekulaev^{168a}, G. A. Chelkov^{79,aw}, M. A. Chelstowska³⁶, B. Chen⁷⁸, C. Chen^{60a}, C. H. Chen⁷⁸, H. Chen²⁹, J. Chen^{60a}, J. Chen³⁹, S. Chen¹³⁷, S. J. Chen^{15c}, X. Chen^{15b,av}, Y. Chen⁸², Y.-H. Chen⁴⁶, H. C. Cheng^{63a}, H. J. Cheng^{15a,15d}, A. Cheplakov⁷⁹, E. Cheremushkina¹²³, R. Cherkaoui El Moursli^{35e}, E. Cheu⁷, K. Cheung⁶⁴, T. J. A. Chevalérias¹⁴⁵, L. Chevalier¹⁴⁵, V. Chiarella⁵¹, G. Chiarelli^{71a}, G. Chiodini^{67a}, A. S. Chisholm^{36,21}, A. Chitan^{27b}, I. Chiu¹⁶³, Y. H. Chiu¹⁷⁶, M. V. Chizhov⁷⁹, K. Choi⁶⁵, A. R. Chomont^{72a,72b}, S. Chouridou¹⁶², Y. S. Chow¹²⁰, M. C. Chu^{63a}, J. Chudoba¹⁴¹, A. J. Chuinard¹⁰³, J. J. Chwastowski⁸⁴, L. Chytka¹³⁰, K. M. Ciesla⁸⁴, D. Cinca⁴⁷, V. Cindro⁹¹, I. A. Cioară^{27b}, A. Ciocio¹⁸, F. Ciotto^{69a,69b}, Z. H. Citron¹⁸⁰, M. Citterio^{68a}, D. A. Ciubotaru^{27b}, B. M. Ciungu¹⁶⁷, A. Clark⁵⁴, M. R. Clark³⁹, P. J. Clark⁵⁰, C. Clement^{45a,45b}, Y. Coadou¹⁰¹, M. Cobal^{66a,66c}, A. Coccaro^{55b}, J. Cochran⁷⁸, H. Cohen¹⁶¹, A. E. C. Coimbra³⁶, L. Colasurdo¹¹⁹, B. Cole³⁹, A. P. Colijn¹²⁰, J. Collot⁵⁸, P. Conde Muño^{140a,f}, E. Coniavitis⁵², S. H. Connell^{33b}, I. A. Connelly⁵⁷, S. Constantinescu^{27b}, F. Conventi^{69a,ay}, A. M. Cooper-Sarkar¹³⁵, F. Cormier¹⁷⁵, K. J. R. Cormier¹⁶⁷, L. D. Corpe⁹⁴, M. Corradi^{72a,72b}, E. E. Corrigan⁹⁶, F. Corriveau^{103,ad}, A. Cortes-Gonzalez³⁶, M. J. Costa¹⁷⁴, F. Costanza⁵, D. Costanzo¹⁴⁹, G. Cowan⁹³, J. W. Cowley³², J. Crane¹⁰⁰, K. Cranmer¹²⁴, S. J. Crawley⁵⁷, R. A. Creager¹³⁷, S. Crépe-Renaudin⁵⁸, F. Crescioli¹³⁶, M. Cristinziani²⁴, V. Croft¹²⁰, G. Crosetti^{41a,41b}, A. Cueto⁵, T. Cuhadar Donszelmann¹⁴⁹, A. R. Cukierman¹⁵³, S. Czekierda⁸⁴, P. Czodrowski³⁶, M. J. Da Cunha Sargedas De Sousa^{60b}, J. V. Da Fonseca Pinto^{80b}, C. Da Via¹⁰⁰, W. Dabrowski^{83a}, T. Dado^{28a}, S. Dahbi^{35e}, T. Dai¹⁰⁵, C. Dallapiccola¹⁰², M. Dam⁴⁰, G. D'amen^{23a,23b}, V. D'Amico^{74a,74b}, J. Damp⁹⁹, J. R. Dandoy¹³⁷, M. F. Daneri³⁰, N. P. Dang¹⁸¹, N. D. Dann¹⁰⁰, M. Danninger¹⁷⁵, V. Dao³⁶, G. Darbo^{55b}, O. Dartsis⁵, A. Dattagupta¹³¹, T. Daubney⁴⁶, S. D'Auria^{68a,68b}, W. Davey²⁴, C. David⁴⁶, T. Davidek¹⁴³, D. R. Davis⁴⁹, I. Dawson¹⁴⁹, K. De⁸, R. De Asmundis^{69a}, M. De Beurs¹²⁰, S. De Castro^{23a,23b}, S. De Cecco^{72a,72b}, N. De Groot¹¹⁹, P. de Jong¹²⁰, H. De la Torre¹⁰⁶, A. De Maria^{15c}, D. De Pedis^{72a}, A. De Salvo^{72a}, U. De Sanctis^{73a,73b}, M. De Santis^{73a,73b}, A. De Santo¹⁵⁶, K. De Vasconcelos Corga¹⁰¹, J. B. De Vivie De Regie¹³², C. Debenedetti¹⁴⁶, D. V. Dedovich⁷⁹, A. M. Deiana⁴², M. Del Gaudio^{41a,41b}, J. Del Peso⁹⁸, Y. Delabat Diaz⁴⁶, D. Delgove¹³², F. Deliot^{145,q}, C. M. Delitzsch⁷, M. Della Pietra^{69a,69b}, D. Della Volpe⁵⁴, A. Dell'Acqua³⁶, L. Dell'Asta^{73a,73b}, M. Delmastro⁵, C. Delporte¹³², P. A. Delsart⁵⁸, D. A. DeMarco¹⁶⁷, S. Demers¹⁸³, M. Demichev⁷⁹, G. Demontigny¹⁰⁹, S. P. Denisov¹²³, D. Denysiuk¹²⁰, L. D'Ermo¹³⁶, D. Derendarz⁸⁴, J. E. Derkaoui^{35d}, F. Derue¹³⁶, P. Dervan⁹⁰, K. Desch²⁴, C. Deterre⁴⁶, K. Dette¹⁶⁷, C. Deutsch²⁴, M. R. Devesa³⁰, P. O. Deviveiros³⁶, A. Dewhurst¹⁴⁴, S. Dhaliwal²⁶, F. A. Di Bello⁵⁴, A. Di Ciaccio^{73a,73b}, L. Di Ciaccio⁵, W. K. Di Clemente¹³⁷, C. Di Donato^{69a,69b}, A. Di Girolamo³⁶, G. Di Gregorio^{71a,71b}, B. Di Micco^{74a,74b}, R. Di Nardo¹⁰², K. F. Di Petrillo⁵⁹, R. Di Sipio¹⁶⁷, D. Di Valentino³⁴, C. Diaconu¹⁰¹, F. A. Dias⁴⁰, T. Dias Do Vale^{140a}, M. A. Diaz^{147a}, J. Dickinson¹⁸, E. B. Diehl¹⁰⁵, J. Dietrich¹⁹, S. Díez Cornell⁴⁶, A. Dimitrievska¹⁸, W. Ding^{15b}, J. Dingfelder²⁴, F. Dittus³⁶, F. Djama¹⁰¹, T. Djobava^{159b}, J. I. Djuvsland¹⁷, M. A. B. Do Vale^{80c}, M. Dobre^{27b}, D. Dodsworth²⁶, C. Doglioni⁹⁶, J. Dolejsi¹⁴³, Z. Dolezal¹⁴³, M. Donadelli^{80d}, J. Donini³⁸, A. D'onofrio⁹², M. D'Onofrio⁹⁰, J. Dopke¹⁴⁴, A. Doria^{69a}, M. T. Dova⁸⁸, A. T. Doyle⁵⁷, E. Drechsler¹⁵², E. Dreyer¹⁵², T. Dreyer⁵³, A. S. Drobac¹⁷⁰, Y. Duan^{60b}, F. Dubinin¹¹⁰, M. Dubovsky^{28a}, A. Dubreuil⁵⁴, E. Duchovni¹⁸⁰, G. Duckeck¹¹⁴, A. Ducourthial¹³⁶, O. A. Ducu¹⁰⁹, D. Duda¹¹⁵, A. Dudarev³⁶, A. C. Dudder⁹⁹, E. M. Duffield¹⁸, L. Dufflot¹³², M. Dührssen³⁶, C. Dülken¹⁸², M. Dumancic¹⁸⁰, A. E. Dumitriu^{27b}, A. K. Duncan⁵⁷, M. Dunford^{61a}, A. Duperrin¹⁰¹, H. Duran Yildiz^{4a}, M. Düren⁵⁶, A. Durglishvili^{159b}, D. Duschinger⁴⁸, B. Dutta⁴⁶, D. Duvnjak¹, G. I. Dyckes¹³⁷, M. Dyndal³⁶, S. Dysch¹⁰⁰, B. S. Dziedzic⁸⁴, K. M. Ecker¹¹⁵, R. C. Edgar¹⁰⁵, T. Eifert³⁶, G. Eigen¹⁷, K. Einsweiler¹⁸, T. Ekelof¹⁷², M. El Kacimi^{35c}, R. El Kosseifi¹⁰¹, V. Ellajosyula¹⁷², M. Ellert¹⁷², F. Ellinghaus¹⁸², A. A. Elliot⁹², N. Ellis³⁶, J. Elmsheuser²⁹, M. Elsing³⁶, D. Emelianov¹⁴⁴, A. Emerman³⁹, Y. Enari¹⁶³, J. S. Ennis¹⁷⁸, M. B. Epland⁴⁹, J. Erdmann⁴⁷, A. Ereditato²⁰, M. Errenst³⁶, M. Escalier¹³²

C. Escobar¹⁷⁴, O. Estrada Pastor¹⁷⁴, E. Etzion¹⁶¹, H. Evans⁶⁵, A. Ezhilov¹³⁸, F. Fabbri⁵⁷, L. Fabbri^{23a,23b}, V. Fabiani¹¹⁹, G. Facini⁹⁴, R. M. Faisca Rodrigues Pereira^{140a}, R. M. Fakhruddinov¹²³, S. Falciano^{72a}, P. J. Falke⁵, S. Falke⁵, J. Faltova¹⁴³, Y. Fang^{15a}, Y. Fang^{15a}, G. Fanourakis⁴⁴, M. Fanti^{68a,68b}, A. Farbin⁸, A. Farilla^{74a}, E. M. Farina^{70a,70b}, T. Farooque¹⁰⁶, S. Farrell¹⁸, S. M. Farrington¹⁷⁸, P. Farthouat³⁶, F. Fassi^{35c}, P. Fassnacht³⁶, D. Fassouliotis⁹, M. Fauci Giannelli⁵⁰, W. J. Fawcett³², L. Fayard¹³², O. L. Fedin^{138,o}, W. Fedorko¹⁷⁵, M. Feickert⁴², S. Feigl¹³⁴, L. Feligioni¹⁰¹, A. Fell¹⁴⁹, C. Feng^{60b}, E. J. Feng³⁶, M. Feng⁴⁹, M. J. Fenton⁵⁷, A. B. Fenyuk¹²³, J. Ferrando⁴⁶, A. Ferrante¹⁷³, A. Ferrari¹⁷², P. Ferrari¹²⁰, R. Ferrari^{70a}, D. E. Ferreira de Lima^{61b}, A. Ferrer¹⁷⁴, D. Ferrere⁵⁴, C. Ferretti¹⁰⁵, F. Fiedler⁹⁹, A. Filipčić⁹¹, F. Filthaut¹¹⁹, K. D. Finelli²⁵, M. C. N. Fiolhais^{140a}, L. Fiorini¹⁷⁴, F. Fischer¹¹⁴, W. C. Fisher¹⁰⁶, I. Fleck¹⁵¹, P. Fleischmann¹⁰⁵, R. R. M. Fletcher¹³⁷, T. Flick¹⁸², B. M. Flierl¹¹⁴, L. F. Flores¹³⁷, L. R. Flores Castillo^{63a}, F. M. Follega^{75a,75b}, N. Fomin¹⁷, J. H. Foo¹⁶⁷, G. T. Forcolin^{75a,75b}, A. Formica¹⁴⁵, F. A. Förster¹⁴, A. C. Forti¹⁰⁰, A. G. Foster²¹, M. G. Foti¹³⁵, D. Fournier¹³², H. Fox⁸⁹, P. Francavilla^{71a,71b}, S. Francescato^{72a,72b}, M. Franchini^{23a,23b}, S. Franchino^{61a}, D. Francis³⁶, L. Franconi²⁰, M. Franklin⁵⁹, A. N. Fray⁹², B. Freund¹⁰⁹, W. S. Freund^{80b}, E. M. Freundlich⁴⁷, D. C. Frizzell¹²⁸, D. Froidevaux³⁶, J. A. Frost¹³⁵, C. Fukunaga¹⁶⁴, E. Fullana Torregrosa¹⁷⁴, E. Fumagalli^{55a,55b}, T. Fusayasu¹¹⁶, J. Fuster¹⁷⁴, A. Gabrielli^{23a,23b}, A. Gabrielli¹⁸, G. P. Gach^{83a}, S. Gadatsch⁵⁴, P. Gadow¹¹⁵, G. Gagliardi^{55a,55b}, L. G. Gagnon¹⁰⁹, C. Galea^{27b}, B. Galhardo^{140a}, G. E. Gallardo¹³⁵, E. J. Gallas¹³⁵, B. J. Gallop¹⁴⁴, P. Gallus¹⁴², G. Galster⁴⁰, R. Gamboa Goni⁹², K. K. Gan¹²⁶, S. Ganguly¹⁸⁰, J. Gao^{60a}, Y. Gao⁹⁰, Y. S. Gao^{31,1}, C. García¹⁷⁴, J. E. García Navarro¹⁷⁴, J. A. García Pascual^{15a}, C. Garcia-Argos⁵², M. Garcia-Sciveres¹⁸, R. W. Gardner³⁷, N. Garelli¹⁵³, S. Gargiulo⁵², V. Garonne¹³⁴, A. Gaudiello^{55a,55b}, G. Gaudio^{70a}, I. L. Gavrilenko¹¹⁰, A. Gavriljuk¹¹¹, C. Gay¹⁷⁵, G. Gaycken²⁴, E. N. Gazis¹⁰, A. A. Geanta^{27b}, C. N. P. Gee¹⁴⁴, J. Geisen⁵³, M. Geisen⁹⁹, M. P. Geisler^{61a}, C. Gemme^{55b}, M. H. Genest⁵⁸, C. Geng¹⁰⁵, S. Gentile^{72a,72b}, S. George⁹³, T. Gerialis⁴⁴, L. O. Gerlach⁵³, P. Gessinger-Befurt⁹⁹, G. Gessner⁴⁷, S. Ghasemi¹⁵¹, M. Ghasemi Bostanabad¹⁷⁶, M. Ghneimat²⁴, A. Ghosh⁷⁷, B. Giacobbe^{23b}, S. Giagu^{72a,72b}, N. Giangiacomi^{23a,23b}, P. Giannetti^{71a}, A. Giannini^{69a,69b}, S. M. Gibson⁹³, M. Gignac¹⁴⁶, D. Gillberg³⁴, G. Gilles¹⁸², D. M. Gingrich^{3,ax}, M. P. Giordani^{66a,66c}, F. M. Giorgi^{23b}, P. F. Giraud¹⁴⁵, G. Giugliarelli^{66a,66c}, D. Giugni^{68a}, F. Giuli^{73a,73b}, S. Gkaitatzis¹⁶², I. Gkialas^{9,h}, E. L. Gkoukousis¹⁴, P. Gkoutoumis¹⁰, L. K. Gladilin¹¹³, C. Glasman⁹⁸, J. Glatzer¹⁴, P. C. F. Glaysher⁴⁶, A. Glazov⁴⁶, M. Goblirsch-Kolb²⁶, S. Goldfarb¹⁰⁴, T. Golling⁵⁴, D. Golubkov¹²³, A. Gomes^{140a,140b}, R. Goncalves Gama⁵³, R. Gonçalo^{140a,140b}, G. Gonella⁵², L. Gonella²¹, A. Gongadze⁷⁹, F. Gonnella²¹, J. L. Gonski⁵⁹, S. González de la Hoz¹⁷⁴, S. Gonzalez-Sevilla⁵⁴, G. R. Gonzalvo Rodriguez¹⁷⁴, L. Goossens³⁶, P. A. Gorbounov¹¹¹, H. A. Gordon²⁹, B. Gorini³⁶, E. Gorini^{67a,67b}, A. Gorišek⁹¹, A. T. Goshaw⁴⁹, C. Gössling⁴⁷, M. I. Gostkin⁷⁹, C. A. Gottardo²⁴, M. Gouighri^{35b}, D. Goujdami^{35c}, A. G. Goussiou¹⁴⁸, N. Govender^{33b,a}, C. Goy⁵, E. Gozani¹⁶⁰, I. Grabowska-Bold^{83a}, E. C. Graham⁹⁰, J. Gramling¹⁷¹, E. Gramstad¹³⁴, S. Grancagnolo¹⁹, M. Grandi¹⁵⁶, V. Gratchev¹³⁸, P. M. Gravila^{27f}, F. G. Gravili^{67a,67b}, C. Gray⁵⁷, H. M. Gray¹⁸, C. Grefe²⁴, K. Gregersen⁹⁶, I. M. Gregor⁴⁶, P. Grenier¹⁵³, K. Grevtsov⁴⁶, N. A. Grieser¹²⁸, J. Griffiths⁸, A. A. Grillo¹⁴⁶, K. Grimm^{31,k}, S. Grinstein^{14,x}, J.-F. Grivaz¹³², S. Groh⁹⁹, E. Gross¹⁸⁰, J. Grosse-Knetter⁵³, Z. J. Grout⁹⁴, C. Grud¹⁰⁵, A. Grummer¹¹⁸, L. Guan¹⁰⁵, W. Guan¹⁸¹, J. Guenther³⁶, A. Guerguichon¹³², F. Guescini¹¹⁵, D. Guest¹⁷¹, R. Gugel⁵², B. Gui¹²⁶, T. Guillemin⁵, S. Guindon³⁶, U. Gul⁵⁷, J. Guo^{60c}, W. Guo¹⁰⁵, Y. Guo^{60a,s}, Z. Guo¹⁰¹, R. Gupta⁴⁶, S. Gurbuz^{12c}, G. Gustavino¹²⁸, P. Gutierrez¹²⁸, C. Gutsche⁹⁴, C. Guyot¹⁴⁵, M. P. Guzik^{83a}, C. Gwenlan¹³⁵, C. B. Gwilliam⁹⁰, A. Haas¹²⁴, C. Haber¹⁸, H. K. Hadavand⁸, N. Haddad^{35e}, A. Hadeef^{60a}, S. Hageböck³⁶, M. Hagihara¹⁶⁹, M. Haleem¹⁷⁷, J. Haley¹²⁹, G. Halladjian¹⁰⁶, G. D. Hallewell¹⁰¹, K. Hamacher¹⁸², P. Hamal¹³⁰, K. Hamano¹⁷⁶, H. Hamdaoui^{35e}, G. N. Hamity¹⁴⁹, K. Han^{60a,ak}, L. Han^{60a}, S. Han^{15a,15d}, K. Hanagaki^{81,v}, M. Hance¹⁴⁶, D. M. Handl¹¹⁴, B. Haney¹³⁷, R. Hankache¹³⁶, P. Hanke^{61a}, E. Hansen⁹⁶, J. B. Hansen⁴⁰, J. D. Hansen⁴⁰, M. C. Hansen²⁴, P. H. Hansen⁴⁰, E. C. Hanson¹⁰⁰, K. Hara¹⁶⁹, A. S. Hard¹⁸¹, T. Harenberg¹⁸², S. Harkusha¹⁰⁷, P. F. Harrison¹⁷⁸, N. M. Hartmann¹¹⁴, Y. Hasegawa¹⁵⁰, A. Hasib⁵⁰, S. Hassani¹⁴⁵, S. Haug²⁰, R. Hauser¹⁰⁶, L. B. Havener³⁹, M. Havranek¹⁴², C. M. Hawkes²¹, R. J. Hawking³⁶, D. Hayden¹⁰⁶, C. Hayes¹⁵⁵, R. L. Hayes¹⁷⁵, C. P. Hays¹³⁵, J. M. Hays⁹², H. S. Hayward⁹⁰, S. J. Haywood¹⁴⁴, F. He^{60a}, M. P. Heath⁵⁰, V. Hedberg⁹⁶, L. Heelan⁸, S. Heer²⁴, K. K. Heidegger⁵², W. D. Heidorn⁷⁸, J. Heilman³⁴, S. Heim⁴⁶, T. Heim¹⁸, B. Heinemann^{46,as}, J. J. Heinrich¹³¹, L. Heinrich³⁶, C. Heinz⁵⁶, J. Hejbal¹⁴¹, L. Helary^{61b}, A. Held¹⁷⁵, S. Hellesund¹³⁴, C. M. Helling¹⁴⁶, S. Hellman^{45a,45b}, C. Helsen³⁶, R. C. W. Henderson⁸⁹, Y. Heng¹⁸¹, S. Henkelmann¹⁷⁵, A. M. Henriques Correia³⁶, G. H. Herbert¹⁹, H. Herde²⁶, V. Herget¹⁷⁷, Y. Hernández Jiménez^{33c}, H. Herr⁹⁹, M. G. Herrmann¹¹⁴, T. Herrmann⁴⁸, G. Herten⁵², R. Hertenberger¹¹⁴, L. Hervas³⁶, T. C. Herwig¹³⁷, G. G. Hesketh⁹⁴, N. P. Hessay^{168a}, A. Higashida¹⁶³, S. Higashino⁸¹, E. Higón-Rodríguez¹⁷⁴, K. Hildebrand³⁷, E. Hill¹⁷⁶, J. C. Hill³², K. K. Hill²⁹, K. H. Hiller⁴⁶, S. J. Hillier²¹, M. Hils⁴⁸, I. Hinchliffe¹⁸, F. Hinterkeuser²⁴, M. Hirose¹³³, S. Hirose⁵², D. Hirschbuehl¹⁸², B. Hiti⁹¹, O. Hladik¹⁴¹, D. R. Hlaluku^{33c}, X. Hoad⁵⁰, J. Hobbs¹⁵⁵, N. Hod¹⁸⁰, M. C. Hodgkinson¹⁴⁹, A. Hoecker³⁶, F. Hoenig¹¹⁴, D. Hohn⁵², D. Hohov¹³², T. R. Holmes³⁷, M. Holzbock¹¹⁴, L.B.A.H Hommels³², S. Honda¹⁶⁹, T. Honda⁸¹, T. M. Hong¹³⁹, A. Hönle¹¹⁵, B. H. Hooberman¹⁷³, W. H. Hopkins⁶, Y. Horii¹¹⁷, P. Horn⁴⁸, L. A. Horyn³⁷, J.-Y. Hostachy⁵⁸, A. Hostiuc¹⁴⁸,

S. Hou¹⁵⁸, A. Houmada^{35a}, J. Howarth¹⁰⁰, J. Hoya⁸⁸, M. Hrabovsky¹³⁰, J. Hrdinka⁷⁶, I. Hristova¹⁹, J. Hrivnac¹³², A. Hrynevich¹⁰⁸, T. Hryn'ova⁵, P. J. Hsu⁶⁴, S.-C. Hsu¹⁴⁸, Q. Hu²⁹, S. Hu^{60c}, Y. Huang^{15a}, Z. Hubacek¹⁴², F. Hubaut¹⁰¹, M. Huebner²⁴, F. Huegging²⁴, T. B. Huffman¹³⁵, M. Huhtinen³⁶, R. F. H. Hunter³⁴, P. Huo¹⁵⁵, A. M. Hupe³⁴, N. Huseynov^{79.af}, J. Huston¹⁰⁶, J. Huth⁵⁹, R. Hyneman¹⁰⁵, S. Hyrych^{28a}, G. Iacobucci⁵⁴, G. Iakovidis²⁹, I. Ibragimov¹⁵¹, L. Iconomidou-Fayard¹³², Z. Idrissi^{35e}, P. I. Iengo³⁶, R. Ignazzi⁴⁰, O. Igonkina^{120.z.*}, R. Iguchi¹⁶³, T. Iizawa⁵⁴, Y. Ikegami⁸¹, M. Ikeno⁸¹, D. Iliadis¹⁶², N. Ilic¹¹⁹, F. Iltzsche⁴⁸, G. Introzzi^{70a,70b}, M. Iodice^{74a}, K. Iordanidou^{168a}, V. Ippolito^{72a,72b}, M. F. Isacson¹⁷², M. Ishino¹⁶³, M. Ishitsuka¹⁶⁵, W. Islam¹²⁹, C. Issever¹³⁵, S. Istin¹⁶⁰, F. Ito¹⁶⁹, J. M. Iturbe Ponce^{63a}, R. Iuppa^{75a,75b}, A. Ivina¹⁸⁰, H. Iwasaki⁸¹, J. M. Izen⁴³, V. Izzo^{69a}, P. Jacka¹⁴¹, P. Jackson¹, R. M. Jacobs²⁴, B. P. Jaeger¹⁵², V. Jain², G. Jäkel¹⁸², K. B. Jakobi⁹⁹, K. Jakobs⁵², S. Jakobsen⁷⁶, T. Jakoubek¹⁴¹, J. Jamieson⁵⁷, K. W. Janas^{83a}, R. Jansky⁵⁴, J. Janssen²⁴, M. Janus⁵³, P. A. Janus^{83a}, G. Jarlskog⁹⁶, N. Javadov^{79.af}, T. Javůrek³⁶, M. Javurkova⁵², F. Jeanneau¹⁴⁵, L. Jeanty¹³¹, J. Jejelava^{159a.ag}, A. Jelinskas¹⁷⁸, P. Jenni^{52.b}, J. Jeong⁴⁶, N. Jeong⁴⁶, S. Jézéquel⁵, H. Ji¹⁸¹, J. Jia¹⁵⁵, H. Jiang⁷⁸, Y. Jiang^{60a}, Z. Jiang^{153.p}, S. Jiggins⁵², F. A. Jimenez Morales³⁸, J. Jimenez Pena¹⁷⁴, S. Jin^{15c}, A. Jinaru^{27b}, O. Jinnouchi¹⁶⁵, H. Jivan^{33c}, P. Johansson¹⁴⁹, K. A. Johns⁷, C. A. Johnson⁶⁵, K. Jon-And^{45a,45b}, R. W. L. Jones⁸⁹, S. D. Jones¹⁵⁶, S. Jones⁷, T. J. Jones⁹⁰, J. Jongmanns^{61a}, P. M. Jorge^{140a}, J. Jovicevic³⁶, X. Ju¹⁸, J. J. Junggeburth¹¹⁵, A. Juste Rozas^{14.x}, A. Kaczmarska⁸⁴, M. Kado^{72a,72b}, H. Kagan¹²⁶, M. Kagan¹⁵³, C. Kahra⁹⁹, T. Kaji¹⁷⁹, E. Kajomovitz¹⁶⁰, C. W. Kalderon⁹⁶, A. Kaluza⁹⁹, A. Kamenshchikov¹²³, L. Kanjir⁹¹, Y. Kano¹⁶³, V. A. Kantserov¹¹², J. Kanzaki⁸¹, L. S. Kaplan¹⁸¹, D. Kar^{33c}, M. J. Kareem^{168b}, E. Karentzos¹⁰, S. N. Karpov⁷⁹, Z. M. Karpova⁷⁹, V. Kartvelishvili⁸⁹, A. N. Karyukhin¹²³, L. Kashif¹⁸¹, R. D. Kass¹²⁶, A. Kastanas^{45a,45b}, Y. Kataoka¹⁶³, C. Kato^{60c,60d}, J. Katzy⁴⁶, K. Kawade⁸², K. Kawagoe⁸⁷, T. Kawaguchi¹¹⁷, T. Kawamoto¹⁶³, G. Kawamura⁵³, E. F. Kay¹⁷⁶, V. F. Kazanin^{122a,122b}, R. Keeler¹⁷⁶, R. Kehoe⁴², J. S. Keller³⁴, E. Kellermann⁹⁶, D. Kelsey¹⁵⁶, J. J. Kempster²¹, J. Kendrick²¹, O. Kepka¹⁴¹, S. Kersten¹⁸², B. P. Kerševan⁹¹, S. Ketabchi Haghighat¹⁶⁷, M. Khader¹⁷³, F. Khalil-Zada¹³, M. Khandoga¹⁴⁵, A. Khanov¹²⁹, A. G. Kharlamov^{122a,122b}, T. Kharlamova^{122a,122b}, E. E. Khoda¹⁷⁵, A. Khodinov¹⁶⁶, T. J. Kho⁵⁴, E. Khramov⁷⁹, J. Khubua^{159b}, S. Kido⁸², M. Kiehn⁵⁴, C. R. Kilby⁹³, Y. K. Kim³⁷, N. Kimura^{66a,66c}, O. M. Kind¹⁹, B. T. King^{90.*}, D. Kirchmeier⁴⁸, J. Kirk¹⁴⁴, A. E. Kiryunin¹¹⁵, T. Kishimoto¹⁶³, D. P. Kisliuk¹⁶⁷, V. Kitali⁴⁶, O. Kivernyk⁵, E. Kladiva^{28b.*}, T. Klapdor-Kleingrothaus⁵², M. Klassen^{61a}, M. H. Klein¹⁰⁵, M. Klein⁹⁰, U. Klein⁹⁰, K. Kleinknecht⁹⁹, P. Klimek¹²¹, A. Klimentov²⁹, T. Klingl²⁴, T. Klioutchnikova³⁶, F. F. Klitzner¹¹⁴, P. Kluit¹²⁰, S. Kluth¹¹⁵, E. Kneringer⁷⁶, E. B. F. G. Knoops¹⁰¹, A. Knue⁵², D. Kobayashi⁸⁷, T. Kobayashi¹⁶³, M. Kobel⁴⁸, M. Kocian¹⁵³, P. Kodys¹⁴³, P. T. Koenig²⁴, T. Koffas³⁴, N. M. Köhler¹¹⁵, T. Koi¹⁵³, M. Kolb^{61b}, I. Koletsou⁵, T. Komarek¹³⁰, T. Kondo⁸¹, N. Kondrashova^{60c}, K. Köneke⁵², A. C. König¹¹⁹, T. Kono¹²⁵, R. Konoplich^{124.an}, V. Konstantinides⁹⁴, N. Konstantinidis⁹⁴, B. Konya⁹⁶, R. Kopeliansky⁶⁵, S. Koperny^{83a}, K. Korcyl⁸⁴, K. Kordas¹⁶², G. Koren¹⁶¹, A. Korn⁹⁴, I. Korolkov¹⁴, E. V. Korolkova¹⁴⁹, N. Korotkova¹¹³, O. Kortner¹¹⁵, S. Kortner¹¹⁵, T. Kosek¹⁴³, V. V. Kostyukhin²⁴, A. Kotwal⁴⁹, A. Koulouris¹⁰, A. Kourkoumeli-Charalampidi^{70a,70b}, C. Kourkoumelis⁹, E. Kourlitis¹⁴⁹, V. Kouskoura²⁹, A. B. Kowalewska⁸⁴, R. Kowalewski¹⁷⁶, C. Kozakai¹⁶³, W. Kozanecki¹⁴⁵, A. S. Kozhin¹²³, V. A. Kramarenko¹¹³, G. Kramberger⁹¹, D. Krasnoperov^{60a}, M. W. Krasny¹³⁶, A. Krasznahorkay³⁶, D. Krauss¹¹⁵, J. A. Kremer^{83a}, J. Kretzschmar⁹⁰, P. Krieger¹⁶⁷, F. Krieter¹¹⁴, A. Krishnan^{61b}, K. Krizka¹⁸, K. Kroeninger⁴⁷, H. Kroha¹¹⁵, J. Kroll¹⁴¹, J. Kroll¹³⁷, J. Krstic¹⁶, U. Kruchonak⁷⁹, H. Krüger²⁴, N. Krumnack⁷⁸, M. C. Kruse⁴⁹, J. A. Krzysiak⁸⁴, T. Kubota¹⁰⁴, S. Kuday^{4b}, J. T. Kuechler⁴⁶, S. Kuehn³⁶, A. Kugel^{61a}, T. Kuhl⁴⁶, V. Kukhtin⁷⁹, R. Kukla¹⁰¹, Y. Kulchitsky^{107.aj}, S. Kuleshov^{147b}, Y. P. Kulinich¹⁷³, M. Kuna⁵⁸, T. Kunigo⁸⁵, A. Kupco¹⁴¹, T. Kupfer⁴⁷, O. Kuprash⁵², H. Kurashige⁸², L. L. Kurchaninov^{168a}, Y. A. Kurochkin¹⁰⁷, A. Kurova¹¹², M. G. Kurth^{15a,15d}, E. S. Kuwertz³⁶, M. Kuze¹⁶⁵, A. K. Kvam¹⁴⁸, J. Kvita¹³⁰, T. Kwan¹⁰³, A. La Rosa¹¹⁵, L. La Rotonda^{41a,41b}, F. La Ruffa^{41a,41b}, C. Lacasta¹⁷⁴, F. Lacava^{72a,72b}, D. P. J. Lack¹⁰⁰, H. Lacker¹⁹, D. Lacour¹³⁶, E. Ladygin⁷⁹, R. Lafaye⁵, B. Laforge¹³⁶, T. Lagouri^{33c}, S. Lai⁵³, S. Lammers⁶⁵, W. Lampl⁷, C. Lampoudis¹⁶², E. Lançon²⁹, U. Landgraf⁵², M. P. J. Landon⁹², M. C. Lanfermann⁵⁴, V. S. Lang⁴⁶, J. C. Lange⁵³, R. J. Langenberg³⁶, A. J. Lankford¹⁷¹, F. Lanni²⁹, K. Lantzsch²⁴, A. Lanza^{70a}, A. Lapertosa^{55a,55b}, S. Laplace¹³⁶, J. F. Laporte¹⁴⁵, T. Lari^{68a}, F. Lasagni Manghi^{23a,23b}, M. Lassnig³⁶, T. S. Lau^{63a}, A. Laudrain¹³², A. Laurier³⁴, M. Lavorgna^{69a,69b}, M. Lazzaroni^{68a,68b}, B. Le¹⁰⁴, O. Le Dortz¹³⁶, E. Le Guirriec¹⁰¹, M. LeBlanc⁷, T. LeCompte⁶, F. Ledroit-Guillon⁵⁸, C. A. Lee²⁹, G. R. Lee¹⁷, L. Lee⁵⁹, S. C. Lee¹⁵⁸, S. J. Lee³⁴, B. Lefebvre^{168a}, M. Lefebvre¹⁷⁶, F. Legger¹¹⁴, C. Leggett¹⁸, K. Lehmann¹⁵², N. Lehmann¹⁸², G. Lehmann Miotto³⁶, W. A. Leight⁴⁶, A. Leisos^{162.w}, M. A. L. Leite^{80d}, C. E. Leitgeb¹¹⁴, R. Leitner¹⁴³, D. Lellouch^{180.*}, K. J. C. Leney⁴², T. Lenz²⁴, B. Lenzi³⁶, R. Leone⁷, S. Leone^{71a}, C. Leonidopoulos⁵⁰, A. Leopold¹³⁶, G. Lerner¹⁵⁶, C. Leroy¹⁰⁹, R. Les¹⁶⁷, C. G. Lester³², M. Levchenko¹³⁸, J. Levêque⁵, D. Levin¹⁰⁵, L. J. Levinson¹⁸⁰, D. J. Lewis²¹, B. Li^{15b}, B. Li¹⁰⁵, C.-Q. Li^{60a}, F. Li^{60c}, H. Li^{60a}, H. Li^{60b}, J. Li^{60c}, K. Li¹⁵³, L. Li^{60c}, M. Li^{15a}, Q. Li^{15a,15d}, Q. Y. Li^{60a}, S. Li^{60c,60d}, X. Li⁴⁶, Y. Li⁴⁶, Z. Li^{60b}, Z. Liang^{15a}, B. Liberti^{73a}, A. Liblong¹⁶⁷, K. Lie^{63c}, S. Liem¹²⁰, C. Y. Lin³², K. Lin¹⁰⁶, T. H. Lin⁹⁹, R. A. Linck⁶⁵, J. H. Lindon²¹, A. L. Lioni⁵⁴, E. Lipeles¹³⁷, A. Lipniacka¹⁷, M. Lisovyi^{61b}, T. M. Liss^{173.au}, A. Lister¹⁷⁵, A. M. Litke¹⁴⁶

J. D. Little⁸, B. Liu^{78.ac}, B. L. Liu⁶, H. B. Liu²⁹, H. Liu¹⁰⁵, J. B. Liu^{60a}, J. K. K. Liu¹³⁵, K. Liu¹³⁶, M. Liu^{60a}, P. Liu¹⁸, Y. Liu^{15a,15d}, Y. L. Liu¹⁰⁵, Y. W. Liu^{60a}, M. Livan^{70a,70b}, A. Lleres⁵⁸, J. Llorente Merino^{15a}, S. L. Lloyd⁹², C. Y. Lo^{63b}, F. Lo Sterzo⁴², E. M. Lobodzinska⁴⁶, P. Loch⁷, S. Loffredo^{73a,73b}, T. Lohse¹⁹, K. Lohwasser¹⁴⁹, M. Lokajicek¹⁴¹, J. D. Long¹⁷³, R. E. Long⁸⁹, L. Longo³⁶, K. A. Looper¹²⁶, J. A. Lopez^{147b}, I. Lopez Paz¹⁰⁰, A. Lopez Solis¹⁴⁹, J. Lorenz¹¹⁴, N. Lorenzo Martinez⁵, M. Losada²², P. J. Lösel¹¹⁴, A. Lösle⁵², X. Lou⁴⁶, X. Lou^{15a}, A. Lounis¹³², J. Love⁶, P. A. Love⁸⁹, J. J. Lozano Bahilo¹⁷⁴, M. Lu^{60a}, Y. J. Lu⁶⁴, H. J. Lubatti¹⁴⁸, C. Luci^{72a,72b}, A. Lucotte⁵⁸, C. Luedtke⁵², F. Luehring⁶⁵, I. Luise¹³⁶, L. Luminari^{72a}, B. Lund-Jensen¹⁵⁴, M. S. Lutz¹⁰², D. Lynn²⁹, R. Lysak¹⁴¹, E. Lytken⁹⁶, F. Lyu^{15a}, V. Lyubushkin⁷⁹, T. Lyubushkina⁷⁹, H. Ma²⁹, L. L. Ma^{60b}, Y. Ma^{60b}, G. Maccarrone⁵¹, A. Macchiolo¹¹⁵, C. M. Macdonald¹⁴⁹, J. Machado Miguens¹³⁷, D. Madaffari¹⁷⁴, R. Madar³⁸, W. F. Mader⁴⁸, N. Madysa⁴⁸, J. Maeda⁸², K. Maekawa¹⁶³, S. Maeland¹⁷, T. Maeno²⁹, M. Maerker⁴⁸, A. S. Maevskiy¹¹³, V. Magerl⁵², N. Magini⁷⁸, D. J. Mahon³⁹, C. Maidantchik^{80b}, T. Maier¹¹⁴, A. Maio^{140a,140b,140d}, O. Majersky^{28a}, S. Majewski¹³¹, Y. Makida⁸¹, N. Makovec¹³², B. Malaescu¹³⁶, Pa. Malecki⁸⁴, V. P. Maleev¹³⁸, F. Malek⁵⁸, U. Mallik⁷⁷, D. Malon⁶, C. Malone³², S. Maltezos¹⁰, S. Malyukov³⁶, J. Mamuzic¹⁷⁴, G. Mancini⁵¹, I. Mandić⁹¹, L. Manhaes de Andrade Filho^{80a}, I. M. Maniatis¹⁶², J. Manjarres Ramos⁴⁸, K. H. Mankinen⁹⁶, A. Mann¹¹⁴, A. Manousos⁷⁶, B. Mansoulie¹⁴⁵, I. Manthos¹⁶², S. Manzoni¹²⁰, A. Marantis¹⁶², G. Marcea³⁰, L. Marchese¹³⁵, G. Marchiori¹³⁶, M. Marcisovsky¹⁴¹, C. Marcon⁹⁶, C. A. Marin Tobon³⁶, M. Marjanovic³⁸, F. Marroquim^{80b}, Z. Marshall¹⁸, M. U. F. Martensson¹⁷², S. Marti-Garcia¹⁷⁴, C. B. Martin¹²⁶, T. A. Martin¹⁷⁸, V. J. Martin⁵⁰, B. Martin dit Latour¹⁷, L. Martinelli^{74a,74b}, M. Martinez^{14.x}, V. I. Martinez Outschoorn¹⁰², S. Martin-Haugh¹⁴⁴, V. S. Martoiu^{27b}, A. C. Martyniuk⁹⁴, A. Marzin³⁶, S. R. Maschek¹¹⁵, L. Masetti⁹⁹, T. Mashimo¹⁶³, R. Mashinistov¹¹⁰, J. Masik¹⁰⁰, A. L. Maslennikov^{122a,122b}, L. H. Mason¹⁰⁴, L. Massa^{73a,73b}, P. Massarotti^{69a,69b}, P. Mastrandrea^{71a,71b}, A. Mastroberardino^{41a,41b}, T. Masubuchi¹⁶³, A. Matic¹¹⁴, P. Mättig²⁴, J. Maurer^{27b}, B. Maček⁹¹, S. J. Maxfield⁹⁰, D. A. Maximov^{122a,122b}, R. Mazini¹⁵⁸, I. Maznas¹⁶², S. M. Mazza¹⁴⁶, S. P. Mc Kee¹⁰⁵, T. G. McCarthy¹¹⁵, L. I. McClymont⁹⁴, W. P. McCormack¹⁸, E. F. McDonald¹⁰⁴, J. A. McFayden³⁶, M. A. McKay⁴², K. D. McLean¹⁷⁶, S. J. McMahan¹⁴⁴, P. C. McNamara¹⁰⁴, C. J. McNicol¹⁷⁸, R. A. McPherson^{176.ad}, J. E. Mdhului^{33c}, Z. A. Meadows¹⁰², S. Meehan¹⁴⁸, T. Megy⁵², S. Mehlhase¹¹⁴, A. Mehta⁹⁰, T. Meideck⁵⁸, B. Meirose⁴³, D. Melini¹⁷⁴, B. R. Mellado Garcia^{33c}, J. D. Mellenthin⁵³, M. Melo^{28a}, F. Meloni⁴⁶, A. Melzer²⁴, S. B. Menary¹⁰⁰, E. D. Mendes Gouveia^{140a,140e}, L. Meng³⁶, X. T. Meng¹⁰⁵, S. Menke¹¹⁵, E. Meoni^{41a,41b}, S. Mergelmeyer¹⁹, S. A. M. Merkt¹³⁹, C. Merlassino²⁰, P. Mermod⁵⁴, L. Merola^{69a,69b}, C. Meroni^{68a}, O. Meshkov^{113,110}, J. K. R. Meshreki¹⁵¹, A. Messina^{72a,72b}, J. Metcalfe⁶, A. S. Mete¹⁷¹, C. Meyer⁶⁵, J. Meyer¹⁶⁰, J.-P. Meyer¹⁴⁵, H. Meyer Zu Theenhausen^{61a}, F. Miano¹⁵⁶, R. P. Middleton¹⁴⁴, L. Mijović⁵⁰, G. Mikenberg¹⁸⁰, M. Mikestikova¹⁴¹, M. Mikuz⁹¹, H. Mildner¹⁴⁹, M. Milesi¹⁰⁴, A. Milic¹⁶⁷, D. A. Millar⁹², D. W. Miller³⁷, A. Milov¹⁸⁰, D. A. Milstead^{45a,45b}, R. A. Mina^{153.p}, A. A. Minaenko¹²³, M. Miñano Moya¹⁷⁴, I. A. Minashvili^{159b}, A. I. Mincer¹²⁴, B. Mindur^{83a}, M. Mineev⁷⁹, Y. Minegishi¹⁶³, Y. Ming¹⁸¹, L. M. Mir¹⁴, A. Mirto^{67a,67b}, K. P. Mistry¹³⁷, T. Mitani¹⁷⁹, J. Mitrevski¹¹⁴, V. A. Mitsou¹⁷⁴, M. Mittal^{60c}, A. Miucci²⁰, P. S. Miyagawa¹⁴⁹, A. Mizukami⁸¹, J. U. Mjörnmark⁹⁶, T. Mkrtychyan¹⁸⁴, M. Mlynarikova¹⁴³, T. Moa^{45a,45b}, K. Mochizuki¹⁰⁹, P. Mogg⁵², S. Mohapatra³⁹, R. Moles-Valls²⁴, M. C. Mondragon¹⁰⁶, K. Mönig⁴⁶, J. Monk⁴⁰, E. Monnier¹⁰¹, A. Montalbano¹⁵², J. Montejo Berlingen³⁶, M. Montella⁹⁴, F. Monticelli⁸⁸, S. Monzani^{68a}, N. Morange¹³², D. Moreno²², M. Moreno Llácer³⁶, C. Moreno Martinez¹⁴, P. Morettini^{55b}, M. Morgenstern¹²⁰, S. Morgenstern⁴⁸, D. Mori¹⁵², M. Morii⁵⁹, M. Morinaga¹⁷⁹, V. Morisbak¹³⁴, A. K. Morley³⁶, G. Mornacchi³⁶, A. P. Morris⁹⁴, L. Morvaj¹⁵⁵, P. Moschovakos³⁶, B. Moser¹²⁰, M. Mosidze^{159b}, T. Moskalets¹⁴⁵, H. J. Moss¹⁴⁹, J. Moss^{31.m}, K. Motohashi¹⁶⁵, E. Mountricha³⁶, E. J. W. Moyse¹⁰², S. Muanza¹⁰¹, J. Mueller¹³⁹, R. S. P. Mueller¹¹⁴, D. Muenstermann⁸⁹, G. A. Mullier⁹⁶, J. L. Munoz Martinez¹⁴, F. J. Munoz Sanchez¹⁰⁰, P. Murin^{28b}, W. J. Murray^{178,144}, A. Murrone^{68a,68b}, M. Muškinja¹⁸, C. Mwewa^{33a}, A. G. Myagkov^{123,ao}, J. Myers¹³¹, M. Myska¹⁴², B. P. Nachman¹⁸, O. Nackenhorst⁴⁷, A. Nag Nag⁴⁸, K. Nagai¹³⁵, K. Nagano⁸¹, Y. Nagasaka⁶², M. Nagel⁵², E. Nagy¹⁰¹, A. M. Nairz³⁶, Y. Nakahama¹¹⁷, K. Nakamura⁸¹, T. Nakamura¹⁶³, I. Nakano¹²⁷, H. Nanjo¹³³, F. Napolitano^{61a}, R. F. Naranjo Garcia⁴⁶, R. Narayan⁴², D. I. Narriars Villar^{61a}, I. Naryshkin¹³⁸, T. Naumann⁴⁶, G. Navarro²², H. A. Neal^{105.*}, P. Y. Nechaeva¹¹⁰, F. Nechansky⁴⁶, T. J. Neep²¹, A. Negri^{70a,70b}, M. Negrini^{23b}, C. Nellist⁵³, M. E. Nelson¹³⁵, S. Nemecek¹⁴¹, P. Nemethy¹²⁴, M. Nessi^{36.d}, M. S. Neubauer¹⁷³, M. Neumann¹⁸², P. R. Newman²¹, T. Y. Ng^{63c}, Y. S. Ng¹⁹, Y. W. Y. Ng¹⁷¹, H. D. N. Nguyen¹⁰¹, T. Nguyen Manh¹⁰⁹, E. Nibigira³⁸, R. B. Nickerson¹³⁵, R. Nicolaidou¹⁴⁵, D. S. Nielsen⁴⁰, J. Nielsen¹⁴⁶, N. Nikiforou¹¹, V. Nikolaenko^{123,ao}, I. Nikolic-Audit¹³⁶, K. Nikolopoulos²¹, P. Nilsson²⁹, H. R. Nindhito⁵⁴, Y. Ninomiya⁸¹, A. Nisati^{72a}, N. Nishu^{60c}, R. Nisius¹¹⁵, I. Nitsche⁴⁷, T. Nitta¹⁷⁹, T. Nobe¹⁶³, Y. Noguchi⁸⁵, I. Nomidis¹³⁶, M. A. Nomura²⁹, M. Nordberg³⁶, N. Norjoharuddeen¹³⁵, T. Novak⁹¹, O. Novgorodova⁴⁸, R. Novotny¹⁴², L. Nozka¹³⁰, K. Ntekas¹⁷¹, E. Nurse⁹⁴, F. G. Oakham^{34.ax}, H. Oberlack¹¹⁵, J. Ocariz¹³⁶, A. Ochi⁸², I. Ochoa³⁹, J. P. Ochoa-Ricoux^{147a}, K. O'Connor²⁶, S. Oda⁸⁷, S. Odaka⁸¹, S. Oerdek⁵³, A. Ogrodnik^{83a}, A. Oh¹⁰⁰, S. H. Oh⁴⁹, C. C. Ohm¹⁵⁴, H. Oide^{55a,55b}, M. L. Ojeda¹⁶⁷, H. Okawa¹⁶⁹, Y. Okazaki⁸⁵, Y. Okumura¹⁶³, T. Okuyama⁸¹, A. Olariu^{27b}, L. F. Oleiro Seabra^{140a}, S. A. Olivares Pino^{147a}, D. Oliveira Damazio²⁹, J. L. Oliver¹, M. J. R. Olsson¹⁷¹,

A. Olszewski⁸⁴, J. Olszowska⁸⁴, D. C. O’Neil¹⁵², A. Onofre^{140a,140e}, K. Onogi¹¹⁷, P. U. E. Onyisi¹¹, H. Oppen¹³⁴, M. J. Oreglia³⁷, G. E. Orellana⁸⁸, Y. Oren¹⁶¹, D. Orestano^{74a,74b}, N. Orlando¹⁴, R. S. Orr¹⁶⁷, V. O’Shea⁵⁷, R. Ospanov^{60a}, G. Otero y Garzon³⁰, H. Otono⁸⁷, M. Ouchrif^{35d}, J. Ouellette²⁹, F. Ould-Saada¹³⁴, A. Ouraou¹⁴⁵, Q. Ouyang^{15a}, M. Owen⁵⁷, R. E. Owen²¹, V. E. Ozcan^{12c}, N. Ozturk⁸, J. Pacalt¹³⁰, H. A. Pacey³², K. Pachal⁴⁹, A. Pacheco Pages¹⁴, C. Padilla Aranda¹⁴, S. Pagan Griso¹⁸, M. Paganini¹⁸³, G. Palacino⁶⁵, S. Palazzo⁵⁰, S. Palestini³⁶, M. Palka^{83b}, D. Pallin³⁸, I. Panagoulas¹⁰, C. E. Pandini³⁶, J. G. Panduro Vazquez⁹³, P. Pani⁴⁶, G. Panizzo^{66a,66c}, L. Paolozzi⁵⁴, C. Papadatos¹⁰⁹, K. Papageorgiou^{9,h}, A. Paramonov⁶, D. Paredes Hernandez^{63b}, S. R. Paredes Saenz¹³⁵, B. Parida¹⁶⁶, T. H. Park¹⁶⁷, A. J. Parker⁸⁹, M. A. Parker³², F. Parodi^{55a,55b}, E. W. P. Parrish¹²¹, J. A. Parsons³⁹, U. Parzefall⁵², L. Pascual Dominguez¹³⁶, V. R. Pascuzzi¹⁶⁷, J. M. P. Pasner¹⁴⁶, E. Pasqualucci^{72a}, S. Passaggio^{55b}, F. Pastore⁹³, P. Pasuwan^{45a,45b}, S. Pataraja⁹⁹, J. R. Pater¹⁰⁰, A. Pathak¹⁸¹, T. Pauly³⁶, B. Pearson¹¹⁵, M. Pedersen¹³⁴, L. Pedraza Diaz¹¹⁹, R. Pedro^{140a}, T. Peiffer⁵³, S. V. Peleganchuk^{122a,122b}, O. Penc¹⁴¹, H. Peng^{60a}, B. S. Peralva^{80a}, M. M. Perego¹³², A. P. Pereira Peixoto^{140a}, D. V. Perepelitsa²⁹, F. Peri¹⁹, L. Perini^{68a,68b}, H. Pernegger³⁶, S. Perrella^{69a,69b}, K. Peters⁴⁶, R. F. Y. Peters¹⁰⁰, B. A. Petersen³⁶, T. C. Petersen⁴⁰, E. Petit¹⁰¹, A. Petridis¹, C. Petridou¹⁶², P. Petroff¹³², M. Petrov¹³⁵, F. Petrucci^{74a,74b}, M. Pettee¹⁸³, N. E. Pettersson¹⁰², K. Petukhova¹⁴³, A. Peyaud¹⁴⁵, R. Pezoa^{147b}, L. Pezzotti^{70a,70b}, T. Pham¹⁰⁴, F. H. Phillips¹⁰⁶, P. W. Phillips¹⁴⁴, M. W. Phipps¹⁷³, G. Piacquadio¹⁵⁵, E. Pianori¹⁸, A. Picazio¹⁰², R. H. Pickles¹⁰⁰, R. Piegai³⁰, D. Pietreanu^{27b}, J. E. Pilcher³⁷, A. D. Pilkington¹⁰⁰, M. Pinamonti^{73a,73b}, J. L. Pinfold³, M. Pitt¹⁸⁰, L. Pizzimento^{73a,73b}, M.-A. Pleier²⁹, V. Pleskot¹⁴³, E. Plotnikova⁷⁹, D. Pluth⁷⁸, P. Podberezko^{122a,122b}, R. Poettgen⁹⁶, R. Poggi⁵⁴, L. Poggioli¹³², I. Pogrebnyak¹⁰⁶, D. Pohl²⁴, I. Pokharel⁵³, G. Polesello^{70a}, A. Poley¹⁸, A. Policicchio^{72a,72b}, R. Polifka¹⁴³, A. Polini^{23b}, C. S. Pollard⁴⁶, V. Polychronakos²⁹, D. Ponomarenko¹¹², L. Pontecorvo³⁶, S. Popa^{27a}, G. A. Popeneciu^{27d}, D. M. Portillo Quintero⁵⁸, S. Pospisil¹⁴², K. Potamianos⁴⁶, I. N. Potrap⁷⁹, C. J. Potter³², H. Potti¹¹, T. Poulsen⁹⁶, J. Poveda³⁶, T. D. Powell¹⁴⁹, G. Pownall⁴⁶, M. E. Pozo Astigarraga³⁶, P. Pralavorio¹⁰¹, S. Prell⁷⁸, D. Price¹⁰⁰, M. Primavera^{67a}, S. Prince¹⁰³, M. L. Proffitt¹⁴⁸, N. Proklova¹¹², K. Prokofiev^{63c}, F. Prokoshin⁷⁹, S. Protopopescu²⁹, J. Proudfoot⁶, M. Przybycien^{83a}, D. Pudzha¹³⁸, A. Puri¹⁷³, P. Puzo¹³², J. Qian¹⁰⁵, Y. Qin¹⁰⁰, A. Quadt⁵³, M. Queitsch-Maitland⁴⁶, A. Qureshi¹, P. Rados¹⁰⁴, F. Ragusa^{68a,68b}, G. Rahal⁹⁷, J. A. Raine⁵⁴, S. Rajagopalan²⁹, A. Ramirez Morales⁹², K. Ran^{15a,15d}, T. Rashid¹³², S. Raspopov⁵, M. G. Ratti^{68a,68b}, D. M. Rauch⁴⁶, F. Rauscher¹¹⁴, S. Rave⁹⁹, B. Ravina¹⁴⁹, I. Ravinovich¹⁸⁰, J. H. Rawling¹⁰⁰, M. Raymond³⁶, A. L. Read¹³⁴, N. P. Readioff⁵⁸, M. Reale^{67a,67b}, D. M. Rebuffi^{70a,70b}, A. Redelbach¹⁷⁷, G. Redlinger²⁹, K. Reeves⁴³, L. Rehnisch¹⁹, J. Reichert¹³⁷, D. Reikher¹⁶¹, A. Reiss⁹⁹, A. Rej¹⁵¹, C. Rembser³⁶, M. Renda^{27b}, M. Rescigno^{72a}, S. Resconi^{68a}, E. D. Resseguie¹³⁷, S. Rettie¹⁷⁵, E. Reynolds²¹, O. L. Rezanova^{122a,122b}, P. Reznicek¹⁴³, E. Ricci^{75a,75b}, R. Richter¹¹⁵, S. Richter⁴⁶, E. Richter-Was^{83b}, O. Ricken²⁴, M. Ridel¹³⁶, P. Rieck¹¹⁵, C. J. Riegel¹⁸², O. Rifki⁴⁶, M. Rijssenbeek¹⁵⁵, A. Rimoldi^{70a,70b}, M. Rimoldi⁴⁶, L. Rinaldi^{23b}, G. Ripellino¹⁵⁴, B. Ristic⁸⁹, E. Ritsch³⁶, I. Riu¹⁴, J. C. Rivera Vergara¹⁷⁶, F. Rizatdinova¹²⁹, E. Rizvi⁹², C. Rizzi³⁶, R. T. Roberts¹⁰⁰, S. H. Robertson^{103,ad}, M. Robin⁴⁶, D. Robinson³², J. E. M. Robinson⁴⁶, C. M. Robles Gajardo^{147b}, A. Robson⁵⁷, E. Rocco⁹⁹, C. Roda^{71a,71b}, S. Rodriguez Bosca¹⁷⁴, A. Rodriguez Perez¹⁴, D. Rodriguez Rodriguez¹⁷⁴, A. M. Rodríguez Vera^{168b}, S. Roe³⁶, O. Røhne¹³⁴, R. Röhrig¹¹⁵, C. P. A. Roland⁶⁵, J. Roloff⁵⁹, A. Romaniouk¹¹², M. Romano^{23a,23b}, N. Rompotis⁹⁰, M. Ronzani¹²⁴, L. Roos¹³⁶, S. Rosati^{72a}, K. Rosbach⁵², G. Rosin¹⁰², B. J. Rosser¹³⁷, E. Rossi⁴⁶, E. Rossi^{74a,74b}, E. Rossi^{69a,69b}, L. P. Rossi^{55b}, L. Rossini^{68a,68b}, R. Rosten¹⁴, M. Rotaru^{27b}, J. Rothberg¹⁴⁸, D. Rousseau¹³², G. Rovelli^{70a,70b}, D. Roy^{33c}, A. Rozanov¹⁰¹, Y. Rozen¹⁶⁰, X. Ruan^{33c}, F. Rubbo¹⁵³, F. Rühr⁵², A. Ruiz-Martinez¹⁷⁴, A. Rummeler³⁶, Z. Rurikova⁵², N. A. Rusakovich⁷⁹, H. L. Russell¹⁰³, L. Rustige^{38,47}, J. P. Rutherford⁷, E. M. Rüttinger^{46,j}, Y. F. Ryabov¹³⁸, M. Rybar³⁹, G. Rybkin¹³², A. Ryzhov¹²³, G. F. Rzehorz⁵³, P. Sabatini⁵³, G. Sabato¹²⁰, S. Sacerdoti¹³², H.F.-W. Sadrozinski¹⁴⁶, R. Sadykov⁷⁹, F. Safai Tehrani^{72a}, B. Safarzadeh Samani¹⁵⁶, P. Saha¹²¹, S. Saha¹⁰³, M. Sahinsoy^{61a}, A. Sahu¹⁸², M. Saimpert⁴⁶, M. Saito¹⁶³, T. Saito¹⁶³, H. Sakamoto¹⁶³, A. Sakharov^{124,an}, D. Salamani⁵⁴, G. Salamanna^{74a,74b}, J. E. Salazar Loyola^{147b}, P. H. Sales De Bruin¹⁷², D. Salihagic^{115,*}, A. Salnikov¹⁵³, J. Salt¹⁷⁴, D. Salvatore^{41a,41b}, F. Salvatore¹⁵⁶, A. Salvucci^{63a,63b,63c}, A. Salzburger³⁶, J. Samarati³⁶, D. Sammel⁵², D. Sampsonidis¹⁶², D. Sampsonidou¹⁶², J. Sánchez¹⁷⁴, A. Sanchez Pineda^{66a,66c}, H. Sandaker¹³⁴, C. O. Sander⁴⁶, I. G. Sanderswood⁸⁹, M. Sandhoff¹⁸², C. Sandoval²², D. P. C. Sankey¹⁴⁴, M. Sannino^{55a,55b}, Y. Sano¹¹⁷, A. Sansoni⁵¹, C. Santoni³⁸, H. Santos^{140a,140b}, S. N. Santpur¹⁸, A. Santra¹⁷⁴, A. Saponov⁷⁹, J. G. Saraiva^{140a,140d}, O. Sasaki⁸¹, K. Sato¹⁶⁹, E. Sauvan⁵, P. Savard^{167,ax}, N. Savic¹¹⁵, R. Sawada¹⁶³, C. Sawyer¹⁴⁴, L. Sawyer^{95,al}, C. Sbarra^{23b}, A. Sbrizzi^{23a}, T. Scanlon⁹⁴, J. Schaarschmidt¹⁴⁸, P. Schacht¹¹⁵, B. M. Schachtner¹¹⁴, D. Schaefer³⁷, L. Schaefer¹³⁷, J. Schaeffer⁹⁹, S. Schaepe³⁶, U. Schäfer⁹⁹, A. C. Schaffer¹³², D. Schaille¹¹⁴, R. D. Schamberger¹⁵⁵, N. Scharmberg¹⁰⁰, V. A. Schegelsky¹³⁸, D. Scheirich¹⁴³, F. Schenck¹⁹, M. Schernau¹⁷¹, C. Schiavi^{55a,55b}, S. Schier¹⁴⁶, L. K. Schildgen²⁴, Z. M. Schillaci²⁶, E. J. Schioppa³⁶, M. Schioppa^{41a,41b}, K. E. Schleicher⁵², S. Schlenker³⁶, K. R. Schmidt-Sommerfeld¹¹⁵, K. Schmieden³⁶, C. Schmitt⁹⁹, S. Schmitt⁴⁶, S. Schmitz⁹⁹, J. C. Schmoeckel⁴⁶, U. Schnoor⁵², L. Schoeffel¹⁴⁵, A. Schoening^{61b}, P. G. Scholer⁵²,

E. Schopf¹³⁵, M. Schott⁹⁹, J. F. P. Schouwenberg¹¹⁹, J. Schovancova³⁶, S. Schramm⁵⁴, F. Schroeder¹⁸², A. Schulte⁹⁹, H.-C. Schultz-Coulon^{61a}, M. Schumacher⁵², B. A. Schumm¹⁴⁶, Ph. Schune¹⁴⁵, A. Schwartzman¹⁵³, T. A. Schwarz¹⁰⁵, Ph. Schwemling¹⁴⁵, R. Schwienhorst¹⁰⁶, A. Sciandra¹⁴⁶, G. Sciolla²⁶, M. Scodreggio⁴⁶, M. Scornajenghi^{41a,41b}, F. Scuri^{71a}, F. Scutti¹⁰⁴, L. M. Scyboz¹¹⁵, C. D. Sebastiani^{72a,72b}, P. Seema¹⁹, S. C. Seidel¹¹⁸, A. Seiden¹⁴⁶, T. Seiss³⁷, J. M. Seixas^{80b}, G. Sekhniaidze^{69a}, K. Sekhon¹⁰⁵, S. J. Sekula⁴², N. Semprini-Cesari^{23a,23b}, S. Sen⁴⁹, S. Senkin³⁸, C. Serfon⁷⁶, L. Serin¹³², L. Serkin^{66a,66b}, M. Sessa^{60a}, H. Severini¹²⁸, F. Sforza¹⁷⁰, A. Sfyrly⁵⁴, E. Shabalina⁵³, J. D. Shahinian¹⁴⁶, N. W. Shaikh^{45a,45b}, D. Shaked Renous¹⁸⁰, L. Y. Shan^{15a}, R. Shang¹⁷³, J. T. Shank²⁵, M. Shapiro¹⁸, A. Sharma¹³⁵, A. S. Sharma¹, P. B. Shatalov¹¹¹, K. Shaw¹⁵⁶, S. M. Shaw¹⁰⁰, A. Shcherbakova¹³⁸, Y. Shen¹²⁸, N. Sherafati³⁴, A. D. Sherman²⁵, P. Sherwood⁹⁴, L. Shi^{158.at}, S. Shimizu⁸¹, C. O. Shimmin¹⁸³, Y. Shimogama¹⁷⁹, M. Shimojima¹¹⁶, I. P. J. Shipsey¹³⁵, S. Shirabe⁸⁷, M. Shiyakova^{79.aa}, J. Shlomi¹⁸⁰, A. Shmeleva¹¹⁰, M. J. Shochet³⁷, S. Shojaii¹⁰⁴, D. R. Shope¹²⁸, S. Shrestha¹²⁶, E. Shulga¹⁸⁰, P. Sicho¹⁴¹, A. M. Sickles¹⁷³, P. E. Sidebo¹⁵⁴, E. Sideras Haddad^{33c}, O. Sidiropoulou³⁶, A. Sidoti^{23a,23b}, F. Siegert⁴⁸, Dj. Sijacki¹⁶, M. Silva Jr.¹⁸¹, M. V. Silva Oliveira^{80a}, S. B. Silverstein^{45a}, S. Simion¹³², E. Simioni⁹⁹, R. Simoniello⁹⁹, S. Simsek^{12b}, P. Sinervo¹⁶⁷, N. B. Sinev¹³¹, M. Sioli^{23a,23b}, I. Siral¹⁰⁵, S. Yu. Sivoklov¹¹³, J. Sjölin^{45a,45b}, E. Skorda⁹⁶, P. Skubic¹²⁸, M. Slawinska⁸⁴, K. Sliwa¹⁷⁰, R. Slovak¹⁴³, V. Smakhtin¹⁸⁰, B. H. Smart¹⁴⁴, J. Smiesko^{28a}, N. Smirnov¹¹², S. Yu. Smirnov¹¹², Y. Smirnov¹¹², L. N. Smirnova^{113.t}, O. Smirnova⁹⁶, J. W. Smith⁵³, M. Smizanska⁸⁹, K. Smolek¹⁴², A. Smykiewicz⁸⁴, A. A. Snesarev¹¹⁰, H. L. Snoek¹²⁰, I. M. Snyder¹³¹, S. Snyder²⁹, R. Sobie^{176.ad}, A. M. Soffa¹⁷¹, A. Soffer¹⁶¹, A. Sogaard⁵⁰, F. Sohns⁵³, C. A. Solans Sanchez³⁶, E. Yu. Soldatov¹¹², U. Soldevila¹⁷⁴, A. A. Solodkov¹²³, A. Soloshenko⁷⁹, O. V. Solovyanov¹²³, V. Solovye¹³⁸, P. Sommer¹⁴⁹, H. Son¹⁷⁰, W. Song¹⁴⁴, W. Y. Song^{168b}, A. Sopczak¹⁴², F. Sopkova^{28b}, C. L. Sotiropoulou^{71a,71b}, S. Sottocornola^{70a,70b}, R. Soualah^{66a,66c.g}, A. M. Soukharev^{122a,122b}, D. South⁴⁶, S. Spagnolo^{67a,67b}, M. Spalla¹¹⁵, M. Spangenberg¹⁷⁸, F. Spano⁹³, D. Sperlich⁵², T. M. Spieker^{61a}, R. Spighi^{23b}, G. Spigo³⁶, M. Spina¹⁵⁶, D. P. Spiteri⁷, M. Spousta¹⁴³, A. Stabile^{68a,68b}, B. L. Stamas¹²¹, R. Stamen^{61a}, M. Stamenkovic¹²⁰, E. Stanecka⁸⁴, R. W. Stanek⁶, B. Stanislaus¹³⁵, M. M. Stanitzki⁴⁶, M. Stankaityte¹³⁵, B. Stapf¹²⁰, E. A. Starchenko¹²³, G. H. Stark¹⁴⁶, J. Stark⁵⁸, S. H. Stark⁴⁰, P. Staroba¹⁴¹, P. Starovoitov^{61a}, S. Stärz¹⁰³, R. Staszewski⁸⁴, G. Stavropoulos⁴⁴, M. Stegler⁴⁶, P. Steinberg²⁹, A. L. Steinhebel¹³¹, B. Stelzer¹⁵², H. J. Stelzer¹³⁹, O. Stelzer-Chilton^{168a}, H. Stenzel⁵⁶, T. J. Stevenson¹⁵⁶, G. A. Stewart³⁶, M. C. Stockton³⁶, G. Stoicica^{27b}, M. Stolarski^{140a}, P. Stolte⁵³, S. Stonjek¹¹⁵, A. Straessner⁴⁸, J. Strandberg¹⁵⁴, S. Strandberg^{45a,45b}, M. Strauss¹²⁸, P. Striznec^{28b}, R. Ströhmer¹⁷⁷, D. M. Strom¹³¹, R. Stroynowski⁴², A. Strubig⁵⁰, S. A. Stucci²⁹, B. Stugu¹⁷, J. Stupak¹²⁸, N. A. Styles⁴⁶, D. Su¹⁵³, S. Suchek^{61a}, V. V. Sulin¹¹⁰, M. J. Sullivan⁹⁰, D. M. S. Sultan⁵⁴, S. Sultansoy^{4c}, T. Sumida⁸⁵, S. Sun¹⁰⁵, X. Sun³, K. Suruliz¹⁵⁶, C. J. E. Suster¹⁵⁷, M. R. Sutton¹⁵⁶, S. Suzuki⁸¹, M. Svatos¹⁴¹, M. Swiatlowski³⁷, S. P. Swift², T. Swirski¹⁷⁷, A. Sydorenko⁹⁹, I. Sykora^{28a}, M. Sykora¹⁴³, T. Sykora¹⁴³, D. Ta⁹⁹, K. Tackmann^{46.y}, J. Taenzer¹⁶¹, A. Taffard¹⁷¹, R. Tafirout^{168a}, H. Takai²⁹, R. Takashima⁸⁶, K. Takeda⁸², T. Takeshita¹⁵⁰, E. P. Takeva⁵⁰, Y. Takubo⁸¹, M. Talby¹⁰¹, A. A. Talyshv^{122a,122b}, N. M. Tamir¹⁶¹, J. Tanaka¹⁶³, M. Tanaka¹⁶⁵, R. Tanaka¹³², S. Tapia Araya¹⁷³, S. Tapprogge⁹⁹, A. Tarek Abouelfadl Mohamed¹³⁶, S. Tarem¹⁶⁰, G. Tarna^{27b.c}, G. F. Tartarelli^{68a}, P. Tas¹⁴³, M. Tasevsky¹⁴¹, T. Tashiro⁸⁵, E. Tassi^{41a,41b}, A. Tavares Delgado^{140a,140b}, Y. Tayalati^{35e}, A. J. Taylor⁵⁰, G. N. Taylor¹⁰⁴, W. Taylor^{168b}, A. S. Tee⁸⁹, R. Teixeira De Lima¹⁵³, P. Teixeira-Dias⁹³, H. Ten Kate³⁶, J. J. Teoh¹²⁰, S. Terada⁸¹, K. Terashi¹⁶³, J. Terron⁹⁸, S. Terzo¹⁴, M. Testa⁵¹, R. J. Teuscher^{167.ad}, S. J. Thais¹⁸³, T. Theveneaux-Pelzer⁴⁶, F. Thiele⁴⁰, D. W. Thomas⁹³, J. O. Thomas⁴², J. P. Thomas²¹, A. S. Thompson⁵⁷, P. D. Thompson²¹, L. A. Thomsen¹⁸³, E. Thomson¹³⁷, Y. Tian³⁹, R. E. Tiede Torres⁵³, V. O. Tikhomirov^{110.ap}, Yu. A. Tikhonov^{122a,122b}, S. Timoshenko¹¹², P. Tipton¹⁸³, S. Tisserant¹⁰¹, K. Todome^{23a,23b}, S. Todorova-Nova⁵, S. Todt⁴⁸, J. Tojo⁸⁷, S. Tokár^{28a}, K. Tokushuku⁸¹, E. Tolley¹²⁶, K. G. Tomiwa^{33c}, M. Tomoto¹¹⁷, L. Tompkins^{153.p}, K. Toms¹¹⁸, B. Tong⁵⁹, P. Tornambe¹⁰², E. Torrence¹³¹, H. Torres⁴⁸, E. Torró Pastor¹⁴⁸, C. Toscizi¹³⁵, J. Toth^{101.ab}, D. R. Tovey¹⁴⁹, A. Traeet¹⁷, C. J. Treado¹²⁴, T. Trefzger¹⁷⁷, F. Tresoldi¹⁵⁶, A. Tricoli²⁹, I. M. Trigger^{168a}, S. Trincas-Duvoid¹³⁶, W. Trischuk¹⁶⁷, B. Trocmé⁵⁸, A. Trofymov¹³², C. Troncon^{68a}, M. Trovatelli¹⁷⁶, F. Trovato¹⁵⁶, L. Truong^{33b}, M. Trzebinski⁸⁴, A. Trzupek⁸⁴, F. Tsai⁴⁶, J.C.-L. Tseng¹³⁵, P. V. Tsiarehka^{107.aj}, A. Tsirigotis¹⁶², N. Tsirintanis⁹, V. Tsiskaridze¹⁵⁵, E. G. Tskhadadze^{159a}, M. Tsopoulou¹⁶², I. I. Tsukerman¹¹¹, V. Tsulaia¹⁸, S. Tsuno⁸¹, D. Tsybychev¹⁵⁵, Y. Tu^{63b}, A. Tudorache^{27b}, V. Tudorache^{27b}, T. T. Tulbure^{27a}, A. N. Tuna⁵⁹, S. Turchikhin⁷⁹, D. Turgeman¹⁸⁰, I. Turk Cakir^{4b.u}, R. J. Turner²¹, R. T. Turra^{68a}, P. M. Tuts³⁹, S. Tzamarias¹⁶², E. Tzovara⁹⁹, G. Ucchielli⁴⁷, K. Uchida¹⁶³, I. Ueda⁸¹, M. Ughetto^{45a,45b}, F. Ukegawa¹⁶⁹, G. Unal³⁶, A. Undrus²⁹, G. Unel¹⁷¹, F. C. Ungaro¹⁰⁴, Y. Unno⁸¹, K. Uno¹⁶³, J. Urban^{28b}, P. Urquijo¹⁰⁴, G. Usai⁸, J. Usui⁸¹, Z. Uysal^{12d}, L. Vacavant¹⁰¹, V. Vacek¹⁴², B. Vachon¹⁰³, K. O. H. Vadla¹³⁴, A. Vaidya⁹⁴, C. Valderanis¹¹⁴, E. Valdes Santurio^{45a,45b}, M. Valente⁵⁴, S. Valentinetti^{23a,23b}, A. Valero¹⁷⁴, L. Valéry⁴⁶, R. A. Vallance²¹, A. Vallier³⁶, J. A. Valls Ferrer¹⁷⁴, T. R. Van Daalen¹⁴, P. Van Gemmeren⁶, I. Van Vulpen¹²⁰, M. Vanadia^{73a,73b}, W. Vandelli³⁶, A. Vaniachine¹⁶⁶, D. Vannicola^{72a,72b}, R. Vari^{72a}, E. W. Varnes⁷, C. Varni^{55a,55b}, T. Varol⁴², D. Varouchas¹³², K. E. Varvell¹⁵⁷, M. E. Vasile^{27b}, G. A. Vasquez¹⁷⁶, J. G. Vasquez¹⁸³,

F. Vazeille³⁸, D. Vazquez Furelos¹⁴, T. Vazquez Schroeder³⁶, J. Veatch⁵³, V. Vecchio^{74a,74b}, M. J. Veen¹²⁰, L. M. Veloce¹⁶⁷, F. Veloso^{140a,140c}, S. Veneziano^{72a}, A. Ventura^{67a,67b}, N. Venturi³⁶, A. Verbytskyi¹¹⁵, V. Vercesi^{70a}, M. Verducci^{74a,74b}, C. M. Vergel Infante⁷⁸, C. Vergis²⁴, W. Verkerke¹²⁰, A. T. Vermeulen¹²⁰, J. C. Vermeulen¹²⁰, M. C. Vetterli^{152,ax}, N. Viaux Maira^{147b}, M. Vicente Barreto Pinto⁵⁴, T. Vickey¹⁴⁹, O. E. Vickey Boeriu¹⁴⁹, G. H. A. Viehhauser¹³⁵, L. Vigani¹³⁵, M. Villa^{23a,23b}, M. Villaplana Perez^{68a,68b}, E. Vilucchi⁵¹, M. G. Vincter³⁴, V. B. Vinogradov⁷⁹, A. Vishwakarma⁴⁶, C. Vittori^{23a,23b}, I. Vivarelli¹⁵⁶, M. Vogel¹⁸², P. Vokac¹⁴², S. E. von Buddenbrock^{33c}, E. Von Toerne²⁴, V. Vorobel¹⁴³, K. Vorobev¹¹², M. Vos¹⁷⁴, J. H. Vosseveld⁹⁰, M. Vozak¹⁰⁰, N. Vranjes¹⁶, M. Vranjes Milosavljevic¹⁶, V. Vrba¹⁴², M. Vreeswijk¹²⁰, T. Šfiligoj⁹¹, R. Vuillermet³⁶, I. Vukotic³⁷, T. Ženiš^{28a}, L. Živković¹⁶, P. Wagner²⁴, W. Wagner¹⁸², J. Wagner-Kuhr¹¹⁴, H. Wahlberg⁸⁸, K. Wakamiya⁸², V. M. Walbrecht¹¹⁵, J. Walder⁸⁹, R. Walker¹¹⁴, S. D. Walker⁹³, W. Walkowiak¹⁵¹, V. Wallangen^{45a,45b}, A. M. Wang⁵⁹, C. Wang^{60b}, F. Wang¹⁸¹, H. Wang¹⁸, H. Wang³, J. Wang¹⁵⁷, J. Wang^{61b}, P. Wang⁴², Q. Wang¹²⁸, R.-J. Wang⁹⁹, R. Wang^{60a}, R. Wang⁶, S. M. Wang¹⁵⁸, W. T. Wang^{60a}, W. Wang^{15c,ae}, W. X. Wang^{60a,ae}, Y. Wang^{60a,am}, Z. Wang^{60c}, C. Wanotayaroj⁴⁶, A. Warburton¹⁰³, C. P. Ward³², D. R. Wardrope⁹⁴, N. Warrack⁵⁷, A. Washbrook⁵⁰, A. T. Watson²¹, M. F. Watson²¹, G. Watts¹⁴⁸, B. M. Waugh⁹⁴, A. F. Webb¹¹, S. Webb⁹⁹, C. Weber¹⁸³, M. S. Weber²⁰, S. A. Weber³⁴, S. M. Weber^{61a}, A. R. Weidberg¹³⁵, J. Weingarten⁴⁷, M. Weirich⁹⁹, C. Weiser⁵², P. S. Wells³⁶, T. Wenaus²⁹, T. Wengler³⁶, S. Wenig³⁶, N. Wermes²⁴, M. D. Werner⁷⁸, P. Werner³⁶, M. Wessels^{61a}, T. D. Weston²⁰, K. Whalen¹³¹, N. L. Whallon¹⁴⁸, A. M. Wharton⁸⁹, A. S. White¹⁰⁵, A. White⁸, M. J. White¹, D. Whiteson¹⁷¹, B. W. Whitmore⁸⁹, F. J. Wickens¹⁴⁴, W. Wiedenmann¹⁸¹, M. Wielers¹⁴⁴, N. Wieseotte⁹⁹, C. Wiglesworth⁴⁰, L. A. M. Wiik-Fuchs⁵², F. Wilk¹⁰⁰, H. G. Wilkens³⁶, L. J. Wilkins⁹³, H. H. Williams¹³⁷, S. Williams³², C. Willis¹⁰⁶, S. Willocq¹⁰², J. A. Wilson²¹, I. Wingerter-Seez⁵, E. Winkels¹⁵⁶, F. Winklmeier¹³¹, O. J. Winston¹⁵⁶, B. T. Winter⁵², M. Wittgen¹⁵³, M. Wobisch⁹⁵, A. Wolf⁹⁹, T. M. H. Wolf¹²⁰, R. Wolff¹⁰¹, R. W. Wölker¹³⁵, J. Wollrath⁵², M. W. Wolter⁸⁴, H. Wolters^{140a,140c}, V. W. S. Wong¹⁷⁵, N. L. Woods¹⁴⁶, S. D. Worm²¹, B. K. Wosiek⁸⁴, K. W. Woźniak⁸⁴, K. Wraight⁵⁷, S. L. Wu¹⁸¹, X. Wu⁵⁴, Y. Wu^{60a}, T. R. Wyatt¹⁰⁰, B. M. Wynne⁵⁰, S. Xella⁴⁰, Z. Xi¹⁰⁵, L. Xia¹⁷⁸, D. Xu^{15a}, H. Xu^{60a,c}, L. Xu²⁹, T. Xu¹⁴⁵, W. Xu¹⁰⁵, Z. Xu^{60b}, Z. Xu¹⁵³, B. Yabsley¹⁵⁷, S. Yacoob^{33a}, K. Yajima¹³³, D. P. Yallup⁹⁴, D. Yamaguchi¹⁶⁵, Y. Yamaguchi¹⁶⁵, A. Yamamoto⁸¹, T. Yamanaka¹⁶³, F. Yamane⁸², M. Yamatani¹⁶³, T. Yamazaki¹⁶³, Y. Yamazaki⁸², Z. Yan²⁵, H. J. Yang^{60c,60d}, H. T. Yang¹⁸, S. Yang⁷⁷, X. Yang^{58,60b}, Y. Yang¹⁶³, W.-M. Yao¹⁸, Y. C. Yap⁴⁶, Y. Yasu⁸¹, E. Yatsenko^{60c,60d}, J. Ye⁴², S. Ye²⁹, I. Yeletsikh⁷⁹, M. R. Yexley⁸⁹, E. Yigitbasi²⁵, E. Yildirim⁹⁹, K. Yorita¹⁷⁹, K. Yoshihara¹³⁷, C. J. S. Young³⁶, C. Young¹⁵³, J. Yu⁷⁸, R. Yuan^{60b}, X. Yue^{61a}, S. P. Y. Yuen²⁴, B. Zabinski⁸⁴, G. Zacharis¹⁰, E. Zaffaroni⁵⁴, J. Zahreddine¹³⁶, A. M. Zaitsev^{123,ao}, T. Zakareishvili^{159b}, N. Zakharchuk³⁴, S. Zambito⁵⁹, D. Zanzi³⁶, D. R. Zaripovas⁵⁷, S. V. Zeißner⁴⁷, C. Zeitnitz¹⁸², G. Zemaityte¹³⁵, J. C. Zeng¹⁷³, O. Zenin¹²³, D. Zerwas¹³², M. Zgubič¹³⁵, D. F. Zhang^{15b}, F. Zhang¹⁸¹, G. Zhang^{60a}, G. Zhang^{15b}, H. Zhang^{15c}, J. Zhang⁶, L. Zhang^{15c}, L. Zhang^{60a}, M. Zhang¹⁷³, R. Zhang^{60a}, R. Zhang²⁴, X. Zhang^{60b}, Y. Zhang^{15a,15d}, Z. Zhang^{63a}, Z. Zhang¹³², P. Zhao⁴⁹, Y. Zhao^{60b}, Z. Zhao^{60a}, A. Zhemchugov⁷⁹, Z. Zheng¹⁰⁵, D. Zhong¹⁷³, B. Zhou¹⁰⁵, C. Zhou¹⁸¹, M. S. Zhou^{15a,15d}, M. Zhou¹⁵⁵, N. Zhou^{60c}, Y. Zhou⁷, C. G. Zhu^{60b}, H. L. Zhu^{60a}, H. Zhu^{15a}, J. Zhu¹⁰⁵, Y. Zhu^{60a}, X. Zhuang^{15a}, K. Zhukov¹¹⁰, V. Zhulanov^{122a,122b}, D. Zieminska⁶⁵, N. I. Zimine⁷⁹, S. Zimmermann⁵², Z. Zinonos¹¹⁵, M. Ziolkowski¹⁵¹, G. Zobernig¹⁸¹, A. Zoccoli^{23a,23b}, K. Zoch⁵³, T. G. Zorbas¹⁴⁹, R. Zou³⁷, L. Zwalinski³⁶

¹ Department of Physics, University of Adelaide, Adelaide, Australia

² Physics Department, SUNY Albany, Albany, NY, USA

³ Department of Physics, University of Alberta, Edmonton, AB, Canada

⁴ (a) Department of Physics, Ankara University, Ankara, Turkey; (b) Istanbul Aydin University, Istanbul, Turkey; (c) Division of Physics, TOBB University of Economics and Technology, Ankara, Turkey

⁵ LAPP, Université Grenoble Alpes, Université Savoie Mont Blanc, CNRS/IN2P3, Annecy-le-Vieux, France

⁶ High Energy Physics Division, Argonne National Laboratory, Argonne, IL, USA

⁷ Department of Physics, University of Arizona, Tucson, AZ, USA

⁸ Department of Physics, University of Texas at Arlington, Arlington, TX, USA

⁹ Physics Department, National and Kapodistrian University of Athens, Athens, Greece

¹⁰ Physics Department, National Technical University of Athens, Zografou, Greece

¹¹ Department of Physics, University of Texas at Austin, Austin, TX, USA

¹² (a) Bahcesehir University, Faculty of Engineering and Natural Sciences, Istanbul, Turkey; (b) Istanbul Bilgi University, Faculty of Engineering and Natural Sciences, Istanbul, Turkey; (c) Department of Physics, Bogazici University, Istanbul, Turkey; (d) Department of Physics Engineering, Gaziantep University, Gaziantep, Turkey

¹³ Institute of Physics, Azerbaijan Academy of Sciences, Baku, Azerbaijan

¹⁴ Institut de Física d'Altes Energies (IFAE), Barcelona Institute of Science and Technology, Barcelona, Spain

- 15 (a)Institute of High Energy Physics, Chinese Academy of Sciences, Beijing, China; (b)Physics Department, Tsinghua University, Beijing, China; (c)Department of Physics, Nanjing University, Nanjing, China; (d)University of Chinese Academy of Science (UCAS), Beijing, China
- 16 Institute of Physics, University of Belgrade, Belgrade, Serbia
- 17 Department for Physics and Technology, University of Bergen, Bergen, Norway
- 18 Physics Division, Lawrence Berkeley National Laboratory and University of California, Berkeley, CA, USA
- 19 Institut für Physik, Humboldt Universität zu Berlin, Berlin, Germany
- 20 Albert Einstein Center for Fundamental Physics and Laboratory for High Energy Physics, University of Bern, Bern, Switzerland
- 21 School of Physics and Astronomy, University of Birmingham, Birmingham, UK
- 22 Facultad de Ciencias y Centro de Investigaciones, Universidad Antonio Nariño, Bogotá, Colombia
- 23 (a)Dipartimento di Fisica, INFN Bologna and Università di Bologna, Bologna, Italy; (b)INFN Sezione di Bologna, Bologna, Italy
- 24 Physikalisches Institut, Universität Bonn, Bonn, Germany
- 25 Department of Physics, Boston University, Boston, MA, USA
- 26 Department of Physics, Brandeis University, Waltham, MA, USA
- 27 (a)Transilvania University of Brasov, Brasov, Romania; (b)Horia Hulubei National Institute of Physics and Nuclear Engineering, Bucharest, Romania; (c)Department of Physics, Alexandru Ioan Cuza University of Iasi, Iasi, Romania; (d)National Institute for Research and Development of Isotopic and Molecular Technologies, Physics Department, Cluj Napoca, Romania; (e)University Politehnica Bucharest, Bucharest, Romania; (f)West University in Timisoara, Timisoara, Romania
- 28 (a)Faculty of Mathematics, Physics and Informatics, Comenius University, Bratislava, Slovak Republic; (b)Department of Subnuclear Physics, Institute of Experimental Physics of the Slovak Academy of Sciences, Kosice, Slovak Republic
- 29 Physics Department, Brookhaven National Laboratory, Upton, NY, USA
- 30 Departamento de Física, Universidad de Buenos Aires, Buenos Aires, Argentina
- 31 California State University, Fresno, CA, USA
- 32 Cavendish Laboratory, University of Cambridge, Cambridge, UK
- 33 (a)Department of Physics, University of Cape Town, Cape Town, South Africa; (b)Department of Mechanical Engineering Science, University of Johannesburg, Johannesburg, South Africa; (c)School of Physics, University of the Witwatersrand, Johannesburg, South Africa
- 34 Department of Physics, Carleton University, Ottawa, ON, Canada
- 35 (a)Faculté des Sciences Ain Chock, Réseau Universitaire de Physique des Hautes Energies - Université Hassan II, Casablanca, Morocco; (b)Faculté des Sciences, Université Ibn-Tofail, Kénitra, Morocco; (c)Faculté des Sciences Semlalia, Université Cadi Ayyad, LPHEA-Marrakech, Morocco; (d)Faculté des Sciences, Université Mohamed Premier and LPTPM, Oujda, Morocco; (e)Faculté des sciences, Université Mohammed V, Rabat, Morocco
- 36 CERN, Geneva, Switzerland
- 37 Enrico Fermi Institute, University of Chicago, Chicago, IL, USA
- 38 LPC, Université Clermont Auvergne, CNRS/IN2P3, Clermont-Ferrand, France
- 39 Nevis Laboratory, Columbia University, Irvington, NY, USA
- 40 Niels Bohr Institute, University of Copenhagen, Copenhagen, Denmark
- 41 (a)Dipartimento di Fisica, Università della Calabria, Rende, Italy; (b)INFN Gruppo Collegato di Cosenza, Laboratori Nazionali di Frascati, Frascati, Italy
- 42 Physics Department, Southern Methodist University, Dallas, TX, USA
- 43 Physics Department, University of Texas at Dallas, Richardson, TX, USA
- 44 National Centre for Scientific Research “Demokritos”, Agia Paraskevi, Greece
- 45 (a)Department of Physics, Stockholm University, Sweden; (b)Oskar Klein Centre, Stockholm, Sweden
- 46 Deutsches Elektronen-Synchrotron DESY, Hamburg, Zeuthen, Germany
- 47 Lehrstuhl für Experimentelle Physik IV, Technische Universität Dortmund, Dortmund, Germany
- 48 Institut für Kern- und Teilchenphysik, Technische Universität Dresden, Dresden, Germany
- 49 Department of Physics, Duke University, Durham, NC, USA
- 50 SUPA - School of Physics and Astronomy, University of Edinburgh, Edinburgh, UK
- 51 INFN e Laboratori Nazionali di Frascati, Frascati, Italy
- 52 Physikalisches Institut, Albert-Ludwigs-Universität Freiburg, Freiburg, Germany

- 53 II. Physikalisches Institut, Georg-August-Universität Göttingen, Göttingen, Germany
- 54 Département de Physique Nucléaire et Corpusculaire, Université de Genève, Geneva, Switzerland
- 55 (a)Dipartimento di Fisica, Università di Genova, Genoa, Italy; (b)INFN Sezione di Genova, Genoa, Italy
- 56 II. Physikalisches Institut, Justus-Liebig-Universität Giessen, Giessen, Germany
- 57 SUPA - School of Physics and Astronomy, University of Glasgow, Glasgow, UK
- 58 LPSC, Université Grenoble Alpes, CNRS/IN2P3, Grenoble INP, Grenoble, France
- 59 Laboratory for Particle Physics and Cosmology, Harvard University, Cambridge, MA, USA
- 60 (a)Department of Modern Physics and State Key Laboratory of Particle Detection and Electronics, University of Science and Technology of China, Hefei, China; (b)Institute of Frontier and Interdisciplinary Science and Key Laboratory of Particle Physics and Particle Irradiation (MOE), Shandong University, Qingdao, China; (c)School of Physics and Astronomy, Shanghai Jiao Tong University, KLPPAC-MoE, SKLPPC, Shanghai, China; (d)Tsung-Dao Lee Institute, Shanghai, China
- 61 (a)Kirchhoff-Institut für Physik, Ruprecht-Karls-Universität Heidelberg, Heidelberg, Germany; (b)Physikalisches Institut, Ruprecht-Karls-Universität Heidelberg, Heidelberg, Germany
- 62 Faculty of Applied Information Science, Hiroshima Institute of Technology, Hiroshima, Japan
- 63 (a)Department of Physics, Chinese University of Hong Kong, Shatin, N.T., Hong Kong, China; (b)Department of Physics, University of Hong Kong, Hong Kong, China; (c)Department of Physics and Institute for Advanced Study, Hong Kong University of Science and Technology, Clear Water Bay, Kowloon, Hong Kong, China
- 64 Department of Physics, National Tsing Hua University, Hsinchu, Taiwan
- 65 Department of Physics, Indiana University, Bloomington, IN, USA
- 66 (a)INFN Gruppo Collegato di Udine, Sezione di Trieste, Udine, Italy; (b)ICTP, Trieste, Italy; (c)Dipartimento Politecnico di Ingegneria e Architettura, Università di Udine, Udine, Italy
- 67 (a)INFN Sezione di Lecce, Lecce, Italy; (b)Dipartimento di Matematica e Fisica, Università del Salento, Lecce, Italy
- 68 (a)INFN Sezione di Milano, Milan, Italy; (b)Dipartimento di Fisica, Università di Milano, Milan, Italy
- 69 (a)INFN Sezione di Napoli, Naples, Italy; (b)Dipartimento di Fisica, Università di Napoli, Naples, Italy
- 70 (a)INFN Sezione di Pavia, Pavia, Italy; (b)Dipartimento di Fisica, Università di Pavia, Pavia, Italy
- 71 (a)INFN Sezione di Pisa, Pisa, Italy; (b)Dipartimento di Fisica E. Fermi, Università di Pisa, Pisa, Italy
- 72 (a)INFN Sezione di Roma, Rome, Italy; (b)Dipartimento di Fisica, Sapienza Università di Roma, Rome, Italy
- 73 (a)INFN Sezione di Roma Tor Vergata, Rome, Italy; (b)Dipartimento di Fisica, Università di Roma Tor Vergata, Rome, Italy
- 74 (a)INFN Sezione di Roma Tre, Rome, Italy; (b)Dipartimento di Matematica e Fisica, Università Roma Tre, Rome, Italy
- 75 (a)INFN-TIFPA, Trento, Italy; (b)Università degli Studi di Trento, Trento, Italy
- 76 Institut für Astro- und Teilchenphysik, Leopold-Franzens-Universität, Innsbruck, Austria
- 77 University of Iowa, Iowa City, IA, USA
- 78 Department of Physics and Astronomy, Iowa State University, Ames, IA, USA
- 79 Joint Institute for Nuclear Research, Dubna, Russia
- 80 (a)Departamento de Engenharia Elétrica, Universidade Federal de Juiz de Fora (UFJF), Juiz de Fora, Brazil; (b)Universidade Federal do Rio De Janeiro COPPE/EE/IF, Rio de Janeiro, Brazil; (c)Universidade Federal de São João del Rei (UFSJ), São João del Rei, Brazil; (d)Instituto de Física, Universidade de São Paulo, São Paulo, Brazil
- 81 KEK, High Energy Accelerator Research Organization, Tsukuba, Japan
- 82 Graduate School of Science, Kobe University, Kobe, Japan
- 83 (a)AGH University of Science and Technology, Faculty of Physics and Applied Computer Science, Kraków, Poland; (b)Marian Smoluchowski Institute of Physics, Jagiellonian University, Kraków, Poland
- 84 Institute of Nuclear Physics Polish Academy of Sciences, Kraków, Poland
- 85 Faculty of Science, Kyoto University, Kyoto, Japan
- 86 Kyoto University of Education, Kyoto, Japan
- 87 Research Center for Advanced Particle Physics and Department of Physics, Kyushu University, Fukuoka, Japan
- 88 Instituto de Física La Plata, Universidad Nacional de La Plata and CONICET, La Plata, Argentina
- 89 Physics Department, Lancaster University, Lancaster, UK
- 90 Oliver Lodge Laboratory, University of Liverpool, Liverpool, UK
- 91 Department of Experimental Particle Physics, Jožef Stefan Institute and Department of Physics, University of Ljubljana, Ljubljana, Slovenia
- 92 School of Physics and Astronomy, Queen Mary University of London, London, UK

- ⁹³ Department of Physics, Royal Holloway University of London, Egham, UK
- ⁹⁴ Department of Physics and Astronomy, University College London, London, UK
- ⁹⁵ Louisiana Tech University, Ruston, LA, USA
- ⁹⁶ Fysiska institutionen, Lunds universitet, Lund, Sweden
- ⁹⁷ Centre de Calcul de l'Institut National de Physique Nucléaire et de Physique des Particules (IN2P3), Villeurbanne, France
- ⁹⁸ Departamento de Física Teórica C-15 and CIAFF, Universidad Autónoma de Madrid, Madrid, Spain
- ⁹⁹ Institut für Physik, Universität Mainz, Mainz, Germany
- ¹⁰⁰ School of Physics and Astronomy, University of Manchester, Manchester, UK
- ¹⁰¹ CPPM, Aix-Marseille Université, CNRS/IN2P3, Marseille, France
- ¹⁰² Department of Physics, University of Massachusetts, Amherst, MA, USA
- ¹⁰³ Department of Physics, McGill University, Montreal, QC, Canada
- ¹⁰⁴ School of Physics, University of Melbourne, Victoria, Australia
- ¹⁰⁵ Department of Physics, University of Michigan, Ann Arbor, MI, USA
- ¹⁰⁶ Department of Physics and Astronomy, Michigan State University, East Lansing, MI, USA
- ¹⁰⁷ B.I. Stepanov Institute of Physics, National Academy of Sciences of Belarus, Minsk, Belarus
- ¹⁰⁸ Research Institute for Nuclear Problems of Byelorussian State University, Minsk, Belarus
- ¹⁰⁹ Group of Particle Physics, University of Montreal, Montreal, QC, Canada
- ¹¹⁰ P.N. Lebedev Physical Institute of the Russian Academy of Sciences, Moscow, Russia
- ¹¹¹ Institute for Theoretical and Experimental Physics of the National Research Centre Kurchatov Institute, Moscow, Russia
- ¹¹² National Research Nuclear University MEPhI, Moscow, Russia
- ¹¹³ D.V. Skobeltsyn Institute of Nuclear Physics, M.V. Lomonosov Moscow State University, Moscow, Russia
- ¹¹⁴ Fakultät für Physik, Ludwig-Maximilians-Universität München, Munich, Germany
- ¹¹⁵ Max-Planck-Institut für Physik (Werner-Heisenberg-Institut), Munich, Germany
- ¹¹⁶ Nagasaki Institute of Applied Science, Nagasaki, Japan
- ¹¹⁷ Graduate School of Science and Kobayashi-Maskawa Institute, Nagoya University, Nagoya, Japan
- ¹¹⁸ Department of Physics and Astronomy, University of New Mexico, Albuquerque, NM, USA
- ¹¹⁹ Institute for Mathematics, Astrophysics and Particle Physics, Radboud University Nijmegen/Nikhef, Nijmegen, The Netherlands
- ¹²⁰ Nikhef National Institute for Subatomic Physics and University of Amsterdam, Amsterdam, The Netherlands
- ¹²¹ Department of Physics, Northern Illinois University, DeKalb, IL, USA
- ¹²² ^(a)Budker Institute of Nuclear Physics and NSU, SB RAS, Novosibirsk, Russia; ^(b)Novosibirsk State University Novosibirsk, Novosibirsk, Russia
- ¹²³ Institute for High Energy Physics of the National Research Centre Kurchatov Institute, Protvino, Russia
- ¹²⁴ Department of Physics, New York University, New York, NY, USA
- ¹²⁵ Ochanomizu University, Otsuka, Bunkyo-ku, Tokyo, Japan
- ¹²⁶ Ohio State University, Columbus, OH, USA
- ¹²⁷ Faculty of Science, Okayama University, Okayama, Japan
- ¹²⁸ Homer L. Dodge Department of Physics and Astronomy, University of Oklahoma, Norman, OK, USA
- ¹²⁹ Department of Physics, Oklahoma State University, Stillwater, OK, USA
- ¹³⁰ Palacký University, RCPTM, Joint Laboratory of Optics, Olomouc, Czech Republic
- ¹³¹ Center for High Energy Physics, University of Oregon, Eugene, OR, USA
- ¹³² LAL, Université Paris-Sud, CNRS/IN2P3, Université Paris-Saclay, Orsay, France
- ¹³³ Graduate School of Science, Osaka University, Osaka, Japan
- ¹³⁴ Department of Physics, University of Oslo, Oslo, Norway
- ¹³⁵ Department of Physics, Oxford University, Oxford, UK
- ¹³⁶ LPNHE, Sorbonne Université, Paris Diderot Sorbonne Paris Cité, CNRS/IN2P3, Paris, France
- ¹³⁷ Department of Physics, University of Pennsylvania, Philadelphia, PA, USA
- ¹³⁸ Konstantinov Nuclear Physics Institute of National Research Centre "Kurchatov Institute", PNPI, St. Petersburg, Russia
- ¹³⁹ Department of Physics and Astronomy, University of Pittsburgh, Pittsburgh, PA, USA

- 140 (a)Laboratório de Instrumentação e Física Experimental de Partículas - LIP, Lisbon, Portugal; (b)Departamento de Física, Faculdade de Ciências, Universidade de Lisboa, Lisbon, Portugal; (c)Departamento de Física, Universidade de Coimbra, Coimbra, Portugal; (d)Centro de Física Nuclear da Universidade de Lisboa, Lisboa, Portugal; (e)Departamento de Física, Universidade do Minho, Braga, Portugal; (f)Universidad de Granada, Granada (Spain), Portugal; (g)Dep Física and CEFITEC of Faculdade de Ciências e Tecnologia, Universidade Nova de Lisboa, Caparica, Portugal
- 141 Institute of Physics of the Czech Academy of Sciences, Prague, Czech Republic
- 142 Czech Technical University in Prague, Prague, Czech Republic
- 143 Charles University, Faculty of Mathematics and Physics, Prague, Czech Republic
- 144 Particle Physics Department, Rutherford Appleton Laboratory, Didcot, UK
- 145 IRFU, CEA, Université Paris-Saclay, Gif-sur-Yvette, France
- 146 Santa Cruz Institute for Particle Physics, University of California Santa Cruz, Santa Cruz, CA, USA
- 147 (a)Departamento de Física, Pontificia Universidad Católica de Chile, Santiago, Chile; (b)Departamento de Física, Universidad Técnica Federico Santa María, Valparaíso, Chile
- 148 Department of Physics, University of Washington, Seattle, WA, USA
- 149 Department of Physics and Astronomy, University of Sheffield, Sheffield, UK
- 150 Department of Physics, Shinshu University, Nagano, Japan
- 151 Department Physik, Universität Siegen, Siegen, Germany
- 152 Department of Physics, Simon Fraser University, Burnaby, BC, Canada
- 153 SLAC National Accelerator Laboratory, Stanford, CA, USA
- 154 Physics Department, Royal Institute of Technology, Stockholm, Sweden
- 155 Departments of Physics and Astronomy, Stony Brook University, Stony Brook, NY, USA
- 156 Department of Physics and Astronomy, University of Sussex, Brighton, UK
- 157 School of Physics, University of Sydney, Sydney, Australia
- 158 Institute of Physics, Academia Sinica, Taipei, Taiwan
- 159 (a)E. Andronikashvili Institute of Physics, Iv. Javakishvili Tbilisi State University, Tbilisi, Georgia; (b)High Energy Physics Institute, Tbilisi State University, Tbilisi, Georgia
- 160 Department of Physics, Technion, Israel Institute of Technology, Haifa, Israel
- 161 Raymond and Beverly Sackler School of Physics and Astronomy, Tel Aviv University, Tel Aviv, Israel
- 162 Department of Physics, Aristotle University of Thessaloniki, Thessaloniki, Greece
- 163 International Center for Elementary Particle Physics and Department of Physics, University of Tokyo, Tokyo, Japan
- 164 Graduate School of Science and Technology, Tokyo Metropolitan University, Tokyo, Japan
- 165 Department of Physics, Tokyo Institute of Technology, Tokyo, Japan
- 166 Tomsk State University, Tomsk, Russia
- 167 Department of Physics, University of Toronto, Toronto, ON, Canada
- 168 (a)TRIUMF, Vancouver, BC, Canada; (b)Department of Physics and Astronomy, York University, Toronto, ON, Canada
- 169 Division of Physics and Tomonaga Center for the History of the Universe, Faculty of Pure and Applied Sciences, University of Tsukuba, Tsukuba, Japan
- 170 Department of Physics and Astronomy, Tufts University, Medford, MA, USA
- 171 Department of Physics and Astronomy, University of California Irvine, Irvine, CA, USA
- 172 Department of Physics and Astronomy, University of Uppsala, Uppsala, Sweden
- 173 Department of Physics, University of Illinois, Urbana, IL, USA
- 174 Instituto de Física Corpuscular (IFIC), Centro Mixto Universidad de Valencia - CSIC, Valencia, Spain
- 175 Department of Physics, University of British Columbia, Vancouver, BC, Canada
- 176 Department of Physics and Astronomy, University of Victoria, Victoria, BC, Canada
- 177 Fakultät für Physik und Astronomie, Julius-Maximilians-Universität Würzburg, Würzburg, Germany
- 178 Department of Physics, University of Warwick, Coventry, UK
- 179 Waseda University, Tokyo, Japan
- 180 Department of Particle Physics, Weizmann Institute of Science, Rehovot, Israel
- 181 Department of Physics, University of Wisconsin, Madison, WI, USA
- 182 Fakultät für Mathematik und Naturwissenschaften, Fachgruppe Physik, Bergische Universität Wuppertal, Wuppertal, Germany
- 183 Department of Physics, Yale University, New Haven, CT, USA

184 Yerevan Physics Institute, Yerevan, Armenia

- ^a , Also at Centre for High Performance Computing, CSIR Campus, Rosebank, Cape Town, South Africa
- ^b Also at CERN, Geneva, Switzerland
- ^c Also at CPPM, Aix-Marseille Université, CNRS/IN2P3, Marseille, France
- ^d Also at Département de Physique Nucléaire et Corpusculaire, Université de Genève, Geneva, Switzerland
- ^e Also at Departament de Física de la Universitat Autònoma de Barcelona, Barcelona, Spain
- ^f Also at Departamento de Física, Instituto Superior Técnico, Universidade de Lisboa, Lisbon, Portugal
- ^g Also at Department of Applied Physics and Astronomy, University of Sharjah, Sharjah, United Arab Emirates
- ^h Also at Department of Financial and Management Engineering, University of the Aegean, Chios, Greece
- ⁱ Also at Department of Physics and Astronomy, University of Louisville, Louisville, KY, USA
- ^j Also at Department of Physics and Astronomy, University of Sheffield, Sheffield, UK
- ^k Also at Department of Physics, California State University, East Bay, USA
- ^l Also at Department of Physics, California State University, Fresno, USA
- ^m Also at Department of Physics, California State University, Sacramento, USA
- ⁿ Also at Department of Physics, King's College London, London, UK
- ^o Also at Department of Physics, St. Petersburg State Polytechnical University, St. Petersburg, Russia
- ^p Also at Department of Physics, Stanford University, Stanford CA, USA
- ^q Also at Department of Physics, University of Adelaide, Adelaide, Australia
- ^r Also at Department of Physics, University of Fribourg, Fribourg, Switzerland
- ^s Also at Department of Physics, University of Michigan, Ann Arbor MI, USA
- ^t Also at Faculty of Physics, M.V. Lomonosov Moscow State University, Moscow, Russia
- ^u Also at Giresun University, Faculty of Engineering, Giresun, Turkey
- ^v Also at Graduate School of Science, Osaka University, Osaka, Japan
- ^w Also at Hellenic Open University, Patras, Greece
- ^x Also at Institutio Catalana de Recerca i Estudis Avancats, ICREA, Barcelona, Spain
- ^y Also at Institut für Experimentalphysik, Universität Hamburg, Hamburg, Germany
- ^z Also at Institute for Mathematics, Astrophysics and Particle Physics, Radboud University Nijmegen/Nikhef, Nijmegen, The Netherlands
- ^{aa} Also at Institute for Nuclear Research and Nuclear Energy (INRNE) of the Bulgarian Academy of Sciences, Sofia, Bulgaria
- ^{ab} Also at Institute for Particle and Nuclear Physics, Wigner Research Centre for Physics, Budapest, Hungary
- ^{ac} Also at Institute of High Energy Physics, Chinese Academy of Sciences, Beijing, China
- ^{ad} Also at Institute of Particle Physics (IPP), Vancouver, Canada
- ^{ae} Also at Institute of Physics, Academia Sinica, Taipei, Taiwan
- ^{af} Also at Institute of Physics, Azerbaijan Academy of Sciences, Baku, Azerbaijan
- ^{ag} Also at Institute of Theoretical Physics, Ilia State University, Tbilisi, Georgia
- ^{ah} Also at Instituto de Física Teórica, IFT-UAM/CSIC, Madrid, Spain
- ^{ai} Also at Department of Physics, Istanbul University, Istanbul, Turkey
- ^{aj} Also at Joint Institute for Nuclear Research, Dubna, Russia
- ^{ak} Also at LAL, Université Paris-Sud, CNRS/IN2P3, Université Paris-Saclay, Orsay, France
- ^{al} Also at Louisiana Tech University, Ruston LA, USA
- ^{am} Also at LPNHE, Sorbonne Université, Paris Diderot Sorbonne Paris Cité, CNRS/IN2P3, Paris, France
- ^{an} Also at Manhattan College, New York NY, USA
- ^{ao} Also at Moscow Institute of Physics and Technology State University, Dolgoprudny, Russia
- ^{ap} Also at National Research Nuclear University MEPhI, Moscow, Russia
- ^{aq} Also at Physics Department, An-Najah National University, Nablus, Palestine
- ^{ar} Also at Physics Dept, University of South Africa, Pretoria, South Africa
- ^{as} Also at Physikalisches Institut, Albert-Ludwigs-Universität Freiburg, Freiburg, Germany
- ^{at} Also at School of Physics, Sun Yat-sen University, Guangzhou, China
- ^{au} Also at The City College of New York, New York NY, USA
- ^{av} Also at The Collaborative Innovation Center of Quantum Matter (CICQM), Beijing, China

^{aw} Also at Tomsk State University, Tomsk, and Moscow Institute of Physics and Technology State University, Dolgoprudny, Russia

^{ax} Also at TRIUMF, Vancouver BC, Canada

^{ay} Also at Universita di Napoli Parthenope, Naples, Italy

* Deceased